

Nuclear Science

ISBN 978-92-64-99007-4

OECD/NEA Nuclear Science Committee  
Working Party on the Physics of Plutonium Fuels and Innovative Fuel Cycles

***Physics of Plutonium Recycling***

*Volume VIII*

**Results of a Benchmark Considering  
a High-temperature Reactor (HTR)  
Fuelled with Reactor-grade Plutonium**

**J.G. Hosking, T.D. Newton**  
Serco Assurance

*A Report Produced for Nexia Solutions*

© OECD 2007  
NEA No. 6200

NUCLEAR ENERGY AGENCY  
ORGANISATION FOR ECONOMIC CO-OPERATION AND DEVELOPMENT

## **ORGANISATION FOR ECONOMIC CO-OPERATION AND DEVELOPMENT**

The OECD is a unique forum where the governments of 30 democracies work together to address the economic, social and environmental challenges of globalisation. The OECD is also at the forefront of efforts to understand and to help governments respond to new developments and concerns, such as corporate governance, the information economy and the challenges of an ageing population. The Organisation provides a setting where governments can compare policy experiences, seek answers to common problems, identify good practice and work to co-ordinate domestic and international policies.

The OECD member countries are: Australia, Austria, Belgium, Canada, the Czech Republic, Denmark, Finland, France, Germany, Greece, Hungary, Iceland, Ireland, Italy, Japan, Korea, Luxembourg, Mexico, the Netherlands, New Zealand, Norway, Poland, Portugal, the Slovak Republic, Spain, Sweden, Switzerland, Turkey, the United Kingdom and the United States. The Commission of the European Communities takes part in the work of the OECD.

OECD Publishing disseminates widely the results of the Organisation's statistics gathering and research on economic, social and environmental issues, as well as the conventions, guidelines and standards agreed by its members.

\* \* \*

*This work is published on the responsibility of the Secretary-General of the OECD. The opinions expressed and arguments employed herein do not necessarily reflect the official views of the Organisation or of the governments of its member countries.*

## **NUCLEAR ENERGY AGENCY**

The OECD Nuclear Energy Agency (NEA) was established on 1<sup>st</sup> February 1958 under the name of the OEEC European Nuclear Energy Agency. It received its present designation on 20<sup>th</sup> April 1972, when Japan became its first non-European full member. NEA membership today consists of 28 OECD member countries: Australia, Austria, Belgium, Canada, the Czech Republic, Denmark, Finland, France, Germany, Greece, Hungary, Iceland, Ireland, Italy, Japan, Luxembourg, Mexico, the Netherlands, Norway, Portugal, Republic of Korea, the Slovak Republic, Spain, Sweden, Switzerland, Turkey, the United Kingdom and the United States. The Commission of the European Communities also takes part in the work of the Agency.

The mission of the NEA is:

- to assist its member countries in maintaining and further developing, through international co-operation, the scientific, technological and legal bases required for a safe, environmentally friendly and economical use of nuclear energy for peaceful purposes, as well as
- to provide authoritative assessments and to forge common understandings on key issues, as input to government decisions on nuclear energy policy and to broader OECD policy analyses in areas such as energy and sustainable development.

Specific areas of competence of the NEA include safety and regulation of nuclear activities, radioactive waste management, radiological protection, nuclear science, economic and technical analyses of the nuclear fuel cycle, nuclear law and liability, and public information. The NEA Data Bank provides nuclear data and computer program services for participating countries.

In these and related tasks, the NEA works in close collaboration with the International Atomic Energy Agency in Vienna, with which it has a Co-operation Agreement, as well as with other international organisations in the nuclear field.

### **© OECD 2007**

No reproduction, copy, transmission or translation of this publication may be made without written permission. Applications should be sent to OECD Publishing: [rights@oecd.org](mailto:rights@oecd.org) or by fax (+33-1) 45 24 99 30. Permission to photocopy a portion of this work should be addressed to the Centre Français d'exploitation du droit de Copie (CFC), 20 rue des Grands-Augustins, 75006 Paris, France, fax (+33-1) 46 34 67 19, ([contact@cfcopies.com](mailto:contact@cfcopies.com)) or (for US only) to Copyright Clearance Center (CCC), 222 Rosewood Drive Danvers, MA 01923, USA, fax +1 978 646 8600, [info@copyright.com](mailto:info@copyright.com).

*Cover credit: PBMR, South Africa.*

## **FOREWORD**

This report contains the results submitted for the five phases of the OECD/NEA benchmark concerning a high-temperature reactor (HTR) fuelled with reactor-grade plutonium. The benchmark has been organised under the auspices of the OECD/NEA Working Party on the Physics of Plutonium Fuels and Innovative Fuel Cycles. Specifications for these benchmark phases are reproduced in Appendix A. Although the benchmark has been specifically designed to provide intercomparisons for plutonium and thorium fuels, phases of calculations for uranium fuel have also been included. The purpose of these phases is to identify any increased uncertainties, relative to uranium fuel, that are associated with plutonium and thorium fuel.

The five phases of the benchmark cover:

- Phase 1: An infinite array of fuel pebbles containing uranium fuel.
- Phase 2: An infinite array of fuel pebbles containing plutonium fuel.
- Phase 3: A whole-core calculation for a plutonium-fuelled system.
- Phase 4: A whole-core calculation for a uranium-fuelled system.
- Phase 5: An infinite array of fuel pebbles containing thorium/uranium fuel.

### *Acknowledgements*

Serco Assurance would like to thank all contributors to the benchmark.

The support and sponsorship of Nexia Solutions (formerly BNFL R&T) to the contribution made by Serco Assurance is gratefully acknowledged.



## TABLE OF CONTENTS

Foreword .....	3
<b>Chapter 1 INTRODUCTION.....</b>	<b>7</b>
<b>Chapter 2 METHODS AND CODES USED BY THE PARTICIPANTS .....</b>	<b>9</b>
2.1 Deterministic calculation details .....	9
2.1.1 Resonance shielding.....	9
2.1.2 Double heterogeneity .....	10
2.1.3 Number of energy groups .....	10
<b>Chapter 3 RESULTS .....</b>	<b>13</b>
3.1 Phase 1 .....	13
3.1.1 Phase 1a: Reactivities and reaction rates .....	13
3.1.2 Phase 1b: Reactivities and reaction rates .....	15
3.1.3 Spectra .....	17
3.1.4 Burn-up .....	17
3.2 Phase 2 .....	28
3.2.1 Phase 2a: Reactivities and reaction rates .....	28
3.2.2 Phase 2b: Reactivities and reaction rates .....	30
3.2.3 Spectra .....	32
3.2.4 Burn-up .....	32
3.3 Phase 3 .....	38
3.3.1 Core reactivity.....	38
3.3.2 Spectra .....	39
3.3.3 Cross-sections .....	39
3.4 Phase 4 .....	42
3.4.1 Core reactivity.....	42
3.4.2 Spectra .....	43
3.4.3 Cross-sections .....	44
3.5 Phase 5 .....	45
3.5.1 Phase 5a: Reactivities and reaction rates .....	45
3.5.2 Phase 5b: Reactivities and reaction rates .....	47
3.5.3 Spectra .....	48
3.5.4 Burn-up .....	49
<b>Chapter 4 CONCLUSIONS .....</b>	<b>53</b>
References .....	55
Figures .....	57
Appendix A – Benchmark definition.....	75
Appendix B – Energy group schemes used in the deterministic calculations .....	95



## *Chapter 1*

### **INTRODUCTION**

This report contains results submitted for the five phases of the OECD NEA benchmark for a HTR fuelled with reactor-grade plutonium. The benchmark has been organised as part of the work by the Working Party on the Physics of Plutonium Fuels and Innovative Fuel Cycles. Specifications of these benchmark phases are reproduced in Appendix A of this report. Although the benchmark has been specifically designed to provide inter-comparisons for plutonium and thorium fuels, phases of calculations for uranium fuel have also been included. The purpose of these phases is to identify any increased uncertainties, relative to uranium fuel, that are associated with the plutonium and thorium fuels.

The five phases of the benchmark are defined as follows:

- Phase 1a: Uranium fuel: Cell calculation employing a spherical outer boundary.
- Phase 1b: Uranium fuel: Cell calculation employing a cubic outer boundary.
- Phase 2a: Plutonium fuel: Cell calculation employing a spherical outer boundary.
- Phase 2b: Plutonium fuel: Cell calculation employing a cubic outer boundary.
- Phase 3: Plutonium fuel: Whole-core calculations.
- Phase 4: Uranium fuel: Whole-core calculations.
- Phase 5a: Thorium/uranium fuel: Cell calculation employing a spherical outer boundary.
- Phase 5b: Thorium/uranium fuel: Cell calculation employing a cubic outer boundary.

Participants have been invited to submit results from deterministic calculations and, where appropriate, Monte Carlo calculations. The following participants have submitted results:

- *Participant A*: J.G. Hosking and T.D. Newton, Serco Assurance, UK.
- *Participant B*: O. Koberl, CEA, France.
- *Participant C*: U. Colak, Nuclear Engineering Dept., Hacettepe University, Turkey.
- *Participant D*: M. Tombakoglu, Nuclear Engineering Dept., Hacettepe University, Turkey.
- *Participant E*: P. Morris, Nexia Solutions, UK (formerly BNFL R&T, UK).
- *Participant F*: S. Goluoglu, Nuclear Science & Technology Division, ORNL, USA.



## *Chapter 2*

### **METHODS AND CODES USED BY THE PARTICIPANTS**

Table 2.1 gives an outline of the details of the calculational methods and codes used by each of the benchmark participants.

#### **2.1 Deterministic calculation details**

This subsection contains details of some of the deterministic PBMR modelling methods employed by the participants in order to obtain their submitted results.

##### ***2.1.1 Resonance shielding***

Participant A has used the subgroup treatment within WIMS9 to calculate resonance shielding for  $^{235}\text{U}$  and  $^{238}\text{U}$  in Phases 1 and 4 of the study, for  $^{239}\text{Pu}$  and  $^{240}\text{Pu}$  in Phases 2 and 3 of the study and for  $^{232}\text{Th}$  and  $^{233}\text{U}$  in Phase 5 of the study. All other shieldable nuclides have been treated using equivalence theory. The use of the subgroup treatment allows the effects of the double heterogeneity in the geometry to be accounted for directly in the resonance shielding of the cross-sections.

The subgroup method uses a set of library resonance integrals, interpolated to the correct temperature, that are functions of nuclide, reaction, energy and the scattering power in the problem. These are fitted by a set of subgroup cross-sections and weights for each reaction, energy group and nuclide. An equation is then formed and solved for the subgroup fluxes and the final shielded cross-sections formed from the subgroup cross-sections, weights and fluxes. To treat the double heterogeneity of the particulate fuel a special formation is required for the solution of the subgroup flux equations. This is performed using collision probabilities, treating each energy group in turn. Initially, collision probabilities are solved using the macroscopic subgroup total cross-sections, for the heterogeneous fuel particle with an additional outer layer representing the associated amount of carbon support matrix material. A homogenised version of the particle is then considered and a homogenised subgroup total cross-section is derived which has the same escape probability as the heterogeneous particle. This homogenised subgroup total cross-section is then used in the central region of the pebble to allow collision probabilities to be derived for all the pebble regions. The pebble and particle collision probabilities are then combined to form a full set of collision probabilities for the complete pebble/particle system. These are then used to solve for the subgroup fluxes used in deriving the shielded cross-sections.

Participant B has generated self-shielded cross sections using the APOLLO2 TR model, which is a generalisation of the statistical model and is available for the whole resonance-energy range [2]. In Phases 2 and 3, Participant B has calculated self-shielded cross-sections for all plutonium isotopes.

Participant F has calculated self-shielded cross sections using the CENTRM/PMC/CHOPS modules of the SCALE code system.

### ***2.1.2 Double heterogeneity***

Participant A's treatment of double heterogeneity for deriving neutron fluxes is the same as that described above for the derivation of the subgroup fluxes. Collision probabilities are solved using the macroscopic total cross-sections, for the heterogeneous fuel particle with an additional outer layer representing the associated amount of carbon support matrix material. A homogenised version of the particle is then considered and a homogenised total cross-section is derived which has the same escape probability as the heterogeneous particle. The homogenised total cross-section is then used in the central region of the pebble to allow collision probabilities to be derived for all the pebble regions. The pebble and particle collision probabilities are then combined to form a full set of collision probabilities for the complete pebble/particle system. These are then used to solve for the system fluxes.

The APOLLO2 double heterogeneity treatment used by Participant B is based on assumptions made by J.R. Askew. The main principle of Participant B's method is to apply the escape probability for a single absorbing particle. An assumption is made that there is an isotropic incident flux upon each particle. Slowing-down within the particles is neglected.

Participant F has treated double heterogeneity by first calculating the flux disadvantage factors for the grains and then using these factors to create the homogenised grain/matrix mixture cross-sections. The homogenised cross-sections are used on second pass to create the final resonance-shielded cross-sections that represent the fuel pebbles.

### ***2.1.3 Number of energy groups***

Participant A has used a 172-energy-group scheme for Phases 1, 2 and 5 of the calculations. For Phases 3 and 4, Participant A has used a 10-group energy scheme. The quoted Phase 3 and 4 results from Participant A have been corrected for the energy-group condensation effect of using a 10-group scheme as opposed to the 172-group library scheme. The energy-group boundaries for both the 172-group and 10-group schemes used by Participant A are given in Appendix B.

Participant B has performed calculations using the 172-energy-group scheme provided in Appendix B for all phases of the benchmark.

Participant F has used a 238-group scheme, a description of which is also given in Appendix B.

**Table 2.1. Inter-comparison of methods**

Participant	Calculation type	Code used	Data library used	Notes
Seroe Assurance	Deterministic	WIMS9 [3]	Development WIMS9 library based on JEF2.2 cross-section set.	Phases 1a and 2a employ a collision probability solution.
	Monte Carlo	MONK9 [4] BINGO based on JEF2.2 continuous data.		As there is no facility to perform a critical-buckling search in the MONK Monte Carlo code, critical bucklings must be determined from a series of scoping calculations. As it was not practical to perform numerous Monte Carlo calculations to find the exact critical buckling, the criterion was relaxed. A buckling that gave a value of $k_{\text{effective}}$ within $\pm 250$ pcm of unity was found and taken to be the critical buckling. All particles in every pebble were modelled in both cell and whole core calculations.
CEA	Deterministic	APOLLO2 [5]	CEA93.V6 [6] – based on JEF2.2.	The deterministic whole-core calculations (which employed a transport solution) did not include streaming effects.
	Monte Carlo	TRIPOLI4 [7]	JEF2.2 continuous data.	In the Monte Carlo whole-core calculations, the outer graphite shell of the pebbles was homogenised with the helium coolant to avoid streaming effects. This was done to enable comparisons to be made between the deterministic and Monte Carlo whole-core calculations. The TRIPOLI4 Monte Carlo models included an exact treatment to model the pebbles.
Hacettepe University U. Colak	Deterministic	None submitted	–	–
	Monte Carlo	MCNP-4B	ENDF-B/VI continuous data.	MCNP-4B does not provide a $S(\alpha,\beta)$ treatment for Graphite at a temperature of 1 000 K. Therefore, for the hot calculations, the graphite temperature has been assumed to be 800 K.
Hacettepe University M. Tombakoglu	Deterministic	None submitted	–	–
	Monte Carlo	MCNP-4B + BURN-HUNEM	ENDF/B-VI.2 and V.	A columnar hexagonal unit-cell model is used for Phases 1a, 2a and 3 to achieve a pebble packing fraction of 61%.
Hacettepe University M. Tombakoglu				A cubic unit-cell model is used for Phases 1b and 2b. This provides a pebble packing fraction of 51%.
				In all phases critical bucklings and migration areas are derived from extrapolated lengths, with the extrapolated lengths being calculated using MCNP surface tallies.
Nexia Solutions	Deterministic	VSCOP-99	Data based on ENDF/B-V and JEFF1 libraries.	
	Monte Carlo	None submitted	–	
ORNL	Deterministic	XSDRNPm within SCALE	Data based on ENDF/B-V libraries.	Cell calculations performed with white boundary conditions on the surface of a pebble.
	Monte Carlo	KENO V.a within SCALE	Data based on ENDF/B-V libraries.	XSDRNPm is a 1-D deterministic transport code using S8 quadrature. Cell calculations performed with reflective boundary conditions at the edge of a cube (which contains the pebble).



## *Chapter 3*

## **RESULTS**

The submitted results are given in Tables 3.1 to 3.28. Spectra plots are given in Figures 3.1 to 3.16.

For brevity, calculation results are specified as originating from Participants A, B, C, D, E or F. The letter code used for each of the participants is:

- A. J.G. Hosking and T.D. Newton, Serco Assurance, UK.
- B. O. Koberl, CEA, France.
- C. U. Colak, Nuclear Engineering Department, Hacettepe University, Turkey.
- D. M. Tombakoglu, Nuclear Engineering Department, Hacettepe University, Turkey.
- E. P. Morris, Nexia Solutions, UK (formerly BNFL R&T, UK).
- F. S. Goluoglu, Nuclear Science & Technology Division, ORNL, USA.

### **3.1 Phase 1**

#### ***3.1.1 Phase 1a: Reactivities and reaction rates***

Phase 1a considers a fuel pebble with a reflective boundary condition on the outer surface of the sphere. Results for Monte Carlo calculations are given in Table 3.1 and for deterministic calculations in Table 3.2.

Participant A's Monte Carlo result is for a sphere with an isotropic flux boundary condition at the outer surface, as there is no physical mechanism to model a reflective boundary condition for this type of artificial spherical outer boundary geometry. This explains the artificially high k-effective for Participant A. It is to be noted that, for Phase 1b (a reflected sphere in a box) Participant A's results using the Monte Carlo and deterministic treatments are in good agreement.

Participant C's calculations in Phase 1a were performed for a single fuel element surrounded by a spherical shell containing helium. The boundary condition for Participant C's Phase 1a calculation is not known.

Participant D has modelled a columnar hexagonal unit-cell model to achieve a pebble packing fraction of 61% in this phase of the benchmark. This avoids the difficulty in applying a reflective boundary condition on the surface of a sphere, however, it does not directly correspond to the reflected sphere benchmark.

**Table 3.1. Phase 1a results – Monte Carlo calculations**

Parameter	Units	A	B	C	D	E	F
$k_{inf}$ with zero buckling and at $T = 293.6 \text{ K}$	–	$1.5364 \pm 100 \text{ pcm}$			1.5108		
$B_{cr}^2$ at $T = 293.6 \text{ K}$	$\text{cm}^{-2}$				4.16E-04		
$k_{inf}(B_{cr}^2)$ at $T = 293.6 \text{ K}$	–				1.4455		
$M^2$ at $T = 293.6 \text{ K}$	$\text{cm}^2$				1056.6		
$k_{inf}$ with zero buckling and at $T = 1\,000 \text{ K}$	–	$1.4476 \pm 100 \text{ pcm}$					
$k_{eff}(B_{cr}^2)$ at $T = 1\,000 \text{ K}$ , using $B_{cr}^2$ at $T = 239.6 \text{ K}$	–				0.92366		
$B_{cr}^2$ at $T = 1\,000 \text{ K}$	$\text{cm}^2$				3.46E-04		
$k_{inf}(B_{cr}^2)$ at $T = 1\,000 \text{ K}$	–				1.3699		
$M^2$ at $T = 1\,000 \text{ K}$	$\text{cm}^2$				1032.9		
$\rho^{238}$	–				9.2657		
$\delta^{235}$	–				0.1349		
$\delta^{238}$	–				0.0043		
C	–				0.5212		

$\rho^{238} = {}^{238}\text{U}_{cap}(\text{epithermal})/{}^{238}\text{U}_{cap}(\text{thermal})$ : ratio of epithermal to thermal  ${}^{238}\text{U}$  captures.

$\delta^{235} = {}^{235}\text{U}_{fis}(\text{epithermal})/{}^{235}\text{U}_{fis}(\text{thermal})$ : ratio of epithermal to thermal  ${}^{235}\text{U}$  fissions.

$\delta^{238} = {}^{238}\text{U}_{fis}/{}^{235}\text{U}_{fis}$ : ratio of fissions in  ${}^{238}\text{U}$  to fissions in  ${}^{235}\text{U}$ .

C =  ${}^{238}\text{U}_{cap}/{}^{235}\text{U}_{fis}$ : ratio of captures in  ${}^{238}\text{U}$  to fissions in  ${}^{235}\text{U}$ .

**Table 3.2. Phase 1a results – deterministic calculations**

Parameter	Units	A	B	C	D	E	F
$k_{inf}$ with zero buckling and at $T = 293.6 \text{ K}$	–	1.51759	1.52232			1.50600	1.50748
$B_{cr}^2$ at $T = 293.6 \text{ K}$	$\text{cm}^{-2}$	4.408E-04	4.512E-4				4.130E-04
$k_{inf}(B_{cr}^2)$ at $T = 293.6 \text{ K}$	–	1.46064	1.46511				1.455
$M^2$ at $T = 293.6 \text{ K}$	$\text{cm}^2$	1045.0	1030.788				1101.6
$k_{inf}$ with zero buckling and at $T = 1\,000 \text{ K}$	–	1.42629				1.43126	1.40773
$k_{eff}(B_{cr}^2)$ at $T = 1\,000 \text{ K}$ , using $B_{cr}^2$ at $T = 239.6 \text{ K}$	–	0.90036	0.90130				0.89483
$B_{cr}^2$ at $T = 1\,000 \text{ K}$	$\text{cm}^2$	3.369E-04	3.455E-4				3.088E-04
$k_{inf}(B_{cr}^2)$ at $T = 1\,000 \text{ K}$	–	1.36483	1.37096				1.352
$M^2$ at $T = 1\,000 \text{ K}$	$\text{cm}^2$	1082.9	1073.6				1139.8
$\rho^{238}$	–	9.334387	9.198128				9.519364
$\delta^{235}$	–	0.132525	0.132625				0.129738
$\delta^{238}$	–	0.004091	0.004208				0.003992
C	–	0.528724	0.520845				0.535737

Participant A has used collision probabilities with a white outer boundary condition to model the sphere in the deterministic treatment. Participants B and E have also used a white boundary condition in these calculations.

Deterministic solutions for k-infinity at room temperature for Participants A and B are in very reasonable agreement (473 pcm) with the APOLLO2 result slightly higher, as has been observed in other benchmarks. The reaction rate ratios are also in reasonable agreement. Both participants have used JEF2.2 nuclear data.

Participants E and F also show close agreement between their results (148 pcm) at room temperature. Here both participants have used ENDF/B-V nuclear data.

The relatively large difference between the cell reactivities calculated by Participants E and F and those calculated by Participants A and B, about 1 320 pcm, is probably at least partly due to the different nuclear data set employed.

There is a noticeable, unexplained, difference between Participants E and F results at 1 000 K.

Participants A and B have used the following expressions to calculate  $k_{\text{inf}}(B^2_{\text{cr}})$  and the migration area:

$$k_{\text{inf}}(B^2_{\text{cr}}) = P/A$$

where P is the productions in the solution to which a critical buckling has been applied and A is the absorptions in the solution to which a critical buckling has been applied:

$$M^2 = (k_{\text{inf}}(B^2_{\text{cr}}) - 1)/B^2_{\text{cr}}.$$

Using these expressions, the migration area, buckling and  $k_{\text{inf}}(B^2_{\text{cr}})$  are consistent.

### **3.1.2 Phase 1b: Reactivities and reaction rates**

Participant A is not able to give Monte Carlo results for reaction rates in cases where there is an applied buckling. In these cases the MONK code solves the k-infinity calculation and reports reaction rates for k-infinity, not k-effective. In addition, a prediction of k-effective with the applied buckling is given.

The geometry in Participant C's Phase 1b model consists of a cubic array assembled from cubic unit cells. The critical size and buckling were evaluated by performing a series of calculations in order to ascertain the critical configuration.

The deterministic reaction rate ratios from Participant A for Phases 1a and 1b are very similar; the only major difference in the two benchmark phases is the outer boundary condition. Given the very similar deterministic results from Participants A and B for Phase 1a, it can be concluded that these two participants are in good agreement for Phase 1 of the benchmark.

The Monte Carlo and deterministic calculations from Participant A are in good agreement. For k-infinity at room temperature the difference is  $(1.5222 - 1.51785) 435$  pcm. At temperature, using the critical buckling at 293.6 K the difference is  $(0.9013 - 0.90040) 90$  pcm. This also suggests that the Monte Carlo and deterministic evaluations of the temperature coefficient are in good agreement.

**Table 3.3. Phase 1b results – Monte Carlo calculations**

Parameter	Units	A	B	C	D	E	F
$k_{\text{inf}}$ with zero buckling and at $T = 293.6 \text{ K}$	–	$1.5222 \pm 100 \text{ pcm}$		1.50697	1.5107		$1.50770 \pm 43 \text{ pcm}$
$B_{\text{cr}}^2$ at $T = 293.6 \text{ K}$	$\text{cm}^{-2}$	2.64E-04			2.56E-04		
$k_{\text{inf}}(B_{\text{cr}}^2)$ at $T = 293.6 \text{ K}$	–				1.4504		
$M^2$ at $T = 293.6 \text{ K}$	$\text{cm}^2$				1706.7		
$k_{\text{inf}}$ with zero buckling and at $T = 1\,000 \text{ K}$	–	$1.4329 \pm 100 \text{ pcm}$					$1.40889 \pm 47 \text{ pcm}$
$k_{\text{eff}}(B_{\text{cr}}^2)$ at $T = 1\,000 \text{ K}$ , using $B_{\text{cr}}^2$ at $T = 239.6 \text{ K}$	–	$0.9013 \pm 100 \text{ pcm}$			0.92372		
$B_{\text{cr}}^2$ at $T = 1\,000 \text{ K}$	$\text{cm}^2$	2.03E-4			2.05E-04		
$k_{\text{inf}}(B_{\text{cr}}^2)$ at $T = 1\,000 \text{ K}$	–				1.3702		
$M^2$ at $T = 1\,000 \text{ K}$	$\text{cm}^2$				1766.2		
$\rho^{238}$	–				9.1751		
$\delta^{235}$	–				0.1325		
$\delta^{238}$	–				0.0042		
C	–				0.5178		

**Table 3.4. Phase 1b results – deterministic calculations**

Parameter	Units	A	B	C	D	E	F
$k_{\text{inf}}$ with zero buckling and at $T = 293.6 \text{ K}$	–	1.51785					
$B_{\text{cr}}^2$ at $T = 293.6 \text{ K}$	$\text{cm}^{-2}$	3.245E-04					
$k_{\text{inf}}(B_{\text{cr}}^2)$ at $T = 293.6 \text{ K}$	–	1.48131					
$M^2$ at $T = 293.6 \text{ K}$	$\text{cm}^2$	1483.2					
$k_{\text{inf}}$ with zero buckling and at $T = 1\,000 \text{ K}$	–	1.42668					
$k_{\text{eff}}(B_{\text{cr}}^2)$ at $T = 1\,000 \text{ K}$ , using $B_{\text{cr}}^2$ at $T = 239.6 \text{ K}$	–	0.90040					
$B_{\text{cr}}^2$ at $T = 1\,000 \text{ K}$	$\text{cm}^2$	2.480E-04					
$k_{\text{inf}}(B_{\text{cr}}^2)$ at $T = 1\,000 \text{ K}$	–	1.38343					
$M^2$ at $T = 1\,000 \text{ K}$	$\text{cm}^2$	1546.1					
$\rho^{238}$	–	9.323949					
$\delta^{235}$	–	0.132374					
$\delta^{238}$	–	0.004086					
C	–	0.528246					

The k-infinity (at room temperature) from the Monte Carlo calculation of Participant D is about 1 150 pcm lower than that of Participant A and Participant F's is about 1 450 pcm lower. Participant A used JEF2.2 nuclear data while Participants D and F used ENDF/B-V data. Participant C's Monte Carlo estimate of k-infinity (at room temperature) is 1 523 pcm lower, ENDF/B-VI data was used. The reaction rate ratios, while being in reasonable agreement for Participants A and D, are significantly different for Participant C, suggesting large differences between ENDF/B-V and ENDF/B-VI data.

There is also a large difference between Participant F's Monte Carlo evaluation of the cell reactivity at 1 000 K and the equivalent reactivity from Participant A.

### **3.1.3 Spectra**

The spectrum for the Phase 1a Monte Carlo calculation submitted by Participant D is given in Figure 3.1. The form of this spectrum appears to be in reasonable agreement with the Phase 1 spectra from other participants (Figures 3.2 to 3.4).

Figure 3.2 shows the spectra for deterministic calculations for Phase 1a from Participants A, B and F.

Figure 3.3 compares the Phase 1b Monte Carlo spectra provided by Participants C and D. However, it is not stated as to which material or averaged materials Participant C's spectrum applies.

Figure 3.4 shows the deterministic solution spectra from Participant A for both Phases 1a and 1b averaged over the matrix and fuel particles. It illustrates that the spectra from the two benchmark phases are almost identical.

### **3.1.4 Burn-up**

Participant A's results from the burn-up calculation of Phase 1 (Tables 3.5, 3.9, 3.12 and 3.14) indicate that irradiation in a critical spectrum, as opposed to a case where no buckling is applied, increases  $^{238}\text{U}$  losses through capture and enhances the build-up of plutonium isotopes.

The results from Participant A for Phase 1a and Phase 1b are essentially identical.

For the majority of nuclides, the results from Participant A and B agree to within ~5%. However, there are significantly larger differences between their results for  $^{237}\text{Np}$ ,  $^{238}\text{Pu}$ ,  $^{234}\text{U}$  and  $^{237}\text{U}$  (although these nuclides are only present in trace quantities).

The  $^{239}\text{Pu}$  content at 80 GWd/Te from Participant E indicates a higher  $^{238}\text{U}$  capture cross-section in ENDF/B-V than JEF2.2, Participant A's calculation. The results are also consistent with a lower  $^{239}\text{Pu}$  capture cross-section in ENDF/B-V than JEF2.2.

**Table 3.5. Phase 1a – Monte Carlo calculations – results from Participant D – irradiation with a buckling included**

Units are  $\times 10^{24}$  atoms  $\text{cm}^{-3}$

Nuclide	0 MWd/te	10 000 MWd/te	20 000 MWd/te	30 000 MWd/te	40 000 MWd/te	50 000 MWd/te	60 000 MWd/te	70 000 MWd/te	80 000 MWd/te
<sup>241</sup> Am	0.00E+00	9.01E-09	1.03E-07	3.54E-07	7.61E-07	1.26E-06	1.79E-06	2.27E-06	2.64E-06
<sup>242m</sup> Am	0.00E+00	6.43E-11	1.17E-09	5.00E-09	1.21E-08	2.15E-08	3.17E-08	4.10E-08	4.80E-08
<sup>243</sup> Am	0.00E+00	8.01E-10	2.20E-08	1.34E-07	4.58E-07	1.10E-06	2.21E-06	3.86E-06	6.09E-06
<sup>242</sup> Cm	0.00E+00	4.41E-10	9.91E-09	5.05E-08	1.43E-07	2.92E-07	4.93E-07	7.30E-07	9.78E-07
<sup>243</sup> Cm	0.00E+00	7.24E-13	3.41E-11	2.80E-10	1.10E-09	2.93E-09	6.10E-09	1.08E-08	1.68E-08
<sup>244</sup> Cm	0.00E+00	1.51E-11	9.21E-10	9.16E-09	4.38E-08	1.43E-07	3.60E-07	7.72E-07	1.46E-06
<sup>245</sup> Cm	0.00E+00	6.64E-14	9.38E-12	1.35E-10	8.81E-10	3.42E-09	1.04E-08	2.57E-08	5.45E-08
<sup>237</sup> Np	0.00E+00	4.08E-07	1.59E-06	3.28E-06	5.55E-06	8.22E-06	1.11E-05	1.42E-05	1.73E-05
<sup>238</sup> Pu	0.00E+00	1.17E-08	9.76E-08	3.30E-07	7.83E-07	1.53E-06	2.63E-06	4.09E-06	5.93E-06
<sup>239</sup> Pu	0.00E+00	9.10E-05	1.45E-04	1.78E-04	1.98E-04	2.08E-04	2.09E-04	2.08E-04	2.04E-04
<sup>240</sup> Pu	0.00E+00	1.00E-05	2.85E-05	4.73E-05	6.37E-05	7.74E-05	8.74E-05	9.53E-05	1.01E-04
<sup>241</sup> Pu	0.00E+00	1.70E-06	9.74E-06	2.24E-05	3.68E-05	5.04E-05	6.24E-05	7.09E-05	7.68E-05
<sup>242</sup> Pu	0.00E+00	5.99E-08	7.30E-07	2.75E-06	6.54E-06	1.22E-05	1.97E-05	2.86E-05	3.88E-05
<sup>233</sup> U	0.00E+00	1.49E-13	8.73E-13	1.26E-12	1.87E-12	2.79E-12	4.13E-12	5.44E-12	6.96E-12
<sup>234</sup> U	0.00E+00	2.05E-09	3.83E-09	5.97E-09	8.94E-09	1.36E-08	2.09E-08	3.17E-08	4.73E-08
<sup>235</sup> U	1.93E-03	1.65E-03	1.42E-03	1.21E-03	1.03E-03	8.70E-04	7.26E-04	5.99E-04	4.87E-04
<sup>236</sup> U	0.00E+00	4.71E-05	8.69E-05	1.21E-04	1.51E-04	1.75E-04	1.97E-04	2.14E-04	2.29E-04
<sup>237</sup> U	0.00E+00	5.03E-08	1.00E-07	1.36E-07	1.85E-07	2.25E-07	2.60E-07	2.96E-07	3.22E-07
<sup>238</sup> U	2.13E-02	2.12E-02	2.10E-02	2.09E-02	2.08E-02	2.06E-02	2.05E-02	2.03E-02	2.01E-02

**Table 3.6. Phase 1a – deterministic calculations – results from Participant A – irradiation with a buckling included**

Units are  $\times 10^{24}$  atoms  $\text{cm}^{-3}$

Nuclide	0 MWd/te	10 000 MWd/te	20 000 MWd/te	30 000 MWd/te	40 000 MWd/te	50 000 MWd/te	60 000 MWd/te	70 000 MWd/te	80 000 MWd/te
<sup>241</sup> Am	1.0000E-19	1.0698E-08	1.1378E-07	3.8085E-07	8.0081E-07	1.3076E-06	1.8184E-06	2.2585E-06	2.5740E-06
<sup>242m</sup> Am	1.0000E-19	6.8437E-11	1.1400E-09	4.6793E-09	1.1030E-08	1.9305E-08	2.8030E-08	3.5735E-08	4.1310E-08
<sup>243</sup> Am	1.0000E-19	9.4636E-10	2.3366E-08	1.3683E-07	4.4932E-07	1.0791E-06	2.1319E-06	3.6873E-06	5.7942E-06
<sup>242</sup> Cm	1.0000E-19	6.6307E-10	1.3499E-08	6.5549E-08	1.7938E-07	3.6050E-07	5.9777E-07	8.6935E-07	1.1492E-06
<sup>243</sup> Cm	1.0000E-19	1.1398E-12	4.9366E-11	3.7924E-10	1.4504E-09	3.7987E-09	7.8427E-09	1.3747E-08	2.1371E-08
<sup>244</sup> Cm	1.0000E-19	1.9097E-11	1.0102E-09	9.4126E-09	4.3472E-08	1.3713E-07	3.4057E-07	7.1841E-07	1.3467E-06
<sup>245</sup> Cm	1.0000E-19	9.9221E-14	1.0739E-11	1.5171E-10	9.3609E-10	3.6688E-09	1.0782E-08	2.5950E-08	5.3883E-08
<sup>237</sup> Np	1.0000E-19	3.7784E-07	1.3792E-06	2.8115E-06	4.5399E-06	6.4493E-06	8.4671E-06	1.0529E-05	1.2575E-05
<sup>238</sup> Pu	1.0000E-19	1.2780E-08	9.8382E-08	3.2236E-07	7.5109E-07	1.4440E-06	2.4444E-06	3.7714E-06	5.4153E-06
<sup>239</sup> Pu	1.0000E-19	9.4500E-05	1.4725E-04	1.7653E-04	1.9198E-04	1.9871E-04	1.9959E-04	1.9632E-04	1.8997E-04
<sup>240</sup> Pu	1.0000E-19	1.1547E-05	3.2197E-05	5.2328E-05	6.9334E-05	8.2811E-05	9.3076E-05	1.0064E-04	1.0601E-04
<sup>241</sup> Pu	1.0000E-19	2.0356E-06	1.0809E-05	2.4506E-05	3.9761E-05	5.4046E-05	6.5891E-05	7.4635E-05	8.0148E-05
<sup>242</sup> Pu	1.0000E-19	7.4614E-08	8.5056E-07	3.1262E-06	7.3402E-06	1.3578E-05	2.1692E-05	3.1413E-05	4.2425E-05
<sup>233</sup> U	1.0000E-19	1.4148E-16	5.2408E-16	1.1199E-15	1.9675E-15	3.1927E-15	5.0167E-15	7.7460E-15	1.1740E-14
<sup>234</sup> U	1.0000E-19	2.0000E-09	3.8253E-09	5.8570E-09	8.6782E-09	1.3054E-08	1.9874E-08	3.0069E-08	4.4498E-08
<sup>235</sup> U	1.9259E-03	1.6584E-03	1.4321E-03	1.2341E-03	1.0585E-03	9.0208E-04	7.6245E-04	6.3787E-04	5.2695E-04
<sup>236</sup> U	1.0000E-19	4.6823E-05	8.6056E-05	1.1984E-04	1.4915E-04	1.7457E-04	1.9653E-04	2.1535E-04	2.3130E-04
<sup>237</sup> U	1.0000E-19	4.6237E-08	8.3292E-08	1.1473E-07	1.4045E-07	1.6334E-07	1.8424E-07	2.0352E-07	2.2146E-07
<sup>238</sup> U	2.1288E-02	2.1153E-02	2.1013E-02	2.0868E-02	2.0718E-02	2.0564E-02	2.0406E-02	2.0244E-02	2.0077E-02

**Table 3.7. Phase 1a – deterministic calculations – results from Participant B – irradiation with a buckling included**

Units are  $\times 10^{24}$  atoms  $\text{cm}^{-3}$

Nuclide	0 MWd/te	10 000 MWd/te	20 000 MWd/te	30 000 MWd/te	40 000 MWd/te	50 000 MWd/te	60 000 MWd/te	70 000 MWd/te	80 000 MWd/te
<sup>241</sup> Am	-	1.11E-08	1.17E-07	3.87E-07	8.04E-07	1.30E-06	1.79E-06	2.20E-06	2.49E-06
<sup>242m</sup> Am	-	0.00E+00							
<sup>243</sup> Am	-	1.04E-09	2.53E-08	1.47E-07	4.78E-07	1.14E-06	2.24E-06	3.85E-06	6.01E-06
<sup>242</sup> Cm	-	7.09E-10	1.42E-08	6.84E-08	1.85E-07	3.69E-07	6.07E-07	8.75E-07	1.15E-06
<sup>243</sup> Cm	-	1.24E-12	5.30E-11	4.02E-10	1.52E-09	3.95E-09	8.08E-09	1.40E-08	2.17E-08
<sup>244</sup> Cm	-	2.16E-11	1.12E-09	1.03E-08	4.71E-08	1.47E-07	3.63E-07	7.61E-07	1.42E-06
<sup>245</sup> Cm	-	1.17E-13	1.21E-11	1.68E-10	1.03E-09	3.98E-09	1.16E-08	2.76E-08	5.69E-08
<sup>237</sup> Np	-	4.25E-07	1.63E-06	3.46E-06	5.77E-06	8.44E-06	1.13E-05	1.43E-05	1.74E-05
<sup>238</sup> Pu	-	1.36E-08	1.12E-07	3.79E-07	9.01E-07	1.76E-06	3.00E-06	4.66E-06	6.72E-06
<sup>239</sup> Pu	-	9.34E-05	1.45E-04	1.72E-04	1.86E-04	1.92E-04	1.92E-04	1.89E-04	1.82E-04
<sup>240</sup> Pu	-	1.18E-05	3.25E-05	5.24E-05	6.91E-05	8.22E-05	9.20E-05	9.92E-05	1.04E-04
<sup>241</sup> Pu	-	2.11E-06	1.11E-05	2.49E-05	3.99E-05	5.38E-05	6.51E-05	7.32E-05	7.81E-05
<sup>242</sup> Pu	-	8.00E-08	9.02E-07	3.28E-06	7.65E-06	1.41E-05	2.23E-05	3.21E-05	4.32E-05
<sup>233</sup> U	-	0.00E+00							
<sup>234</sup> U	-	2.18E-09	4.20E-09	6.49E-09	9.76E-09	1.50E-08	2.32E-08	3.57E-08	5.34E-08
<sup>235</sup> U	1.93E-03	1.65E-03	1.42E-03	1.22E-03	1.05E-03	8.88E-04	7.48E-04	6.24E-04	5.13E-04
<sup>236</sup> U	-	4.77E-05	8.73E-05	1.21E-04	1.50E-04	1.74E-04	1.95E-04	2.13E-04	2.27E-04
<sup>237</sup> U	-	5.34E-08	1.03E-07	1.48E-07	1.90E-07	2.27E-07	2.61E-07	2.92E-07	3.20E-07
<sup>238</sup> U	2.13E-02	2.12E-02	2.10E-02	2.09E-02	2.07E-02	2.06E-02	2.04E-02	2.03E-02	2.01E-02

**Table 3.8. Phase 1a – Monte Carlo calculations – results from Participant D – irradiation with a buckling included**

Units are  $\times 10^{24}$  atoms  $\text{cm}^{-3}$

Nuclide	0 MWd/te	10 000 MWd/te	20 000 MWd/te	30 000 MWd/te	40 000 MWd/te	50 000 MWd/te	60 000 MWd/te	70 000 MWd/te	80 000 MWd/te
$^{241}\text{Am}$	0.00E+00	9.01E-09	1.04E-07	3.66E-07	8.01E-07	1.35E-06	1.96E-06	2.53E-06	3.05E-06
$^{242m}\text{Am}$	0.00E+00	6.43E-11	1.18E-09	5.17E-09	1.27E-08	2.32E-08	3.52E-08	4.76E-08	5.81E-08
$^{243}\text{Am}$	0.00E+00	8.01E-10	2.30E-08	1.39E-07	4.80E-07	1.18E-06	2.39E-06	4.23E-06	6.65E-06
$^{242}\text{Cm}$	0.00E+00	4.41E-10	9.96E-09	5.15E-08	1.47E-07	3.02E-07	5.10E-07	7.62E-07	1.03E-06
$^{243}\text{Cm}$	0.00E+00	7.24E-13	3.50E-11	2.81E-10	1.15E-09	3.15E-09	6.62E-09	1.17E-08	1.85E-08
$^{244}\text{Cm}$	0.00E+00	1.51E-11	9.73E-10	9.32E-09	4.75E-08	1.59E-07	4.03E-07	8.80E-07	1.67E-06
$^{245}\text{Cm}$	0.00E+00	6.64E-14	9.91E-12	1.43E-10	9.80E-10	4.38E-09	1.31E-08	3.37E-08	6.92E-08
$^{237}\text{Np}$	0.00E+00	4.08E-07	1.69E-06	3.63E-06	5.96E-06	8.78E-06	1.19E-05	1.56E-05	1.87E-05
$^{238}\text{Pu}$	0.00E+00	1.17E-08	1.03E-07	3.54E-07	8.50E-07	1.66E-06	2.84E-06	4.46E-06	6.50E-06
$^{239}\text{Pu}$	0.00E+00	9.10E-05	1.51E-04	1.82E-04	2.08E-04	2.30E-04	2.36E-04	2.41E-04	2.45E-04
$^{240}\text{Pu}$	0.00E+00	1.00E-05	2.89E-05	4.77E-05	6.33E-05	7.66E-05	8.88E-05	9.63E-05	1.03E-04
$^{241}\text{Pu}$	0.00E+00	1.70E-06	9.86E-06	2.34E-05	3.90E-05	5.43E-05	6.72E-05	7.95E-05	8.78E-05
$^{242}\text{Pu}$	0.00E+00	5.99E-08	7.29E-07	2.81E-06	6.70E-06	1.24E-05	1.98E-05	2.85E-05	3.85E-05
$^{233}\text{U}$	0.00E+00	1.49E-13	1.70E-12	3.02E-12	3.53E-12	5.73E-12	6.80E-12	1.15E-11	1.32E-11
$^{234}\text{U}$	0.00E+00	2.05E-09	4.23E-09	6.58E-09	9.96E-09	1.52E-08	2.31E-08	3.52E-08	5.24E-08
$^{235}\text{U}$	1.93E-03	1.65E-03	1.42E-03	1.21E-03	1.04E-03	8.79E-04	7.42E-04	6.21E-04	5.16E-04
$^{236}\text{U}$	0.00E+00	4.71E-05	8.68E-05	1.20E-04	1.50E-04	1.74E-04	1.95E-04	2.11E-04	2.25E-04
$^{237}\text{U}$	0.00E+00	5.03E-08	1.08E-07	1.55E-07	1.90E-07	2.38E-07	2.81E-07	3.33E-07	3.34E-07
$^{238}\text{U}$	2.13E-02	2.12E-02	2.10E-02	2.09E-02	2.07E-02	2.06E-02	2.04E-02	2.02E-02	2.00E-02

**Table 3.9. Phase 1a – deterministic calculations – results from Participant A – irradiation with no buckling included**

Units are  $\times 10^{24}$  atoms  $\text{cm}^{-3}$

Nuclide	0 MWd/te	10 000 MWd/te	20 000 MWd/te	30 000 MWd/te	40 000 MWd/te	50 000 MWd/te	60 000 MWd/te	70 000 MWd/te	80 000 MWd/te
<sup>241</sup> Am	1.0000E-19	8.9324E-09	9.7320E-08	3.3087E-07	7.0257E-07	1.1538E-06	1.6096E-06	2.0036E-06	2.2902E-06
<sup>242m</sup> Am	1.0000E-19	5.6583E-11	9.6480E-10	4.0179E-09	9.5569E-09	1.6820E-08	2.4510E-08	3.1351E-08	3.6416E-08
<sup>243</sup> Am	1.0000E-19	7.3494E-10	1.9121E-08	1.1672E-07	3.9643E-07	9.7895E-07	1.9792E-06	3.4903E-06	5.5752E-06
<sup>242</sup> Cm	1.0000E-19	5.5376E-10	1.1678E-08	5.8185E-08	1.6227E-07	3.3057E-07	5.5326E-07	8.0946E-07	1.0738E-06
<sup>243</sup> Cm	1.0000E-19	8.7861E-13	3.9993E-11	3.1959E-10	1.2615E-09	3.3882E-09	7.1352E-09	1.2702E-08	1.9982E-08
<sup>244</sup> Cm	1.0000E-19	1.3625E-11	7.6810E-10	7.5433E-09	3.6425E-08	1.1936E-07	3.0640E-07	6.6530E-07	1.2794E-06
<sup>245</sup> Cm	1.0000E-19	6.3452E-14	7.4094E-12	1.1162E-10	7.2792E-10	2.9941E-09	9.1853E-09	2.2987E-08	4.9511E-08
<sup>237</sup> Np	1.0000E-19	3.3204E-07	1.2423E-06	2.5822E-06	4.2378E-06	6.1042E-06	8.1111E-06	1.0194E-05	1.2293E-05
<sup>238</sup> Pu	1.0000E-19	1.0816E-08	8.5968E-08	2.8871E-07	6.8625E-07	1.3409E-06	2.2999E-06	3.5867E-06	5.1960E-06
<sup>239</sup> Pu	1.0000E-19	8.3734E-05	1.3124E-04	1.5830E-04	1.7338E-04	1.8097E-04	1.8362E-04	1.8286E-04	1.7965E-04
<sup>240</sup> Pu	1.0000E-19	1.0531E-05	3.0007E-05	4.9456E-05	6.6143E-05	7.9507E-05	8.9765E-05	9.7379E-05	1.0283E-04
<sup>241</sup> Pu	1.0000E-19	1.7137E-06	9.3778E-06	2.1713E-05	3.5767E-05	4.9174E-05	6.0518E-05	6.9165E-05	7.5016E-05
<sup>242</sup> Pu	1.0000E-19	6.3895E-08	7.5672E-07	2.8596E-06	6.8549E-06	1.2879E-05	2.0816E-05	3.0404E-05	4.1311E-05
<sup>233</sup> U	1.0000E-19	8.8739E-17	3.4425E-16	7.7086E-16	1.4209E-15	2.4229E-15	4.0017E-15	6.4838E-15	1.0281E-14
<sup>234</sup> U	1.0000E-19	1.5874E-09	3.1092E-09	4.8841E-09	7.4351E-09	1.1480E-08	1.7879E-08	2.7545E-08	4.1338E-08
<sup>235</sup> U	1.9259E-03	1.6564E-03	1.4252E-03	1.2213E-03	1.0400E-03	8.7869E-04	7.3538E-04	6.0855E-04	4.9699E-04
<sup>236</sup> U	1.0000E-19	4.6321E-05	8.5768E-05	1.2007E-04	1.4997E-04	1.7593E-04	1.9826E-04	2.1723E-04	2.3308E-04
<sup>237</sup> U	1.0000E-19	4.1166E-08	7.65553E-08	1.0821E-07	1.3533E-07	1.6036E-07	1.8392E-07	2.0623E-07	2.2751E-07
<sup>238</sup> U	2.1288E-02	2.1168E-02	2.1040E-02	2.0904E-02	2.0762E-02	2.0613E-02	2.0457E-02	2.0294E-02	2.0125E-02

**Table 3.10. Phase 1a – deterministic calculations – results from Participant E – irradiation with no buckling included**

Units are  $\times 10^{24}$  atoms  $\text{cm}^{-3}$

Nuclide	0 MWd/te	10 000 MWd/te	20 000 MWd/te	30 000 MWd/te	40 000 MWd/te	50 000 MWd/te	60 000 MWd/te	70 000 MWd/te	80 000 MWd/te
<sup>241</sup> Am	0.0000E+00	4.25E-09	5.53E-08	2.17E-07	5.21E-07	9.50E-07	1.46E-06	1.96E-06	2.44E-06
<sup>242m</sup> Am	0.0000E+00	2.59E-11	5.48E-10	2.66E-09	7.21E-09	1.41E-08	2.27E-08	3.13E-08	3.93E-08
<sup>243</sup> Am	0.0000E+00	2.66E-10	8.37E-09	5.78E-08	2.17E-07	5.87E-07	1.28E-06	2.42E-06	4.12E-06
<sup>242</sup> Cm	0.0000E+00	1.37E-10	3.53E-09	2.06E-08	6.55E-08	1.50E-07	2.78E-07	4.48E-07	6.46E-07
<sup>243</sup> Cm	0.0000E+00	2.59E-13	1.44E-11	1.32E-10	5.87E-10	1.75E-09	4.02E-09	7.76E-09	1.31E-08
<sup>244</sup> Cm	0.0000E+00	4.38E-12	3.02E-10	3.34E-09	1.79E-08	6.44E-08	1.80E-07	4.21E-07	8.69E-07
<sup>245</sup> Cm	0.0000E+00	0.000E+00							
<sup>237</sup> Np	0.0000E+00	3.47E-07	1.44E-06	3.19E-06	5.53E-06	8.33E-06	1.15E-05	1.49E-05	1.85E-05
<sup>238</sup> Pu	0.0000E+00	8.35E-09	7.46E-08	2.63E-07	6.38E-07	1.27E-06	2.21E-06	3.47E-06	5.10E-06
<sup>239</sup> Pu	0.0000E+00	8.84E-05	1.54E-04	2.00E-04	2.30E-04	2.47E-04	2.59E-04	2.64E-04	2.64E-04
<sup>240</sup> Pu	0.0000E+00	5.84E-06	1.89E-05	3.42E-05	4.89E-05	6.21E-05	7.31E-05	8.20E-05	8.88E-05
<sup>241</sup> Pu	0.0000E+00	8.08E-07	5.29E-06	1.38E-05	2.49E-05	3.70E-05	4.85E-05	5.82E-05	6.57E-05
<sup>242</sup> Pu	0.0000E+00	2.19E-08	3.10E-07	1.33E-06	3.51E-06	7.20E-06	1.24E-05	1.93E-05	2.74E-05
<sup>233</sup> U	0.0000E+00	9.46E-13	1.86E-12	2.78E-12	3.78E-12	4.85E-12	6.04E-12	7.29E-12	8.56E-12
<sup>234</sup> U	0.0000E+00	1.73E-05	1.64E-05	1.55E-05	1.46E-05	1.37E-05	1.28E-05	1.20E-05	1.11E-05
<sup>235</sup> U	1.9259E-03	1.65E-03	1.40E-03	1.17E-03	9.76E-04	7.99E-04	6.44E-04	5.08E-04	3.93E-04
<sup>236</sup> U	0.0000E+00	4.76E-05	8.95E-05	1.26E-04	1.58E-04	1.85E-04	2.08E-04	2.25E-04	2.40E-04
<sup>237</sup> U	0.0000E+00	4.42E-08	9.35E-08	1.41E-07	1.88E-07	2.34E-07	2.80E-07	3.21E-07	3.59E-07
<sup>238</sup> U	2.1288E-02	2.12E-02	2.10E-02	2.08E-02	2.06E-02	2.04E-02	2.04E-02	2.02E-02	2.02E-02

**Table 3.11. Phase 1b – Monte Carlo calculations – results from Participant D – irradiation with a buckling included**

Units are  $\times 10^{24}$  atoms  $\text{cm}^{-3}$

Nuclide	0 MWd/te	10 000 MWd/te	20 000 MWd/te	30 000 MWd/te	40 000 MWd/te	50 000 MWd/te	60 000 MWd/te	70 000 MWd/te	80 000 MWd/te
<sup>241</sup> Am	0.00E+00	9.10E-09	1.03E-07	7.77E-07	1.30E-06	1.83E-06	2.29E-06	2.64E-06	2.85E-06
<sup>242m</sup> Am	0.00E+00	6.50E-11	1.17E-09	1.22E-08	2.21E-08	3.23E-08	4.15E-08	4.81E-08	5.22E-08
<sup>243</sup> Am	0.00E+00	8.36E-10	2.22E-08	4.55E-07	1.13E-06	2.27E-06	3.97E-06	6.25E-06	9.12E-06
<sup>242</sup> Cm	0.00E+00	4.46E-10	9.88E-09	1.44E-07	2.98E-07	5.04E-07	7.41E-07	9.85E-07	1.22E-06
<sup>243</sup> Cm	0.00E+00	7.19E-13	3.46E-11	1.11E-09	2.97E-09	6.19E-09	1.09E-08	1.69E-08	2.39E-08
<sup>244</sup> Cm	0.00E+00	1.57E-11	9.29E-10	4.40E-08	1.44E-07	3.65E-07	7.83E-07	1.49E-06	2.59E-06
<sup>245</sup> Cm	0.00E+00	7.24E-14	9.01E-12	8.73E-10	3.55E-09	1.07E-08	2.62E-08	5.48E-08	1.03E-07
<sup>237</sup> Np	0.00E+00	3.95E-07	1.56E-06	5.60E-06	8.34E-06	1.12E-05	1.43E-05	1.73E-05	2.04E-05
<sup>238</sup> Pu	0.00E+00	1.12E-08	9.54E-08	7.85E-07	1.55E-06	2.65E-06	4.13E-06	5.96E-06	8.13E-06
<sup>239</sup> Pu	0.00E+00	9.09E-05	1.47E-04	1.97E-04	2.07E-04	2.09E-04	2.09E-04	2.04E-04	1.99E-04
<sup>240</sup> Pu	0.00E+00	1.00E-05	2.85E-05	6.22E-05	7.46E-05	8.56E-05	9.44E-05	1.01E-04	1.06E-04
<sup>241</sup> Pu	0.00E+00	1.71E-06	9.71E-06	3.80E-05	5.19E-05	6.24E-05	7.04E-05	7.62E-05	7.92E-05
<sup>242</sup> Pu	0.00E+00	6.05E-08	7.28E-07	6.64E-06	1.24E-05	2.00E-05	2.88E-05	3.88E-05	4.96E-05
<sup>233</sup> U	0.00E+00	1.22E-12	2.20E-12	3.52E-12	5.21E-12	6.16E-12	6.95E-12	8.62E-12	9.39E-12
<sup>234</sup> U	0.00E+00	2.01E-09	4.02E-09	8.99E-09	1.38E-08	2.10E-08	3.20E-08	4.76E-08	6.85E-08
<sup>235</sup> U	1.93E-03	1.65E-03	1.42E-03	1.03E-03	8.71E-04	7.27E-04	6.00E-04	4.88E-04	3.90E-04
<sup>236</sup> U	0.00E+00	4.71E-05	8.69E-05	1.51E-04	1.75E-04	1.97E-04	2.14E-04	2.28E-04	2.39E-04
<sup>237</sup> U	0.00E+00	4.87E-08	9.84E-08	1.85E-07	2.31E-07	2.55E-07	2.94E-07	3.23E-07	3.53E-07
<sup>238</sup> U	2.13E-02	2.12E-02	2.10E-02	2.08E-02	2.06E-02	2.05E-02	2.03E-02	2.01E-02	2.00E-02

**Table 3.12. Phase 1b – deterministic calculations – results from Participant A – irradiation with a buckling included**

Units are  $\times 10^{24}$  atoms  $\text{cm}^{-3}$

Nuclide	0 MWd/te	10 000 MWd/te	20 000 MWd/te	30 000 MWd/te	40 000 MWd/te	50 000 MWd/te	60 000 MWd/te	70 000 MWd/te	80 000 MWd/te
$^{241}\text{Am}$	1.0000E-19	1.0700E-08	1.1381E-07	3.8098E-07	8.0114E-07	1.3083E-06	1.8194E-06	2.2599E-06	2.5760E-06
$^{242m}\text{Am}$	1.0000E-19	6.8449E-11	1.1403E-09	4.6808E-09	1.1034E-08	1.9314E-08	2.8046E-08	3.5760E-08	4.1344E-08
$^{243}\text{Am}$	1.0000E-19	9.4648E-10	2.3369E-08	1.3685E-07	4.4939E-07	1.0793E-06	2.1323E-06	3.6879E-06	5.7950E-06
$^{242}\text{Cm}$	1.0000E-19	6.6317E-10	1.3501E-08	6.5562E-08	1.7942E-07	3.6059E-07	5.9792E-07	8.6960E-07	1.1496E-06
$^{243}\text{Cm}$	1.0000E-19	1.1400E-12	4.9376E-11	3.7932E-10	1.4507E-09	3.7996E-09	7.8445E-09	1.3751E-08	2.1377E-08
$^{244}\text{Cm}$	1.0000E-19	1.9099E-11	1.0103E-09	9.4138E-09	4.3477E-08	1.3714E-07	3.4061E-07	7.1848E-07	1.3468E-06
$^{245}\text{Cm}$	1.0000E-19	9.9236E-14	1.0741E-11	1.5174E-10	9.3629E-10	3.6697E-09	1.0785E-08	2.5957E-08	5.3899E-08
$^{237}\text{Np}$	1.0000E-19	3.7785E-07	1.3793E-06	2.8116E-06	4.5402E-06	6.4498E-06	8.4677E-06	1.0530E-05	1.2576E-05
$^{238}\text{Pu}$	1.0000E-19	1.2780E-08	9.8381E-08	3.2236E-07	7.5109E-07	1.4440E-06	2.4444E-06	3.7715E-06	5.4155E-06
$^{239}\text{Pu}$	1.0000E-19	9.4526E-05	1.4730E-04	1.7659E-04	1.9206E-04	1.9880E-04	1.9969E-04	1.9644E-04	1.9009E-04
$^{240}\text{Pu}$	1.0000E-19	1.1550E-05	3.2220E-05	5.2335E-05	6.9339E-05	8.2813E-05	9.3075E-05	1.0064E-04	1.0601E-04
$^{241}\text{Pu}$	1.0000E-19	2.0361E-06	1.0812E-05	2.4514E-05	3.9777E-05	5.4070E-05	6.5922E-05	7.4674E-05	8.0194E-05
$^{242}\text{Pu}$	1.0000E-19	7.4627E-08	8.5072E-07	3.1268E-06	7.3416E-06	1.3580E-05	2.1696E-05	3.1418E-05	4.2431E-05
$^{233}\text{U}$	1.0000E-19	1.4127E-16	5.2334E-16	1.1184E-15	1.9652E-15	3.1896E-15	5.0127E-15	7.7411E-15	1.1735E-14
$^{234}\text{U}$	1.0000E-19	1.9985E-09	3.8227E-09	5.8536E-09	8.6743E-09	1.3050E-08	1.9870E-08	3.0065E-08	4.4495E-08
$^{235}\text{U}$	1.9259E-03	1.6584E-03	1.4322E-03	1.2341E-03	1.0586E-03	9.0215E-04	7.6255E-04	6.3799E-04	5.2709E-04
$^{236}\text{U}$	1.0000E-19	4.6824E-05	8.6056E-05	1.1984E-04	1.4914E-04	1.7456E-04	1.9652E-04	2.1534E-04	2.3129E-04
$^{237}\text{U}$	1.0000E-19	4.6239E-08	8.3296E-08	1.1474E-07	1.4046E-07	1.6334E-07	1.8425E-07	2.0353E-07	2.2146E-07
$^{238}\text{U}$	2.1288E-02	2.1153E-02	2.1013E-02	2.0868E-02	2.0718E-02	2.0564E-02	2.0406E-02	2.0243E-02	2.0077E-02

**Table 3.13. Phase 1b – Monte Carlo calculations – results from Participant D – irradiation with no buckling included**

Units are  $\times 10^{24}$  atoms  $\text{cm}^{-3}$

Nuclide	0 MWd/te	10 000 MWd/te	20 000 MWd/te	30 000 MWd/te	40 000 MWd/te	50 000 MWd/te	60 000 MWd/te	70 000 MWd/te	80 000 MWd/te
$^{241}\text{Am}$	0.00E+00	9.10E-09	9.96E-08	3.49E-07	7.67E-07	1.30E-06	1.89E-06	2.47E-06	2.96E-06
$^{242m}\text{Am}$	0.00E+00	6.50E-11	1.12E-09	4.93E-09	1.22E-08	2.23E-08	3.40E-08	4.58E-08	5.63E-08
$^{243}\text{Am}$	0.00E+00	8.36E-10	2.10E-08	1.35E-07	4.69E-07	1.17E-06	2.32E-06	4.13E-06	6.53E-06
$^{242}\text{Cm}$	0.00E+00	4.46E-10	9.64E-09	4.96E-08	1.42E-07	2.93E-07	4.98E-07	7.45E-07	1.01E-06
$^{243}\text{Cm}$	0.00E+00	7.19E-13	3.24E-11	2.79E-10	1.13E-09	3.06E-09	6.39E-09	1.14E-08	1.81E-08
$^{244}\text{Cm}$	0.00E+00	1.57E-11	8.35E-10	9.23E-09	4.61E-08	1.55E-07	3.96E-07	8.57E-07	1.63E-06
$^{245}\text{Cm}$	0.00E+00	7.24E-14	7.66E-12	1.40E-10	9.73E-10	4.07E-09	1.30E-08	3.21E-08	6.98E-08
$^{237}\text{Np}$	0.00E+00	3.95E-07	1.50E-06	3.37E-06	5.84E-06	8.69E-06	1.18E-05	1.52E-05	1.86E-05
$^{238}\text{Pu}$	0.00E+00	1.12E-08	8.99E-08	3.24E-07	8.05E-07	1.60E-06	2.78E-06	4.37E-06	6.36E-06
$^{239}\text{Pu}$	0.00E+00	9.09E-05	1.39E-04	1.79E-04	2.06E-04	2.22E-04	2.33E-04	2.39E-04	2.41E-04
$^{240}\text{Pu}$	0.00E+00	1.00E-05	2.83E-05	4.62E-05	6.25E-05	7.64E-05	8.69E-05	9.48E-05	1.02E-04
$^{241}\text{Pu}$	0.00E+00	1.71E-06	9.34E-06	2.24E-05	3.77E-05	5.26E-05	6.65E-05	7.80E-05	8.64E-05
$^{242}\text{Pu}$	0.00E+00	6.05E-08	7.18E-07	2.72E-06	6.51E-06	1.21E-05	1.96E-05	2.83E-05	3.83E-05
$^{233}\text{U}$	0.00E+00	1.22E-12	2.18E-12	3.22E-12	3.63E-12	5.17E-12	7.47E-12	8.11E-12	9.65E-12
$^{234}\text{U}$	0.00E+00	2.01E-09	3.77E-09	6.06E-09	9.19E-09	1.41E-08	2.19E-08	3.37E-08	5.04E-08
$^{235}\text{U}$	1.93E-03	1.65E-03	1.42E-03	1.21E-03	1.03E-03	8.72E-04	7.33E-04	6.12E-04	5.07E-04
$^{236}\text{U}$	0.00E+00	4.71E-05	8.66E-05	1.21E-04	1.51E-04	1.75E-04	1.96E-04	2.13E-04	2.26E-04
$^{237}\text{U}$	0.00E+00	4.87E-08	9.29E-08	1.51E-07	2.00E-07	2.39E-07	2.80E-07	3.11E-07	3.51E-07
$^{238}\text{U}$	2.13E-02	2.12E-02	2.11E-02	2.09E-02	2.08E-02	2.06E-02	2.04E-02	2.02E-02	2.01E-02

**Table 3.14. Phase 1b – deterministic calculations – results from Participant A – irradiation with no buckling included**

Units are  $\times 10^{24}$  atoms  $\text{cm}^{-3}$

Nuclide	0 MWd/te	10 000 MWd/te	20 000 MWd/te	30 000 MWd/te	40 000 MWd/te	50 000 MWd/te	60 000 MWd/te	70 000 MWd/te	80 000 MWd/te
<sup>241</sup> Am	1.0000E-19	8.9348E-09	9.7354E-08	3.3101E-07	7.0290E-07	1.1544E-06	1.6106E-06	2.0050E-06	2.2920E-06
<sup>242m</sup> Am	1.0000E-19	5.6597E-11	9.6509E-10	4.0194E-09	9.5612E-09	1.6829E-08	2.4526E-08	3.1374E-08	3.6447E-08
<sup>243</sup> Am	1.0000E-19	7.3507E-10	1.9125E-08	1.1675E-07	3.9653E-07	9.7919E-07	1.9797E-06	3.4911E-06	5.5763E-06
<sup>242</sup> Cm	1.0000E-19	5.5388E-10	1.1681E-08	5.8201E-08	1.6231E-07	3.3066E-07	5.5342E-07	8.0971E-07	1.0742E-06
<sup>243</sup> Cm	1.0000E-19	8.7883E-13	4.0004E-11	3.1968E-10	1.2619E-09	3.3892E-09	7.1373E-09	1.2706E-08	1.9988E-08
<sup>244</sup> Cm	1.0000E-19	1.3627E-11	7.6826E-10	7.5450E-09	3.6433E-08	1.1939E-07	3.0647E-07	6.6542E-07	1.2795E-06
<sup>245</sup> Cm	1.0000E-19	6.3467E-14	7.4115E-12	1.1165E-10	7.2817E-10	2.9952E-09	9.1886E-09	2.2995E-08	4.9529E-08
<sup>237</sup> Np	1.0000E-19	3.3222E-07	1.2429E-06	2.5832E-06	4.2395E-06	6.1063E-06	8.1136E-06	1.0197E-05	1.2296E-05
<sup>238</sup> Pu	1.0000E-19	1.0821E-08	8.6005E-08	2.8882E-07	6.8648E-07	1.3413E-06	2.3005E-06	3.5875E-06	5.1972E-06
<sup>239</sup> Pu	1.0000E-19	8.3756E-05	1.3128E-04	1.5836E-04	1.7345E-04	1.8106E-04	1.8372E-04	1.8296E-04	1.7977E-04
<sup>240</sup> Pu	1.0000E-19	1.0533E-05	3.0012E-05	4.9461E-05	6.6146E-05	7.9507E-05	8.9762E-05	9.7373E-05	1.0283E-04
<sup>241</sup> Pu	1.0000E-19	1.7142E-06	9.3812E-06	2.1722E-05	3.5783E-05	4.9197E-05	6.0548E-05	6.9202E-05	7.5060E-05
<sup>242</sup> Pu	1.0000E-19	6.3910E-08	7.5691E-07	2.8603E-06	6.8567E-06	1.2882E-05	2.0821E-05	3.0410E-05	4.1317E-05
<sup>233</sup> U	1.0000E-19	8.8685E-17	3.4406E-16	7.7046E-16	1.4203E-15	2.4221E-15	4.0007E-15	6.4827E-15	1.0280E-14
<sup>234</sup> U	1.0000E-19	1.5869E-09	3.1084E-09	4.8832E-09	7.4345E-09	1.1480E-08	1.7881E-08	2.7549E-08	4.1346E-08
<sup>235</sup> U	1.9259E-03	1.6564E-03	1.4252E-03	1.2213E-03	1.0401E-03	8.7876E-04	7.3548E-04	6.0868E-04	4.9713E-04
<sup>236</sup> U	1.0000E-19	4.6321E-05	8.5767E-05	1.2007E-04	1.4997E-04	1.7592E-04	1.9825E-04	2.1722E-04	2.3306E-04
<sup>237</sup> U	1.0000E-19	4.1187E-08	7.65586E-08	1.0824E-07	1.3538E-07	1.6040E-07	1.8395E-07	2.0625E-07	2.2752E-07
<sup>238</sup> U	2.1288E-02	2.1168E-02	2.1040E-02	2.0904E-02	2.0762E-02	2.0612E-02	2.0456E-02	2.0294E-02	2.0125E-02

## 3.2 Phase 2

### 3.2.1 Phase 2a: Reactivities and reaction rates

Again, Participant A's k-infinity is too high due to the physical inability to model a reflective boundary condition on the surface of a sphere in Monte Carlo calculations.

**Table 3.15. Phase 2a results – Monte Carlo calculations**

Parameter	Units	A	B	C	D	E	F
$k_{\text{inf}}$ with zero buckling and at $T = 293.6 \text{ K}$	–	$1.4805 \pm 100 \text{ pcm}$			1.4573		
$B_{\text{cr}}^2$ at $T = 293.6 \text{ K}$	$\text{cm}^{-2}$				4.50E-04		
$k_{\text{inf}}(B_{\text{cr}}^2)$ at $T = 293.6 \text{ K}$	–				1.4334		
$M^2$ at $T = 293.6 \text{ K}$	$\text{cm}^2$				951.1		
$k_{\text{inf}}$ with zero buckling and at $T = 1\,000 \text{ K}$	–	$1.4068 \pm 100 \text{ pcm}$					
$k_{\text{eff}}(B_{\text{cr}}^2)$ at $T = 1\,000 \text{ K}$ , using $B_{\text{cr}}^2$ at $T = 239.6 \text{ K}$	–				0.97322		
$B_{\text{cr}}^2$ at $T = 1\,000 \text{ K}$	$\text{cm}^{-2}$				4.16E-04		
$k_{\text{inf}}(B_{\text{cr}}^2)$ at $T = 1\,000 \text{ K}$	–				1.3886		
$M^2$ at $T = 1\,000 \text{ K}$	$\text{cm}^2$				925.3		
Reactivity at a pebble irradiation of $1\,500 \text{ MWd/te}$	–				0.9810		
$^{135}\text{Xe}$ number density at a pebble irradiation of $1\,500 \text{ MWd/te}$	$\times 10^{24} \text{ atoms cm}^{-3}$						
$^{135}\text{Xe}$ absorption cross-section at a pebble irradiation of $1\,500 \text{ MWd/te}$	barns						
$\rho^{239}$	–				0.1525		
$\delta^{239}$	–				0.1461		
$\delta^{241}$	–				0.3616		
$F^{241}$	–				0.2475		
$C^8$	–				0.0121		
$C^9$	–				0.5934		
$C^0$	–				0.5698		
$C^1$	–				0.0832		
$C^2$	–				0.0565		

$\rho^{239} = {}^{239}\text{Pu}_{\text{cap}}(\text{epithermal}) / {}^{239}\text{Pu}_{\text{cap}}(\text{thermal})$ : ratio of epithermal to thermal  ${}^{239}\text{Pu}$  captures.

$\delta^{239} = {}^{239}\text{Pu}_{\text{fis}}(\text{epithermal}) / {}^{239}\text{Pu}_{\text{fis}}(\text{thermal})$ : ratio of epithermal to thermal  ${}^{239}\text{Pu}$  fissions.

$\delta^{241} = {}^{241}\text{Pu}_{\text{fis}}(\text{epithermal}) / {}^{241}\text{Pu}_{\text{fis}}(\text{thermal})$ : ratio of epithermal to thermal  ${}^{241}\text{Pu}$  fissions.

$F^{241} = {}^{241}\text{Pu}_{\text{fis}} / {}^{239}\text{Pu}_{\text{fis}}$ : ratio of fissions in  ${}^{241}\text{Pu}$  to fissions in  ${}^{239}\text{Pu}$ .

$C^8 = {}^{238}\text{Pu}_{\text{cap}} / {}^{239}\text{Pu}_{\text{fis}}$ : ratio of captures in  ${}^{238}\text{Pu}$  to fissions in  ${}^{239}\text{Pu}$ .

$C^9 = {}^{239}\text{Pu}_{\text{cap}} / {}^{239}\text{Pu}_{\text{fis}}$ : ratio of captures in  ${}^{239}\text{Pu}$  to fissions in  ${}^{239}\text{Pu}$ .

$C^0 = {}^{240}\text{Pu}_{\text{cap}} / {}^{239}\text{Pu}_{\text{fis}}$ : ratio of captures in  ${}^{240}\text{Pu}$  to fissions in  ${}^{239}\text{Pu}$ .

$C^1 = {}^{241}\text{Pu}_{\text{cap}} / {}^{239}\text{Pu}_{\text{fis}}$ : ratio of captures in  ${}^{241}\text{Pu}$  to fissions in  ${}^{239}\text{Pu}$ .

$C^2 = {}^{242}\text{Pu}_{\text{cap}} / {}^{239}\text{Pu}_{\text{fis}}$ : ratio of captures in  ${}^{242}\text{Pu}$  to fissions in  ${}^{239}\text{Pu}$ .

**Table 3.16. Phase 2a results – deterministic calculations**

Parameter	Units	A	B	C	D	E	F
$k_{\text{inf}}$ with zero buckling and at T = 293.6 K	–	1.46154	1.46369			1.43270	1.47656
$B_{\text{cr}}^2$ at T = 293.6 K	$\text{cm}^{-2}$	3.49E-04	4.803E-4				4.428E-04
$k_{\text{inf}}(B_{\text{cr}}^2)$ at T = 293.6 K	–	1.44325	1.44569				1.458
$M^2$ at T = 293.6 K	$\text{cm}^2$	1 271	927.9				1 034.4
$k_{\text{inf}}$ with zero buckling and at T = 1 000 K	–	1.38884					1.39241
$k_{\text{eff}}(B_{\text{cr}}^2)$ at T = 1 000 K, using $B_{\text{cr}}^2$ at T = 239.6 K	–	0.95562	0.95491				0.94877
$B_{\text{cr}}^2$ at T = 1 000 K	$\text{cm}^2$	3.06E-04	4.194E-4				3.809E-04
$k_{\text{inf}}(B_{\text{cr}}^2)$ at T = 1 000 K	–	1.37491	1.37629				1.379
$M^2$ at T = 1 000 K	$\text{cm}^2$	1 227	897.2				995.0
Reactivity at a pebble irradiation of 1 500 MWd/te	–	1.36772	1.35605				
$^{135}\text{Xe}$ number density at a pebble irradiation of 1 500 MWd/te	$\times 10^{24}$ atoms $\text{cm}^{-3}$	3.4714E-07					
$^{135}\text{Xe}$ absorption cross-section at a pebble irradiation of 1 500 MWd/te	barns	1.2025E+05					
$\rho^{239}$	–	0.14799	0.148241				
$\delta^{239}$	–	0.13904	0.139550				
$\delta^{241}$	–	0.34356	0.291976				
$F^{241}$	–	0.23599	0.239237				
$C^8$	–	0.01070	0.010620				
$C^9$	–	0.60378	0.603985				
$C^0$	–	0.57985	0.576980				
$C^1$	–	0.07887	0.081506				
$C^2$	–	0.05396	0.046782				

Again, good agreement is seen between Participant A and B for deterministic k-infinity calculations and most of the reaction rate ratios at a temperature of 293.6 K. For this plutonium system, the APOLLO2 k-infinity result is 215 pcm higher than WIMS9, a value of 473 pcm higher was seen for the uranium system in Phase 1. The two reaction rate ratios that are in most significant disagreement are  $^{241}\text{Pu}_{\text{fis}}(\text{epithermal})/^{241}\text{Pu}_{\text{fis}}(\text{thermal})$  where Participant A's result is about 25% higher and  $^{242}\text{Pu}_{\text{cap}}/^{239}\text{Pu}_{\text{fis}}$  where Participant A's result is about 11% higher.

Participant D's reaction ratio results are in reasonable agreement with those of Participants A and B. Participant D's estimate of the  $^{241}\text{Pu}_{\text{fis}}(\text{epithermal})/^{241}\text{Pu}_{\text{fis}}(\text{thermal})$  ratio is in better agreement with Participant A, while the  $^{242}\text{Pu}_{\text{cap}}/^{239}\text{Pu}_{\text{fis}}$  ratio is in better agreement with Participant B.

The reactivities from Participants E and F at room temperature are significantly different considering that both have used ENDF/B-V nuclear data. This is thought to be due to the inadequate treatment of plutonium resonances in the VSOP code, Participant E's result. Judging from the result of Participant F, ENDF/B-V predicts higher reactivities than JEF2.2 for plutonium systems. This is the opposite of uranium systems in the Phase 1 calculations where reactivities from ENDF/B-V were lower than JEF2.2.

### 3.2.2 Phase 2b: Reactivities and reaction rates

**Table 3.17. Phase 2b – Monte Carlo calculations**

Parameter	Units	A	B	C	D	E	F
$k_{inf}$ with zero buckling and at $T = 293.6 \text{ K}$	–	$1.4657 \pm 100 \text{ pcm}$		1.44418	1.4575		$1.47717 \pm 34 \text{ pcm}$
$B_{cr}^2$ at $T = 293.6 \text{ K}$	$\text{cm}^{-2}$	2.84E-4			2.77E-04		
$k_{inf}(B_{cr}^2)$ at $T = 293.6 \text{ K}$	–				1.4349		
$M^2$ at $T = 293.6 \text{ K}$	$\text{cm}^2$				1 574.9		
$k_{inf}$ with zero buckling and at $T = 1\ 000 \text{ K}$	–	$1.3928 \pm 100 \text{ pcm}$					$1.39218 \pm 38 \text{ pcm}$
$k_{eff}(B_{cr}^2)$ at $T = 1\ 000 \text{ K}$ , using $B_{cr}^2$ at $T = 239.6 \text{ K}$	–	$0.9571 \pm 100 \text{ pcm}$			0.96482		
$B_{cr}^2$ at $T = 1\ 000 \text{ K}$	$\text{cm}^2$	2.49E-4			2.49E-04		
$k_{inf}(B_{cr}^2)$ at $T = 1\ 000 \text{ K}$	–				1.3884		
$M^2$ at $T = 1\ 000 \text{ K}$	$\text{cm}^2$				1 531.0		
Reactivity at a pebble irradiation of 1 500 MWd/te	–				0.98358		
$^{135}\text{Xe}$ number density at a pebble irradiation of 1 500 MWd/te	$\times 10^{24} \text{ atoms cm}^{-3}$						
$^{135}\text{Xe}$ absorption cross-section at a pebble irradiation of 1 500 MWd/te	barns						
$\rho^{239}$	–						
$\delta^{239}$	–				0.1509		
$\delta^{241}$	–				0.1451		
$F^{241}$	–				0.3572		
$C^8$	–				0.2481		
$C^9$	–				0.0121		
$C^0$	–				0.5927		
$C^1$	–				0.5714		
$C^2$	–				0.0833		

**Table 3.18. Phase 2b – deterministic calculations**

Parameter	Units	A	B	C	D	E	F
$k_{\text{inf}}$ with zero buckling and at $T = 293.6 \text{ K}$	–	1.46154					
$B_{\text{cr}}^2$ at $T = 293.6 \text{ K}$	$\text{cm}^{-2}$	3.49E-04					
$k_{\text{inf}}(B_{\text{cr}}^2)$ at $T = 293.6 \text{ K}$	–	1.44325					
$M^2$ at $T = 293.6 \text{ K}$	$\text{cm}^2$	1272					
$k_{\text{inf}}$ with zero buckling and at $T = 1\,000 \text{ K}$	–	1.38884					
$k_{\text{eff}}(B_{\text{cr}}^2)$ at $T = 1\,000 \text{ K}$ , using $B_{\text{cr}}^2$ at $T = 239.6 \text{ K}$	–	0.95562					
$B_{\text{cr}}^2$ at $T = 1\,000 \text{ K}$	$\text{cm}^2$	3.05E-04					
$k_{\text{inf}}(B_{\text{cr}}^2)$ at $T = 1\,000 \text{ K}$	–	1.37491					
$M^2$ at $T = 1\,000 \text{ K}$	$\text{cm}^2$	1227					
Reactivity at a pebble irradiation of 1 500 MWd/te	–	1.36772					
$^{135}\text{Xe}$ number density at a pebble irradiation of 1 500 MWd/te	$\times 10^{24}$ atoms $\text{cm}^{-3}$	3.4716E-07					
$^{135}\text{Xe}$ absorption cross-section at a pebble irradiation of 1 500 MWd/te	barns	1.2044E+05					
$\rho^{239}$	–	0.14799					
$\delta^{239}$	–	0.13904					
$\delta^{241}$	–	0.34356					
$F^{241}$	–	0.23599					
$C^8$	–	0.01070					
$C^9$	–	0.60378					
$C^0$	–	0.57989					
$C^1$	–	0.07887					
$C^2$	–	0.05396					

Again, the deterministic results from Participant A for Phases 2a and 2b are very similar other than the effect of the outer boundary condition. It can again be concluded that Participants A and B are in close agreement based on the Phase 2a results.

The Monte Carlo and deterministic calculations for Participant A are in good agreement. For  $k$ -infinity the difference is  $(1.4657 - 1.46154)$  416 pcm. At temperature, using the critical buckling at 293.6 K the difference is  $(0.9571 - 0.95622)$  88 pcm. This also suggests the Monte Carlo and deterministic evaluations of the temperature coefficient are in good agreement. It should be noted that, for the plutonium system, the temperature coefficient is only about one half of the value for the uranium system in Phase 1.

Participants D and F, both using ENDF/B-V cross-section data, have very different results, by about 2 000 pcm. Participant D is in reasonable agreement with the JEF2.2 result but Participant F is significantly higher.

Xenon rapidly builds up in the reactor as a poison and reaches equilibrium concentrations after a few days at constant power. In Phases 2a and 2b of the benchmark Participant D calculates this effect, in addition to the change in reactivity when going to 1 000 K, to be a reduction in reactivity of  $(1.4573 - 0.9810) 47\ 630$  pcm for Phase 2a and  $(1.4575 - 0.98358) 47\ 392$  pcm in Phase 2b. Participant A calculates the effect as a reduction by  $(1.46154 - 1.36772) 9\ 382$  pcm in Phase 2a and  $(1.46154 - 1.36772) 9\ 382$  pcm in Phase 2b. Participant B calculates the effect as  $(1.46369 - 1.35605) 10\ 764$  pcm for Phase 2a. There is significant disagreement between the results of Participant D and those from the other participants in this part of the benchmark. There is a large difference between the pebble reactivity at 1 500 MWd/te calculated by Participant A and the equivalent value calculated by Participant B. This result is surprising given the close agreement between Participant A and B's general results for other parts of the benchmark. This could be due to differences in xenon worth and/or xenon number density at 1 500 MWd/te (perhaps resulting from differences in the employed burn-up chain or yield data).

### 3.2.3 Spectra

Figure 3.5 shows the Monte Carlo solution spectrum for Phase 2a from Participant D.

Figure 3.6 shows the spectra for Phase 2a submitted by Participants A, B and F, all using deterministic solutions.

Figure 3.7 shows the Monte Carlo solution spectrum for Phase 2b from Participant D. There appears to be close agreement between this spectrum and that from Participant D for the Phase 2a solution.

No deterministic solutions have been shown for Phase 2b, as these are the same as Phase 2a.

### 3.2.4 Burn-up

The number densities at 0, 10 000, 20 000, 30 000, 40 000, 50 000, 60 000, 70 000, 80 000 MWd/te supplied for Phase 2a or 2b are given in Tables 3.19 to 3.23. The results for Monte Carlo calculations from Participant D for Phases 2a and 2b are essentially identical, Tables 3.19 and 3.22, as are those from Participant A using deterministic methods, Tables 3.20 and 3.23.

The deterministic results from Participants A and B show reasonable agreement. There appears to be a slightly larger accumulation of the higher actinides in Participant B's calculation. The most noticeable differences are for  $^{243}\text{Am}$ ,  $^{245}\text{Cm}$ ,  $^{237}\text{Np}$  and  $^{238}\text{U}$  (although these only occur in trace quantities). The rate of accumulation of  $^{237}\text{Np}$  and  $^{238}\text{U}$  between 10 000 and 80 000 MWd/te is far larger in Participant B's calculation.

**Table 3.19. Phase 2a – Monte Carlo calculations – results from Participant D**

*Units are  $\times 10^{24}$  atoms cm $^{-3}$*

Nuclide	0 MWd/te	10 000 MWd/te	20 000 MWd/te	30 000 MWd/te	40 000 MWd/te	50 000 MWd/te	60 000 MWd/te	70 000 MWd/te	80 000 MWd/te
$^{241}\text{Am}$	0.00E+00	7.12E-06	1.42E-05	2.12E-05	2.81E-05	3.49E-05	4.17E-05	4.84E-05	5.50E-05
$^{242m}\text{Am}$	0.00E+00	9.08E-09	3.58E-08	7.89E-08	1.37E-07	2.08E-07	2.91E-07	3.85E-07	4.90E-07
$^{243}\text{Am}$	0.00E+00	1.02E-05	2.11E-05	3.20E-05	4.23E-05	5.26E-05	6.31E-05	7.34E-05	8.39E-05
$^{242}\text{Cm}$	0.00E+00	4.53E-08	1.90E-07	4.27E-07	7.54E-07	1.16E-06	1.64E-06	2.20E-06	2.83E-06
$^{243}\text{Cm}$	0.00E+00	1.38E-11	1.22E-10	4.22E-10	9.78E-10	1.93E-09	3.30E-09	5.12E-09	7.61E-09
$^{244}\text{Cm}$	0.00E+00	6.56E-08	2.88E-07	6.71E-07	1.22E-06	1.89E-06	2.71E-06	3.68E-06	4.81E-06
$^{245}\text{Cm}$	0.00E+00	8.67E-11	7.78E-10	2.73E-09	6.65E-09	1.32E-08	2.27E-08	3.70E-08	5.50E-08
$^{237}\text{Np}$	0.00E+00	4.00E-10	1.49E-09	3.22E-09	5.57E-09	8.51E-09	1.20E-08	1.62E-08	2.09E-08
$^{238}\text{Pu}$	6.01E-04	5.98E-04	5.96E-04	5.93E-04	5.90E-04	5.87E-04	5.85E-04	5.82E-04	5.79E-04
$^{239}\text{Pu}$	1.24E-02	1.21E-02	1.19E-02	1.16E-02	1.13E-02	1.10E-02	1.07E-02	1.04E-02	1.01E-02
$^{240}\text{Pu}$	5.45E-03	5.45E-03	5.45E-03	5.45E-03	5.45E-03	5.44E-03	5.44E-03	5.43E-03	5.42E-03
$^{241}\text{Pu}$	3.01E-03	3.04E-03	3.08E-03	3.12E-03	3.16E-03	3.19E-03	3.22E-03	3.26E-03	3.28E-03
$^{242}\text{Pu}$	1.55E-03	1.55E-03	1.56E-03	1.56E-03	1.57E-03	1.58E-03	1.58E-03	1.59E-03	1.60E-03
$^{233}\text{U}$	0.00E+00	3.94E-15	1.49E-14	3.27E-14	5.95E-14	9.64E-14	1.34E-13	1.81E-13	2.35E-13
$^{234}\text{U}$	0.00E+00	2.32E-07	4.63E-07	6.90E-07	9.16E-07	1.14E-06	1.36E-06	1.58E-06	1.79E-06
$^{235}\text{U}$	0.00E+00	1.80E-08	3.66E-08	5.60E-08	7.61E-08	9.70E-08	1.19E-07	1.41E-07	1.64E-07
$^{236}\text{U}$	0.00E+00	2.83E-08	5.65E-08	8.47E-08	1.13E-07	1.41E-07	1.69E-07	1.97E-07	2.25E-07
$^{237}\text{U}$	0.00E+00	1.04E-10	1.55E-10	2.00E-10	2.42E-10	2.76E-10	3.29E-10	3.77E-10	4.11E-10
$^{238}\text{U}$	0.00E+00	1.42E-10	2.84E-10	4.26E-10	5.69E-10	7.13E-10	8.57E-10	1.00E-09	1.15E-09

**Table 3.20. Phase 2a – deterministic calculations – results from Participant A**

Units are  $\times 10^{24}$  atoms cm $^{-3}$

Nuclide	0 MWd/te	10 000 MWd/te	20 000 MWd/te	30 000 MWd/te	40 000 MWd/te	50 000 MWd/te	60 000 MWd/te	70 000 MWd/te	80 000 MWd/te
$^{241}\text{Am}$	1.0000E-19	7.0773E-06	1.2700E-05	2.1061E-05	2.7956E-05	3.4778E-05	4.1524E-05	4.8185E-05	5.4757E-05
$^{242m}\text{Am}$	1.0000E-19	7.3501E-09	2.3358E-08	6.2987E-08	1.0919E-07	1.6631E-07	2.3335E-07	3.0938E-07	3.9347E-07
$^{243}\text{Am}$	1.0000E-19	9.9436E-06	1.7864E-05	2.9674E-05	3.9447E-05	4.9158E-05	5.8808E-05	6.8400E-05	7.7935E-05
$^{242}\text{Cm}$	1.0000E-19	5.4956E-08	1.7535E-07	4.7606E-07	8.3051E-07	1.2737E-06	1.8008E-06	2.4071E-06	3.0886E-06
$^{243}\text{Cm}$	1.0000E-19	1.7613E-11	1.0150E-10	4.6140E-10	1.0769E-09	2.0710E-09	3.5236E-09	5.5099E-09	8.0998E-09
$^{244}\text{Cm}$	1.0000E-19	6.8030E-08	2.2040E-07	6.1147E-07	1.0854E-06	1.6928E-06	2.4327E-06	3.3042E-06	4.3063E-06
$^{245}\text{Cm}$	1.0000E-19	1.0003E-10	5.8364E-10	2.6991E-09	6.3862E-09	1.2443E-08	2.1442E-08	3.3945E-08	5.0502E-08
$^{237}\text{Np}$	1.0000E-19	1.4283E-11	6.4505E-11	2.2003E-10	4.2516E-10	6.9895E-10	1.0410E-09	1.4509E-09	1.9282E-09
$^{238}\text{Pu}$	6.0118E-04	5.9873E-04	5.9676E-04	5.9380E-04	5.9134E-04	5.8888E-04	5.8644E-04	5.8402E-04	5.8162E-04
$^{239}\text{Pu}$	1.2447E-02	1.2147E-02	1.1908E-02	1.1552E-02	1.1258E-02	1.0967E-02	1.0677E-02	1.0391E-02	1.0106E-02
$^{240}\text{Pu}$	5.4460E-03	5.4484E-03	5.4492E-03	5.4486E-03	5.4466E-03	5.4431E-03	5.4382E-03	5.4318E-03	5.4241E-03
$^{241}\text{Pu}$	3.0997E-03	3.0523E-03	3.0856E-03	3.1340E-03	3.1729E-03	3.2104E-03	3.2464E-03	3.2808E-03	3.3137E-03
$^{242}\text{Pu}$	1.5454E-03	1.5509E-03	1.5556E-03	1.5632E-03	1.5700E-03	1.5773E-03	1.5849E-03	1.5931E-03	1.6017E-03
$^{233}\text{U}$	1.0000E-19	3.3672E-15	1.0867E-14	3.0006E-14	5.3069E-14	8.2485E-14	1.1815E-13	1.5994E-13	2.0775E-13
$^{234}\text{U}$	1.0000E-19	2.3193E-07	4.1599E-07	6.8959E-07	9.1533E-07	1.1390E-06	1.3607E-06	1.5803E-06	1.7979E-06
$^{235}\text{U}$	1.0000E-19	1.7833E-08	3.2502E-08	5.5160E-08	7.4630E-08	9.4627E-08	1.1514E-07	1.3617E-07	1.5771E-07
$^{236}\text{U}$	1.0000E-19	2.8187E-08	5.0712E-08	8.4451E-08	1.1251E-07	1.4052E-07	1.6847E-07	1.9636E-07	2.2417E-07
$^{237}\text{U}$	1.0000E-19	2.0624E-11	4.8574E-11	9.3792E-11	1.3209E-10	1.7055E-10	2.0910E-10	2.4774E-10	2.8645E-10
$^{238}\text{U}$	1.0000E-19	3.8460E-14	1.7510E-13	6.0459E-13	1.1803E-12	1.9607E-12	2.9513E-12	4.1578E-12	5.5862E-12

**Table 3.21. Phase 2a – deterministic calculations – results from Participant B**

Units are  $\times 10^{24}$  atoms  $\text{cm}^{-3}$

Nuclide	0 MWd/te	10 000 MWd/te	20 000 MWd/te	30 000 MWd/te	40 000 MWd/te	50 000 MWd/te	60 000 MWd/te	70 000 MWd/te	80 000 MWd/te
$^{241}\text{Am}$	–	7.08E-06	1.41E-05	2.11E-05	2.79E-05	3.48E-05	4.15E-05	4.81E-05	5.47E-05
$^{242m}\text{Am}$	–	–	–	–	–	–	–	–	–
$^{243}\text{Am}$	–	2.32E-07	4.62E-07	6.89E-07	9.15E-07	1.14E-06	1.36E-06	1.58E-06	1.79E-06
$^{242}\text{Cm}$	–	5.62E-08	2.20E-07	4.86E-07	8.48E-07	1.30E-06	1.84E-06	2.46E-06	3.15E-06
$^{243}\text{Cm}$	–	1.84E-11	1.45E-10	4.82E-10	1.12E-09	2.16E-09	3.67E-09	5.74E-09	8.44E-09
$^{244}\text{Cm}$	–	7.44E-08	2.97E-07	6.68E-07	1.19E-06	1.85E-06	2.66E-06	3.61E-06	4.70E-06
$^{245}\text{Cm}$	–	1.12E-10	8.95E-10	3.01E-09	7.13E-09	1.39E-08	2.39E-08	3.78E-08	5.63E-08
$^{237}\text{Np}$	–	3.05E-10	1.22E-09	2.73E-09	4.86E-09	7.57E-09	1.09E-08	1.47E-08	1.91E-08
$^{238}\text{Pu}$	6.01E-04	5.99E-04	5.94E-04	5.91E-04	5.89E-04	5.86E-04	5.84E-04	5.81E-04	5.81E-04
$^{239}\text{Pu}$	1.24E-02	1.21E-02	1.18E-02	1.15E-02	1.12E-02	1.09E-02	1.06E-02	1.03E-02	1.01E-02
$^{240}\text{Pu}$	5.45E-03	5.45E-03	5.45E-03	5.45E-03	5.45E-03	5.45E-03	5.44E-03	5.43E-03	5.43E-03
$^{241}\text{Pu}$	3.01E-03	3.05E-03	3.09E-03	3.14E-03	3.17E-03	3.21E-03	3.25E-03	3.28E-03	3.32E-03
$^{242}\text{Pu}$	1.55E-03	1.55E-03	1.56E-03	1.57E-03	1.58E-03	1.58E-03	1.59E-03	1.59E-03	1.60E-03
$^{233}\text{U}$	–	–	–	–	–	–	–	–	–
$^{234}\text{U}$	–	2.31E-07	4.59E-07	6.86E-07	9.10E-07	1.13E-06	1.35E-06	1.57E-06	1.78E-06
$^{235}\text{U}$	–	1.79E-08	3.65E-08	5.57E-08	7.57E-08	9.63E-08	1.18E-07	1.39E-07	1.62E-07
$^{236}\text{U}$	–	2.82E-08	5.64E-08	8.45E-08	1.13E-07	1.41E-07	1.69E-07	1.97E-07	2.24E-07
$^{237}\text{U}$	–	2.11E-11	5.72E-11	9.59E-11	1.35E-10	1.74E-10	2.14E-10	2.53E-10	2.93E-10
$^{238}\text{U}$	0.00E+00	1.41E-10	2.82E-10	4.24E-10	5.66E-10	7.09E-10	8.53E-10	9.98E-10	1.14E-09

**Table 3.22. Phase 2b – Monte Carlo calculations – results from Participant D**

Units are  $\times 10^{24}$  atoms  $\text{cm}^{-3}$

Nuclide	0 MWd/te	10 000 MWd/te	20 000 MWd/te	30 000 MWd/te	40 000 MWd/te	50 000 MWd/te	60 000 MWd/te	70 000 MWd/te	80 000 MWd/te
$^{241}\text{Am}$	0.00E+00	7.12E-06	1.42E-05	2.12E-05	2.81E-05	3.50E-05	4.17E-05	4.84E-05	5.50E-05
$^{242m}\text{Am}$	0.00E+00	9.16E-09	3.59E-08	7.88E-08	1.36E-07	2.08E-07	2.91E-07	3.85E-07	4.90E-07
$^{243}\text{Am}$	0.00E+00	1.11E-05	2.17E-05	3.26E-05	4.28E-05	5.31E-05	6.34E-05	7.40E-05	8.44E-05
$^{242}\text{Cm}$	0.00E+00	4.57E-08	1.90E-07	4.27E-07	7.52E-07	1.16E-06	1.65E-06	2.20E-06	2.83E-06
$^{243}\text{Cm}$	0.00E+00	1.39E-11	1.20E-10	4.17E-10	9.83E-10	1.91E-09	3.23E-09	5.07E-09	7.59E-09
$^{244}\text{Cm}$	0.00E+00	7.15E-08	3.01E-07	6.86E-07	1.24E-06	1.92E-06	2.75E-06	3.73E-06	4.87E-06
$^{245}\text{Cm}$	0.00E+00	9.56E-11	8.00E-10	2.81E-09	6.68E-09	1.33E-08	2.32E-08	3.68E-08	5.51E-08
$^{237}\text{Np}$	0.00E+00	3.99E-10	1.49E-09	3.22E-09	5.57E-09	8.52E-09	1.20E-08	1.62E-08	2.09E-08
$^{238}\text{Pu}$	6.01E-04	5.98E-04	5.96E-04	5.93E-04	5.90E-04	5.87E-04	5.85E-04	5.82E-04	5.79E-04
$^{239}\text{Pu}$	1.24E-02	1.21E-02	1.19E-02	1.16E-02	1.13E-02	1.10E-02	1.07E-02	1.04E-02	1.01E-02
$^{240}\text{Pu}$	5.45E-03	5.45E-03	5.45E-03	5.45E-03	5.44E-03	5.44E-03	5.44E-03	5.43E-03	5.42E-03
$^{241}\text{Pu}$	3.01E-03	3.05E-03	3.09E-03	3.12E-03	3.16E-03	3.19E-03	3.23E-03	3.26E-03	3.29E-03
$^{242}\text{Pu}$	1.55E-03	1.55E-03	1.56E-03	1.56E-03	1.57E-03	1.58E-03	1.58E-03	1.59E-03	1.60E-03
$^{233}\text{U}$	0.00E+00	3.58E-15	1.46E-14	3.43E-14	5.90E-14	9.14E-14	1.35E-13	1.84E-13	2.42E-13
$^{234}\text{U}$	0.00E+00	2.33E-07	4.63E-07	6.90E-07	9.16E-07	1.14E-06	1.36E-06	1.58E-06	1.79E-06
$^{235}\text{U}$	0.00E+00	1.79E-08	3.66E-08	5.60E-08	7.61E-08	9.70E-08	1.19E-07	1.41E-07	1.64E-07
$^{236}\text{U}$	0.00E+00	2.83E-08	5.65E-08	8.47E-08	1.13E-07	1.41E-07	1.69E-07	1.97E-07	2.25E-07
$^{237}\text{U}$	0.00E+00	1.04E-10	1.56E-10	1.98E-10	2.43E-10	2.81E-10	3.20E-10	3.75E-10	4.14E-10
$^{238}\text{U}$	0.00E+00	1.41E-10	2.84E-10	4.26E-10	5.69E-10	7.13E-10	8.57E-10	1.00E-09	1.15E-09

**Table 3.23. Phase 2b – deterministic calculations – results from Participant A**

Units are  $\times 10^{24}$  atoms cm $^{-3}$

Nuclide	0 MWd/te	10 000 MWd/te	20 000 MWd/te	30 000 MWd/te	40 000 MWd/te	50 000 MWd/te	60 000 MWd/te	70 000 MWd/te	80 000 MWd/te
$^{241}\text{Am}$	1.0000E-19	7.0773E-06	1.4100E-05	2.1061E-05	2.7956E-05	3.4780E-05	4.1526E-05	4.8188E-05	5.4760E-05
$^{242m}\text{Am}$	1.0000E-19	7.3507E-09	2.8698E-08	6.2992E-08	1.0920E-07	1.6632E-07	2.3338E-07	3.0941E-07	3.9352E-07
$^{243}\text{Am}$	1.0000E-19	9.9469E-06	1.9845E-05	2.9684E-05	3.9460E-05	4.9174E-05	5.8827E-05	6.8422E-05	7.7960E-05
$^{242}\text{Cm}$	1.0000E-19	5.4960E-08	2.1567E-07	4.7610E-07	8.3058E-07	1.2738E-06	1.8009E-06	2.4074E-06	3.0889E-06
$^{243}\text{Cm}$	1.0000E-19	1.7615E-11	1.3884E-10	4.6147E-10	1.0771E-09	2.0713E-09	3.5242E-09	5.5107E-09	8.1011E-09
$^{244}\text{Cm}$	1.0000E-19	6.8061E-08	2.7219E-07	6.1176E-07	1.0859E-06	1.6935E-06	2.4338E-06	3.3056E-06	4.3082E-06
$^{245}\text{Cm}$	1.0000E-19	1.0009E-10	8.0104E-10	2.7008E-09	6.3901E-09	1.2451E-08	2.1455E-08	3.3965E-08	5.0531E-08
$^{237}\text{Np}$	1.0000E-19	1.4284E-11	8.3620E-11	2.2005E-10	4.2520E-10	6.9901E-10	1.0411E-09	1.4510E-09	1.9284E-09
$^{238}\text{Pu}$	6.0118E-04	5.9873E-04	5.9626E-04	5.9380E-04	5.9134E-04	5.8888E-04	5.8644E-04	5.8402E-04	5.8163E-04
$^{239}\text{Pu}$	1.2447E-02	1.2147E-02	1.1848E-02	1.1552E-02	1.1258E-02	1.0967E-02	1.0677E-02	1.0391E-02	1.0106E-02
$^{240}\text{Pu}$	5.4460E-03	5.4484E-03	5.4492E-03	5.4485E-03	5.4464E-03	5.4428E-03	5.4379E-03	5.4315E-03	5.4237E-03
$^{241}\text{Pu}$	3.0997E-03	3.0523E-03	3.0939E-03	3.1342E-03	3.1731E-03	3.2107E-03	3.2467E-03	3.2812E-03	3.3141E-03
$^{242}\text{Pu}$	1.5454E-03	1.5509E-03	1.5569E-03	1.5632E-03	1.5700E-03	1.5772E-03	1.5849E-03	1.5931E-03	1.6017E-03
$^{233}\text{U}$	1.0000E-19	3.3641E-15	1.3391E-14	2.9979E-14	5.3021E-14	8.2411E-14	1.1804E-13	1.5980E-13	2.0757E-13
$^{234}\text{U}$	1.0000E-19	2.3193E-07	4.6179E-07	6.8959E-07	9.1533E-07	1.1390E-06	1.3607E-06	1.5803E-06	1.7979E-06
$^{235}\text{U}$	1.0000E-19	1.7833E-08	3.6224E-08	5.5160E-08	7.4630E-08	9.4628E-08	1.1515E-07	1.3618E-07	1.5772E-07
$^{236}\text{U}$	1.0000E-19	2.8187E-08	5.6339E-08	8.4449E-08	1.1251E-07	1.4052E-07	1.6847E-07	1.9635E-07	2.2416E-07
$^{237}\text{U}$	1.0000E-19	2.0626E-11	5.5982E-11	9.3801E-11	1.3210E-10	1.7056E-10	2.0912E-10	2.4775E-10	2.8647E-10
$^{238}\text{U}$	1.0000E-19	3.8463E-14	2.2744E-13	6.0462E-13	1.1804E-12	1.9608E-12	2.9514E-12	4.1580E-12	5.5863E-12

### 3.3 Phase 3

#### 3.3.1 Core reactivity

**Table 3.24. Phase 3 – Monte Carlo calculations**

Parameter	Units	A	B	C	D	E	F
Core reactivity at 293.6 K	–	1.3494 ± 100 pcm	1.35714 ± 50 pcm	1.35302	1.347		1.36127 ± 50 pcm
Core reactivity at 1 000 K	–	1.2998 ± 100 pcm	1.31111 ± 50 pcm	1.30577	1.318		1.29879 ± 42 pcm
Core reactivity at an irradiation of 1 500 MWd/te	–				1.294		
Core average $^{135}\text{Xe}$ number density at an irradiation of 1 500 MWd/te	$\times 10^{24}$ atoms $\text{cm}^{-3}$						
Core average $^{135}\text{Xe}$ absorption cross-section at an irradiation of 1 500 MWd/Te	barns						

**Table 3.25. Phase 3 – deterministic calculations**

Parameter	Units	A	B	C	D	E	F
Core reactivity at 293.6 K	–	1.34645	1.35075			1.29827	
Core reactivity at 1 000 K	–	1.29598	1.29820			1.26230	
Core reactivity at an irradiation of 1 500 MWd/te	–	1.28540	1.27818			1.24099	
Core average $^{135}\text{Xe}$ number density at an irradiation of 1 500 MWd/te	$\times 10^{24}$ atoms $\text{cm}^{-3}$	9.1062E-11					
Core average $^{135}\text{Xe}$ absorption cross-section at an irradiation of 1 500 MWd/Te	barns	1.4614E-05					

The mean calculated Monte Carlo core reactivity of all participants at 293.6 K is 1.35356 with a standard deviation between results of ±576 pcm. The outlying results are from Participant D (-657 pcm from the mean) and Participant F (+770 pcm from the mean).

The difference between Participant A's Monte Carlo and deterministic results for the core reactivity at 293.6 K is  $295 \pm 100$  pcm, and that for Participant B is  $639 \pm 50$  pcm. This is relatively good agreement considering the stochastic nature of the pebble arrangement.

For the Monte Carlo calculations, the reactivity reduction in going to power temperatures is 4 960 pcm from Participant A, 4 603 pcm from Participant B, 2 900 pcm from Participant D and 6 248 pcm from Participant F. However, the deterministic calculations of Participants A and B give values of 5 047 pcm and 5 255 pcm, respectively. Participant A's Monte Carlo and deterministic values are in good agreement.

Participant A has included a deterministic evaluation of the whole core xenon reactivity effect, 1 058 pcm. Participant B's deterministic calculation of the same quantity is 2 002 pcm. Participant D gives a Monte Carlo determination of 2 400 pcm.

There is poor agreement between the deterministic calculations of Participant E and those from Participants A and B, however, this may be in part due to ENDF/B-5 relative to JEF2.2 nuclear data. Note, however, that for the plutonium cell calculations of Phase 2 Participant E's results gave higher rather than lower values.

### 3.3.2 Spectra

Figure 3.8 shows the Monte Carlo spectra provided by Participants A, D and F.

Figure 3.9 shows the Monte Carlo and deterministic spectra for Participant A's calculation. There is a general good agreement but with a slight difference at the peak of the low-energy plutonium resonance.

Figure 3.10 compares the deterministic spectra from Participant E and Participant A. There are significant differences between the two spectra, the causes of which are unknown.

### 3.3.3 Cross-sections

**Table 3.26. Phase 3 – Monte Carlo calculations – results from Participant A**

*Specified in units of barns*

Nuclide	<b>10<sup>-5</sup> eV to 0.625 eV</b>	<b>0.625 eV to 9.118 KeV</b>	<b>9.118 KeV to 20 MeV</b>
<i>Capture</i>			
<sup>238</sup> Pu	119 ± 15	13 ± 3	0.6 ± 0.4
<sup>239</sup> Pu	390 ± 6	16 ± 1	0.3 ± 0.1
<sup>240</sup> Pu	148 ± 6	241 ± 5	0.3 ± 0.2
<sup>241</sup> Pu	201 ± 9	16 ± 2	0.6 ± 0.3
<sup>242</sup> Pu	8 ± 2	88 ± 3	0.4 ± 0.3
<i>Fission</i>			
<sup>238</sup> Pu	4 ± 2	2 ± 1	2 ± 1
<sup>239</sup> Pu	654 ± 7	25 ± 1	2.1 ± 0.3
<sup>240</sup> Pu	0.02 ± 0.02	0.2 ± 0.1	0.7 ± 0.2
<sup>241</sup> Pu	567 ± 15	55 ± 4	2.3 ± 0.7
<sup>242</sup> Pu	0 ± 1	0.1 ± 0.1	0.5 ± 0.3

**Table 3.27. Phase 3 – Monte Carlo calculations – results from Participant D***Specified in units of barns*

Nuclide	$10^{-5}$ eV to 0.625 eV	0.625 eV to 9.118 KeV	9.118 KeV to 20 MeV
<i>Capture</i>			
$^{238}\text{Pu}$	145.2	14.64	0.4854
$^{239}\text{Pu}$	374.6	15.57	0.2598
$^{240}\text{Pu}$	153.8	232.4	0.3458
$^{241}\text{Pu}$	204.7	15.31	0.2687
$^{242}\text{Pu}$	7.953	87.78	0.3007
<i>Fission</i>			
$^{238}\text{Pu}$	4.410	2.016	1.4564
$^{239}\text{Pu}$	643.2	24.37	1.8401
$^{240}\text{Pu}$	0.0330	0.1304	0.7523
$^{241}\text{Pu}$	586.05	53.10	2.2042
$^{242}\text{Pu}$	3.9E-04	0.0202	0.5915

**Table 3.28. Phase 3 – Monte Carlo calculations – results from Participant F***Specified in units of barns*

Nuclide	$10^{-5}$ eV to 0.625 eV	0.625 eV to 9.118 KeV	9.118 KeV to 20 MeV
<i>Capture</i>			
$^{238}\text{Pu}$	144.8939	14.5820	0.4750
$^{239}\text{Pu}$	390.5491	16.9366	0.2598
$^{240}\text{Pu}$	155.5297	237.4493	0.3430
$^{241}\text{Pu}$	231.4431	17.8462	0.3085
$^{242}\text{Pu}$	7.9612	108.7398	0.2929
<i>Fission</i>			
$^{238}\text{Pu}$	4.3997	2.1714	1.3790
$^{239}\text{Pu}$	659.8146	24.5275	1.7867
$^{240}\text{Pu}$	0.0299	0.1253	0.6815
$^{241}\text{Pu}$	599.5869	54.1593	2.1294
$^{242}\text{Pu}$	3.918E-04	0.0210	0.5382

**Table 3.29. Phase 3 – deterministic calculations – results from Participant A***Specified in units of barns*

Nuclide	$10^{-5}$ eV to 0.625 eV	0.625 eV to 9.118 KeV	9.118 KeV to 20 MeV
<i>Capture</i>			
$^{238}\text{Pu}$	127.39	13.63	0.36
$^{239}\text{Pu}$	400.59	16.00	0.29
$^{240}\text{Pu}$	151.25	242.89	0.37
$^{241}\text{Pu}$	204.53	15.75	0.44
$^{242}\text{Pu}$	7.37	87.05	0.33
<i>Fission</i>			
$^{238}\text{Pu}$	4.25	2.15	1.47
$^{239}\text{Pu}$	672.95	24.03	1.88
$^{240}\text{Pu}$	0.03	0.24	0.73
$^{241}\text{Pu}$	576.01	53.74	2.24
$^{242}\text{Pu}$	0.01	0.08	0.58

**Table 3.30. Phase 3 – deterministic calculations – results from Participant B***Specified in units of barns*

Nuclide	$10^{-5}$ eV to 0.625 eV	0.625 eV to 9.118 KeV	9.118 KeV to 20 MeV
<i>Capture</i>			
$^{238}\text{Pu}$	127.00	13.57	0.37
$^{239}\text{Pu}$	403.54	16.02	0.29
$^{240}\text{Pu}$	151.68	241.34	0.37
$^{241}\text{Pu}$	207.02	15.61	0.45
$^{242}\text{Pu}$	7.39	91.26	0.33
<i>Fission</i>			
$^{238}\text{Pu}$	4.24	2.14	1.61
$^{239}\text{Pu}$	677.44	24.04	1.97
$^{240}\text{Pu}$	0.03	0.24	0.84
$^{241}\text{Pu}$	581.38	53.55	2.34
$^{242}\text{Pu}$	0.01	0.08	0.66

**Table 3.31. Phase 3 – deterministic calculations – results from Participant E***Specified in units of barns*

Nuclide	Participant E $10^{-5}$ eV to 10 MeV	Participant A $10^{-5}$ eV to 10 MeV
<i>Capture</i>		
$^{238}\text{Pu}$	26.6	27.58
$^{239}\text{Pu}$	75.0	73.87
$^{240}\text{Pu}$	158	138.45
$^{241}\text{Pu}$	40.5	41.35
$^{242}\text{Pu}$	33.3	41.94
<i>Fission</i>		
$^{238}\text{Pu}$	2.03	2.25
$^{239}\text{Pu}$	122	123.27
$^{240}\text{Pu}$	0.349	0.39
$^{241}\text{Pu}$	118	121.21
$^{242}\text{Pu}$	0.184	0.25

The Monte Carlo cross-sections submitted by Participant A and Participant F show differences greater than the scoring statistics for  $^{238}\text{Pu}$ ,  $^{241}\text{Pu}$  and  $^{242}\text{Pu}$  capture and  $^{241}\text{Pu}$  fission reflecting the origin of the nuclear data. Participant D has a lower value, more in agreement with Participant A for  $^{241}\text{Pu}$  and  $^{242}\text{Pu}$  capture and  $^{241}\text{Pu}$  fission despite using the same nuclear data as Participant F.

There is relatively good agreement between the deterministic cross-sections at all energies for Participants A and B reflecting the same origin of nuclear data (JEF2.2).

All deterministic cross-sections from Participant A agree with the Monte Carlo cross-sections from Participant A within the one sigma uncertainty in the Monte Carlo values, except for the thermal  $^{239}\text{Pu}$  fission and capture cross-sections. As these are the most dominant reactions in the problem, and therefore have the best counting statistics, this appears anomalous. However, Figure 3.9 shows the Monte Carlo flux at these thermal energies slightly exceeds that in the deterministic calculation. The reaction rates are therefore in very good agreement. This anomaly is attributed to the accuracy of splitting the Monte Carlo reaction rates into flux and cross-section components.

Participant E was only able to provide one-group cross-sections. Table 3.31 shows these cross-sections, as well as equivalent values from Participant A. It appears that most of the cross-sections are in reasonable agreement for Participants E and A, with the notable exception of  $^{240}\text{Pu}$  and  $^{242}\text{Pu}$  capture. The significantly higher  $^{240}\text{Pu}$  capture cross-section from Participant E could be a contributing factor to the low core reactivities provided by this participant.

### 3.4 Phase 4

#### 3.4.1 Core reactivity

**Table 3.32. Phase 4 – Monte Carlo calculations**

Parameter	Units	A	B	C	D	E	F
Core reactivity ( $k_{\text{eff}}$ ) at 293.6 K	–	$1.3697 \pm 100 \text{ pcm}$	$1.38208 \pm 50 \text{ pcm}$			1.36454	$1.36881 \pm 0.00048$
Core reactivity ( $k_{\text{eff}}$ ) at 1 000 K	–	$1.2863 \pm 100 \text{ pcm}$	$1.30557 \pm 50 \text{ pcm}$			1.30350	$1.27599 \pm 0.00046$
Core reactivity at an irradiation of 1 500 MWd/te – with buckling	–						
Core reactivity at an irradiation of 1 500 MWd/te – without buckling	–					1.24585	
Core average $^{135}\text{Xe}$ number density at an irradiation of 1 500 MWd/te	$\times 10^{24} \text{ atoms cm}^{-3}$						
Core average $^{135}\text{Xe}$ absorption cross-section at an irradiation of 1 500 MWd/Te	barns						
Core migration length	cm						

**Table 3.33. Phase 4 – deterministic calculations**

Parameter	Units	A	B	C	D	E	F
Core reactivity ( $k_{\text{eff}}$ ) at 293.6 K – no streaming correction	–	1.36818	1.37663			1.35018	
Core reactivity ( $k_{\text{eff}}$ ) at 293.6 K – with streaming correction	–					1.34551	
Core reactivity ( $k_{\text{eff}}$ ) at 1 000 K – no streaming correction	–	1.28443	1.29460			1.27078	
Core reactivity ( $k_{\text{eff}}$ ) at 1 000 K – with streaming correction	–					1.26737	
Core reactivity at an irradiation of 1 500 MWd/te – with buckling	–	1.24109	1.25327			1.21118	

**Table 3.33. Phase 4 – deterministic calculations (cont.)**

Parameter	Units	A	B	C	D	E	F
Core reactivity at an irradiation of 1 500 MWd/te – without buckling	–	1.24162					
Core average $^{135}\text{Xe}$ number density at an irradiation of 1 500 MWd/te	$\times 10^{24}$ atoms $\text{cm}^{-3}$	1.0036E-10					
Core average $^{135}\text{Xe}$ absorption cross-section at an irradiation of 1 500 MWd/Te	barns	4.1109E+05					
Core migration length	cm	39.359					

The difference between the Monte Carlo and deterministic (with no streaming correction) results of Participant A at 293.6K is  $152 \pm 100$  pcm. The equivalent difference at 1 000 K is  $187 \pm 100$  pcm. This is good agreement, especially when consideration is made of the stochastic nature of the pebble distribution. As the differences are comparable at both 293.6 K and 1 000 K, this indicates that Participant A's deterministic and Monte Carlo evaluations of the temperature coefficient are in agreement.

Participant B's Monte Carlo estimate of k-effective at room temperature is 1 238 pcm higher than that of Participant A. The reactivity change to 1 000°C is calculated as 8 340 pcm, 7 651 pcm and 9 282 pcm by Participants A, B and F respectively.

There is reasonable agreement between the k-effectives of the deterministic solutions, Participant B being 845 pcm higher than Participant A and Participant E being 1 800 pcm lower. The reactivity to 1 000°C is calculated as 8 375 pcm, 8 203 pcm and 7 940 pcm by Participants A, B and E respectively.

### 3.4.2 Spectra

Figure 3.11 shows a comparison between the Monte Carlo spectra of Participants A and F. There are significant differences between the spectra.

Figure 3.12 shows the Monte Carlo and deterministic 172-group spectra for Participant A's calculation. There is a general good agreement, but with a slight difference at the low-energy peak in the spectrum.

Figure 3.13 shows the Monte Carlo and deterministic four-group spectra for Participant A's calculation. Again, there is a general good agreement between the spectra.

Figure 3.14 shows the deterministic spectrum from Participant E. It has not been possible to make a plot to directly compare the deterministic spectra from Participants E and A, since the VSOP code applies an unknown normalisation factor to the flux data internally. The form of Participant E's deterministic spectrum, however, appears to be comparable to that of Participant A.

### 3.4.3 Cross-sections

**Table 3.34. Monte Carlo calculations – results from Participant A**

*Specified in units of barns*

Nuclide	$10^{-5}$ eV to 20 MeV
<i>Capture</i>	
$^{235}\text{U}$	$19.956 \pm 0.630$
$^{238}\text{U}$	$3.696 \pm 0.065$
<i>Fission</i>	
$^{235}\text{U}$	$98.138 \pm 1.300$
$^{238}\text{U}$	$0.027 \pm 0.003$

**Table 3.35. Monte Carlo calculations – results from Participant D**

*Specified in units of barns*

Nuclide	$10^{-5}$ eV to 20 MeV
<i>Capture</i>	
$^{235}\text{U}$	17.306
$^{238}\text{U}$	3.1518
<i>Fission</i>	
$^{235}\text{U}$	85.859
$^{238}\text{U}$	0.023774

**Table 3.36. Monte Carlo calculations – results from Participant F**

*Specified in units of barns*

Nuclide	$10^{-5}$ eV to 20 MeV
<i>Capture</i>	
$^{235}\text{U}$	24.4629
$^{238}\text{U}$	4.4870
<i>Fission</i>	
$^{235}\text{U}$	115.3191
$^{238}\text{U}$	0.0315

**Table 3.37. Deterministic calculations – results from Participant A**

*Specified in units of barns*

Nuclide	$10^{-5}$ eV to 20 MeV
<i>Capture</i>	
$^{235}\text{U}$	19.788
$^{238}\text{U}$	3.7222
<i>Fission</i>	
$^{235}\text{U}$	96.829
$^{238}\text{U}$	2.73E-02

**Table 3.38. Deterministic calculations – results from Participant B***Specified in units of barns*

Nuclide	$10^{-5}$ eV to 20 MeV
<i>Capture</i>	
$^{235}\text{U}$	19.94
$^{238}\text{U}$	3.67
<i>Fission</i>	
$^{235}\text{U}$	97.63
$^{238}\text{U}$	0.03

**Table 3.39. Deterministic calculations – results from Participant E***Specified in units of barns*

Nuclide	$10^{-5}$ eV to 20 MeV
<i>Capture</i>	
$^{235}\text{U}$	20.7
$^{238}\text{U}$	3.53
<i>Fission</i>	
$^{235}\text{U}$	96.5
$^{238}\text{U}$	0.026

The Monte Carlo cross-sections submitted by Participants A and F appear to be discrepant. Participant A's Monte Carlo and deterministic cross-sections are in good agreement. It is concluded that Participant F's Monte Carlo cross-sections are in error.

Cross-sections for Participants A, B and E are in reasonable agreement.

### 3.5 Phase 5

#### 3.5.1 Phase 5a: Reactivities and reaction rates

**Table 3.40. Phase 5a – Monte Carlo calculations**

Parameter	Units	A	B	C	D	E	F
$k_{\text{inf}}$ with zero buckling and at $T = 293.6\text{ K}$	–	$1.4442 \pm 50\text{ pcm}$			1.46841		
$B_{\text{cr}}^2$ at $T = 293.6\text{ K}$	$\text{cm}^{-2}$				1.73E-4		
$k_{\text{inf}}(B_{\text{cr}}^2)$ at $T = 293.6\text{ K}$	–				1.4549		
$M^2$ at $T = 293.6\text{ K}$	$\text{cm}^2$				2607.8		
$k_{\text{inf}}$ with zero buckling and at $T = 1\,000\text{ K}$	–	$1.4452 \pm 50\text{ pcm}$			1.4573		
$k_{\text{eff}}(B_{\text{cr}}^2)$ at $T = 1\,000\text{ K}$ , using $B_{\text{cr}}^2$ at $T = 239.6\text{ K}$	–				0.89041		
$B_{\text{cr}}^2$ at $T = 1\,000\text{ K}$	$\text{cm}^{-2}$				1.27E-4		
$k_{\text{inf}}(B_{\text{cr}}^2)$ at $T = 1\,000\text{ K}$	–				1.4526		
$M^2$ at $T = 1\,000\text{ K}$	$\text{cm}^2$				3553.2		

**Table 3.40. Phase 5a – Monte Carlo calculations (cont.)**

Parameter	Units	A	B	C	D	E	F
Reactivity at a pebble irradiation of 1 500 MWd/te	–				0.9682		
$^{135}\text{Xe}$ number density at a pebble irradiation of 1 500 MWd/te	$\times 10^{24}$ atoms $\text{cm}^{-3}$				1.95E-08		
$^{135}\text{Xe}$ absorption cross-section at a pebble irradiation of 1 500 MWd/Te	barns				(E < 0.625eV) 1.53935E+6 (E > 0.625eV) 327.45		
$\rho^{232}$	–				0.30452		
$\delta^{233}$	–				0.04946		
$\delta^{232}$	–				0.0001526		
C	–				0.21156		

$\rho^{232} = \frac{\text{Th}_{\text{cap}}(\text{epithermal})}{\text{Th}_{\text{cap}}(\text{thermal})}$ : ratio of epithermal to thermal  $^{232}\text{Th}$  captures.

$\delta^{233} = \frac{\text{U}_{\text{fis}}(\text{epithermal})}{\text{U}_{\text{fis}}(\text{thermal})}$ : ratio of epithermal to thermal  $^{233}\text{U}$  fissions.

$\delta^{232} = \frac{\text{Th}_{\text{fis}}}{\text{U}_{\text{fis}}}$ : ratio of fissions in  $^{232}\text{Th}$  to fissions in  $^{233}\text{U}$ .

C =  $\frac{\text{Th}_{\text{cap}}}{\text{U}_{\text{fis}}}$ : ratio of captures in  $^{232}\text{Th}$  to fissions in  $^{233}\text{U}$ .

**Table 3.41. Phase 5a – deterministic calculations**

Parameter	Units	A	B	C	D	E	F
$k_{\text{inf}}$ with zero buckling and at T = 293.6 K	–	1.46068	1.46269				1.4645
$B_{\text{cr}}^2$ at T = 293.6 K	$\text{cm}^{-2}$	1.738E-04					1.666E-04
$k_{\text{inf}}(B_{\text{cr}}^2)$ at T = 293.6 K	–	1.45351					1.457
$M^2$ at T = 293.6 K	$\text{cm}^2$	2609.1					2743.9
$k_{\text{inf}}$ with zero buckling and at T = 1 000 K	–	1.46114	1.46276				1.46163
$k_{\text{eff}}(B_{\text{cr}}^2)$ at T = 1 000 K, using $B_{\text{cr}}^2$ at T = 239.6 K	–	0.86259					0.87917
$B_{\text{cr}}^2$ at T = 1 000 K	$\text{cm}^{-2}$	1.189E-04					1.195E-04
$k_{\text{inf}}(B_{\text{cr}}^2)$ at T = 1 000 K	–	1.45134					1.452
$M^2$ at T = 1 000 K	$\text{cm}^2$	3794.9					3781.2
Reactivity at a pebble irradiation of 1 500 MWd/te	–	1.39580					
$^{135}\text{Xe}$ number density at a pebble irradiation of 1 500 MWd/te	$\times 10^{24}$ atoms $\text{cm}^{-3}$	1.9792E-08					
$^{135}\text{Xe}$ absorption cross-section at a pebble irradiation of 1 500 MWd/Te	barns	1.0800E+06					
$\rho^{232}$	–	0.33380					
$\delta^{233}$	–	0.051605					
$\delta^{232}$	–	0.0001366					
C	–	0.21176					

As in the previous phases, where a spherical outer boundary is used, a significant difference is found between Participant A's deterministic and Monte Carlo reactivities due to the boundary conditions. This is again the result of using an isotropic flux boundary condition as opposed to a reflective boundary condition at the edge of the sphere.

There is close agreement ( $1.4645 - 1.46068 = 382$  pcm) between the deterministic evaluations of the cell reactivity at 193.6 K provided by Participants A and F. Their deterministic evaluation of cell reactivity at 1 000 K provided are also in agreement ( $1.46163 - 1.46114 = 49$  pcm). This indicates that the deterministic temperature coefficients calculated by these two participants are consistent.

The Monte Carlo calculations from Participant A indicate that changing the temperature from 293.6 K to 1 000 K leads to a small ( $100 \pm 71$  pcm) positive change in cell reactivity, which is also observed in the deterministic calculation from Participant A. The deterministic calculations from Participant F, however, indicate a small (287 pcm) decrease in cell reactivity for the same change. These opposite results may be a result of differences in the nuclear data used by these participants.

### 3.5.2 Phase 5b: Reactivities and reaction rates

**Table 3.42. Phase 5b – Monte Carlo calculations**

Parameter	Units	A	B	C	D	E	F
$k_{\text{inf}}$ with zero buckling and at $T = 293.6$ K	–	$1.4617 \pm 50$ pcm			1.46778		$1.46470 \pm 34$ pcm
$B^2_{\text{cr}}$ at $T = 293.6$ K	$\text{cm}^{-2}$	9.998E-05			9.83E-5		
$k_{\text{inf}}(B^2_{\text{cr}})$ at $T = 293.6$ K	–				1.4599		
$M^2$ at $T = 293.6$ K	$\text{cm}^2$				4565.1		
$k_{\text{inf}}$ with zero buckling and at $T = 1 000$ K	–	$1.4621 \pm 50$ pcm			1.4527		$1.46127 \pm 26$ pcm
$k_{\text{eff}}(B^2_{\text{cr}})$ at $T = 1 000$ K, using $B^2_{\text{cr}}$ at $T = 239.6$ K	–	$0.8659 \pm 100$ pcm			0.89624		
$B^2_{\text{cr}}$ at $T = 1 000$ K	$\text{cm}^{-2}$	6.929E-05			7.35E-5		
$k_{\text{inf}}(B^2_{\text{cr}})$ at $T = 1 000$ K	–				1.4543		
$M^2$ at $T = 1 000$ K	$\text{cm}^2$				6141.0		
Reactivity at a pebble irradiation of 1 500 MWd/te	–				0.96210		
$^{135}\text{Xe}$ number density at a pebble irradiation of 1 500 MWd/te	$\times 10^{24}$ atoms $\text{cm}^{-3}$				1.95E-08		
$^{135}\text{Xe}$ absorption cross-section at a pebble irradiation of 1 500 MWd/te	barns				( $E < 0.625\text{eV}$ ) 1.54044E+6 ( $E > 0.625\text{eV}$ ) 329.98		
$\rho^{232}$	–						
$\delta^{233}$	–				0.30139		
$\delta^{232}$	–				0.04906		
C	–				0.000152		

**Table 3.41. Phase 5b – deterministic calculations**

Parameter	Units	A	B	C	D	E	F
$k_{inf}$ with zero buckling and at T = 293.6 K	–	1.46066					
$B_{cr}^2$ at T = 293.6 K	cm <sup>-2</sup>	1.278E-04					
$k_{inf}(B_{cr}^2)$ at T = 293.6 K	–	1.45313					
$M^2$ at T = 293.6 K	cm <sup>2</sup>	3546.6					
$k_{inf}$ with zero buckling and at T = 1 000 K	–	1.46010					
$k_{eff}(B_{cr}^2)$ at T = 1 000 K, using $B_{cr}^2$ at T = 239.6 K	–	0.86210					
$B_{cr}^2$ at T = 1 000 K	cm <sup>-2</sup>	8.742E-05					
$k_{inf}(B_{cr}^2)$ at T = 1 000 K	–	1.45098					
$M^2$ at T = 1 000 K	cm <sup>2</sup>	5159.0					
Reactivity at a pebble irradiation of 1 500 MWd/te	–	1.39580					
<sup>135</sup> Xe number density at a pebble irradiation of 1 500 MWd/te	x10 <sup>24</sup> atoms cm <sup>-3</sup>	1.9792E-08					
<sup>135</sup> Xe absorption cross-section at a pebble irradiation of 1 500 MWd/te	barns	1.0802E+06					
$\rho^{232}$	–	3.3342E-01					
$\delta^{233}$	–	5.1553E-02					
$\delta^{232}$	–	1.3674E-04					
C	–	2.1171E-01					

Participants A's Phase 5a and Phase 5b deterministic calculations are in close agreement. There is also good agreement ( $1.4617 - 1.46068 = 102 \pm 50$  pcm) between the cell reactivity at 293.6 K evaluated in Participant A's deterministic and Monte Carlo calculations.

The Monte Carlo results from Participants A and F are in reasonable agreement (300 pcm at 293.6 K and 83 pcm at 1 000 K). As in Phase 5a, Participant A's Monte Carlo calculations indicate a small positive effect on reactivity due to increasing the temperature from 293.6 K to 1 000 K. However, Participant A's deterministic calculation for Phase 5b shows a small decrease in reactivity with increased temperature.

### 3.5.3 Spectra

A comparison between the deterministic and Monte Carlo spectra of Participant A is given in Figure 3.15. There is generally good agreement between the spectra, apart from a slight discrepancy at the low-energy peak.

Figure 3.16 shows a comparison of the deterministic spectra for Phase 5a calculated by Participants A and F.

### 3.5.4 Burn-up

The results from Participant A's deterministic Phase 5a and Phase 5b burn-up calculations are essentially identical.

**Table 3.44. Phase 5a – Monte Carlo calculations – results from Participant D**

*Units are  $\times 10^{24}$  atoms cm $^{-3}$*

Nuclide	0 MWd/te	10 000 MWd/te	20 000 MWd/te	30 000 MWd/te	40 000 MWd/te
$^{241}\text{Am}$	0.000E+00	1.490E-23	2.410E-20	1.850E-18	4.310E-17
$^{242m}\text{Am}$	0.000E+00	4.750E-26	1.390E-22	1.450E-20	4.070E-19
$^{243}\text{Am}$	0.000E+00	1.370E-24	6.650E-21	1.110E-18	5.140E-17
$^{242}\text{Cm}$	0.000E+00	1.810E-25	8.060E-22	1.130E-19	4.180E-18
$^{243}\text{Cm}$	0.000E+00	7.800E-29	7.890E-25	1.910E-22	1.070E-20
$^{244}\text{Cm}$	0.000E+00	3.160E-27	4.140E-23	1.230E-20	8.890E-19
$^{245}\text{Cm}$	0.000E+00	1.840E-30	5.200E-26	2.330E-23	2.420E-21
$^{237}\text{Np}$	0.000E+00	1.110E-12	3.370E-11	2.520E-10	1.130E-09
$^{239}\text{Np}$	–	–	–	–	–
$^{233}\text{Pa}$	–	–	–	–	–
$^{238}\text{Pu}$	0.000E+00	5.580E-15	5.090E-13	7.110E-12	4.880E-11
$^{239}\text{Pu}$	0.000E+00	1.120E-16	1.970E-14	4.130E-13	3.770E-12
$^{240}\text{Pu}$	0.000E+00	3.520E-18	1.400E-15	5.010E-14	6.960E-13
$^{241}\text{Pu}$	0.000E+00	6.950E-20	5.930E-17	3.260E-15	6.290E-14
$^{242}\text{Pu}$	0.000E+00	1.060E-21	2.090E-18	2.010E-16	6.100E-15
$^{232}\text{Th}$	2.190E-02	2.190E-02	2.180E-02	2.170E-02	2.160E-02
$^{233}\text{U}$	1.770E-03	1.500E-03	1.260E-03	1.030E-03	8.210E-04
$^{234}\text{U}$	0.000E+00	2.510E-05	4.920E-05	7.190E-05	9.210E-05
$^{235}\text{U}$	0.000E+00	3.980E-07	1.630E-06	3.710E-06	6.710E-06
$^{236}\text{U}$	0.000E+00	3.660E-09	3.390E-08	1.340E-07	3.760E-07
$^{237}\text{U}$	0.000E+00	3.020E-12	4.750E-11	2.480E-10	9.090E-10
$^{238}\text{U}$	0.000E+00	7.940E-14	2.850E-12	2.550E-11	1.410E-10

**Table 3.45. Phase 5a – Monte Carlo calculations – results from Participant A**

Units are  $\times 10^{24}$  atoms  $\text{cm}^{-3}$

Nuclide	0 MWd/te	10 000 MWd/te	20 000 MWd/te	30 000 MWd/te	40 000 MWd/te
$^{241}\text{Am}$	–	–	1.2208E-19	2.9042E-18	5.7578E-17
$^{242m}\text{Am}$	–	–	–	–	5.2853E-19
$^{243}\text{Am}$	–	1.5861E-19	2.3867E-19	1.9677E-18	6.3802E-17
$^{242}\text{Cm}$	–	1.2375E-19	1.5207E-19	5.3034E-19	1.1992E-17
$^{243}\text{Cm}$	–	–	–	–	1.1198E-19
$^{244}\text{Cm}$	–	1.0697E-19	1.1785E-19	1.5439E-19	1.3112E-18
$^{245}\text{Cm}$	–	–	–	–	–
$^{237}\text{Np}$	–	9.9496E-13	2.9057E-11	2.1229E-10	8.9948E-10
$^{239}\text{Np}$	–	2.0318E-17	1.0003E-15	1.0589E-14	6.4397E-14
$^{233}\text{Pa}$	–	4.4700E-05	7.8933E-05	1.0861E-04	1.3858E-04
$^{238}\text{Pu}$	–	1.3659E-14	9.0152E-13	1.1152E-11	7.1504E-11
$^{239}\text{Pu}$	–	2.1454E-16	2.8227E-14	5.2146E-13	4.4200E-12
$^{240}\text{Pu}$	–	8.9592E-18	2.6164E-15	8.2270E-14	1.0675E-12
$^{241}\text{Pu}$	–	2.6592E-19	1.0808E-16	5.0540E-15	8.6047E-14
$^{242}\text{Pu}$	–	1.2465E-19	4.5805E-18	3.6357E-16	9.7929E-15
$^{232}\text{Th}$	2.1947E-02	2.1891E-02	2.1827E-02	2.1752E-02	2.1663E-02
$^{233}\text{U}$	1.7667E-03	1.5044E-03	1.2602E-03	1.0311E-03	8.1643E-04
$^{234}\text{U}$	–	2.5773E-05	5.1248E-05	7.6114E-05	1.0006E-04
$^{235}\text{U}$	–	3.8310E-07	1.5857E-06	3.6722E-06	6.6604E-06
$^{236}\text{U}$	–	3.5405E-09	3.3105E-08	1.3213E-07	3.7556E-07
$^{237}\text{U}$	–	2.6957E-12	4.0229E-11	2.0526E-10	6.9980E-10
$^{238}\text{U}$	–	7.0546E-14	2.4283E-12	2.1371E-11	1.1246E-10

**Table 3.46. Phase 5b – Monte Carlo calculations – results from Participant D**

Units are  $\times 10^{24}$  atoms cm $^{-3}$

Nuclide	0 MWd/te	10 000 MWd/te	20 000 MWd/te	30 000 MWd/te	40 000 MWd/te
$^{241}\text{Am}$	0.00E+00	1.48E-23	2.32E-20	1.84E-18	4.31E-17
$^{242m}\text{Am}$	0.00E+00	4.73E-26	1.34E-22	1.44E-20	4.05E-19
$^{243}\text{Am}$	0.00E+00	1.44E-24	6.54E-21	1.11E-18	4.93E-17
$^{242}\text{Cm}$	0.00E+00	1.81E-25	7.77E-22	1.12E-19	4.15E-18
$^{243}\text{Cm}$	0.00E+00	7.79E-29	7.69E-25	1.88E-22	1.06E-20
$^{244}\text{Cm}$	0.00E+00	3.34E-27	4.06E-23	1.22E-20	8.50E-19
$^{245}\text{Cm}$	0.00E+00	1.98E-30	4.97E-26	2.40E-23	2.29E-21
$^{237}\text{Np}$	0.00E+00	1.08E-12	3.29E-11	2.61E-10	1.12E-09
$^{239}\text{Np}$	–	–	–	–	–
$^{233}\text{Pa}$	–	–	–	–	–
$^{238}\text{Pu}$	0.00E+00	5.49E-15	4.97E-13	7.18E-12	4.93E-11
$^{239}\text{Pu}$	0.00E+00	1.11E-16	1.93E-14	4.13E-13	3.83E-12
$^{240}\text{Pu}$	0.00E+00	3.47E-18	1.36E-15	4.95E-14	7.07E-13
$^{241}\text{Pu}$	0.00E+00	6.92E-20	5.71E-17	3.26E-15	6.33E-14
$^{242}\text{Pu}$	0.00E+00	1.05E-21	2.02E-18	2.00E-16	6.10E-15
$^{232}\text{Th}$	2.19E-02	2.19E-02	2.18E-02	2.17E-02	2.16E-02
$^{233}\text{U}$	1.77E-03	1.50E-03	1.26E-03	1.03E-03	8.21E-04
$^{234}\text{U}$	0.00E+00	2.51E-05	4.92E-05	7.18E-05	9.21E-05
$^{235}\text{U}$	0.00E+00	3.95E-07	1.63E-06	3.74E-06	6.68E-06
$^{236}\text{U}$	0.00E+00	3.63E-09	3.39E-08	1.34E-07	3.76E-07
$^{237}\text{U}$	0.00E+00	2.96E-12	4.64E-11	2.61E-10	8.80E-10
$^{238}\text{U}$	0.00E+00	7.78E-14	2.78E-12	2.63E-11	1.39E-10

**Table 3.47. Phase 5b – deterministic calculations – results from Participant A**

Units are  $\times 10^{24}$  atoms  $\text{cm}^{-3}$

Nuclide	0 MWd/te	10 000 MWd/te	20 000 MWd/te	30 000 MWd/te	40 000 MWd/te
$^{241}\text{Am}$	–	–	1.2208E-19	2.9041E-18	5.7577E-17
$^{242m}\text{Am}$	–	–	–	–	5.2852E-19
$^{243}\text{Am}$	–	1.5861E-19	2.3867E-19	1.9676E-18	6.3800E-17
$^{242}\text{Cm}$	–	1.2375E-19	1.5207E-19	5.3033E-19	1.1992E-17
$^{243}\text{Cm}$	–	–	–	–	1.1198E-19
$^{244}\text{Cm}$	–	1.0697E-19	1.1785E-19	1.5439E-19	1.3111E-18
$^{245}\text{Cm}$	–	–	–	–	1.0000E-19
$^{237}\text{Np}$	–	9.9493E-13	2.9057E-11	2.1228E-10	8.9948E-10
$^{239}\text{Np}$	–	2.0317E-17	1.0002E-15	1.0588E-14	6.4397E-14
$^{233}\text{Pa}$	–	4.4700E-05	7.8933E-05	1.0862E-04	1.3858E-04
$^{238}\text{Pu}$	–	1.3658E-14	9.0149E-13	1.1152E-11	7.1503E-11
$^{239}\text{Pu}$	–	2.1453E-16	2.8226E-14	5.2146E-13	4.4200E-12
$^{240}\text{Pu}$	–	8.9589E-18	2.6163E-15	8.2269E-14	1.0675E-12
$^{241}\text{Pu}$	–	2.6591E-19	1.0807E-16	5.0538E-15	8.6045E-14
$^{242}\text{Pu}$	–	1.2465E-19	4.5803E-18	3.6356E-16	9.7927E-15
$^{232}\text{Th}$	2.1947E-02	2.1891E-02	2.1827E-02	2.1752E-02	2.1663E-02
$^{233}\text{U}$	1.7667E-03	1.5044E-03	1.2602E-03	1.0311E-03	8.1643E-04
$^{234}\text{U}$	–	2.5772E-05	5.1248E-05	7.6114E-05	1.0006E-04
$^{235}\text{U}$	–	3.8309E-07	1.5857E-06	3.6722E-06	6.6604E-06
$^{236}\text{U}$	–	3.5405E-09	3.3105E-08	1.3213E-07	3.7556E-07
$^{237}\text{U}$	–	2.6956E-12	4.0228E-11	2.0526E-10	6.9980E-10
$^{238}\text{U}$	–	7.0544E-14	2.4283E-12	2.1371E-11	1.1246E-10

## *Chapter 4*

### CONCLUSIONS

A benchmark inter-comparison of results has been made for a series of cell and whole core configurations relevant to uranium-, plutonium- and thorium-fuelled pebble bed modular reactors.

Contributions to the benchmark have been made by six teams: Serco Assurance (UK), CEA (France), the Nuclear Engineering Department of Hacettepe University (Turkey, two contributions), Nexia Solutions (UK, formerly BNFL R&T, UK) and the Nuclear Science and Technology Division of ORNL (USA).

According to the participant, ENDF/B-V, ENDF/B-VI and JEF2.2 nuclear data have been applied in both Monte Carlo and deterministic analyses of the benchmark.

Generally, participants using the same nuclear data report similar results, however, there are some differences, particularly in relation to the fuel temperature coefficients and the whole core xenon fission product poisoning effect. There is also evidence of good agreement between Monte Carlo and deterministic solutions for some of the participants despite the difficult nature of the problem stochastic geometry.



## REFERENCES

- [1] Hosking, G., T.D. Newton, *Proposed Benchmark Specification for an HTR Fuelled with Reactor Grade Plutonium (or Reactor Grade Pu/Th and U/Th)*, NEA/NSC/DOC(2003)22 (2003).
- [2] Coste, M., *et al.*, “Self-shielding Calculations by APOLLO2 Code for Fuel Pins with a Temperature Distribution”, *International Conference on Mathematical Methods and Supercomputing for Nuclear Applications*, Saratoga Springs, New York, 5-9 October 1997.
- [3] Newton, T.D., J.L. Hutton, “The Next Generation WIMS Lattice Code: WIMS9”, *PHYSOR 2002*, Seoul, Korea, October 2002.
- [4] Hutton, J.L., Advanced Monte Carlo Features, *PHYSOR 1996*, Japan, September 1996.
- [5] Herbert, A., *et al.*, *APOLLO2: Notice d’Utilisation Version 2.4*, CEA report, SERMA/LENR/RT/98-2478/A (1998).
- [6] Andrieux, C., *Notice d’identification des bibliothèques CEA93.V6 à 172 et 99 groupes*, CEA report, SERMA/LENR/RT/99-2724/A (1999).
- [7] Both, J.P., Y. Pénéliau, “The Monte Carlo Code TRIPOLI-4 and its First Benchmark Interpretations”, *International Conference on the Physics of Reactors PHYSOR 1996*, Mito, Ibaraki, Japan (1996).



## Figures



**Figure 3.1. Phase 1a – Monte Carlo calculation: Critical fuel spectrum normalised to unit integral**

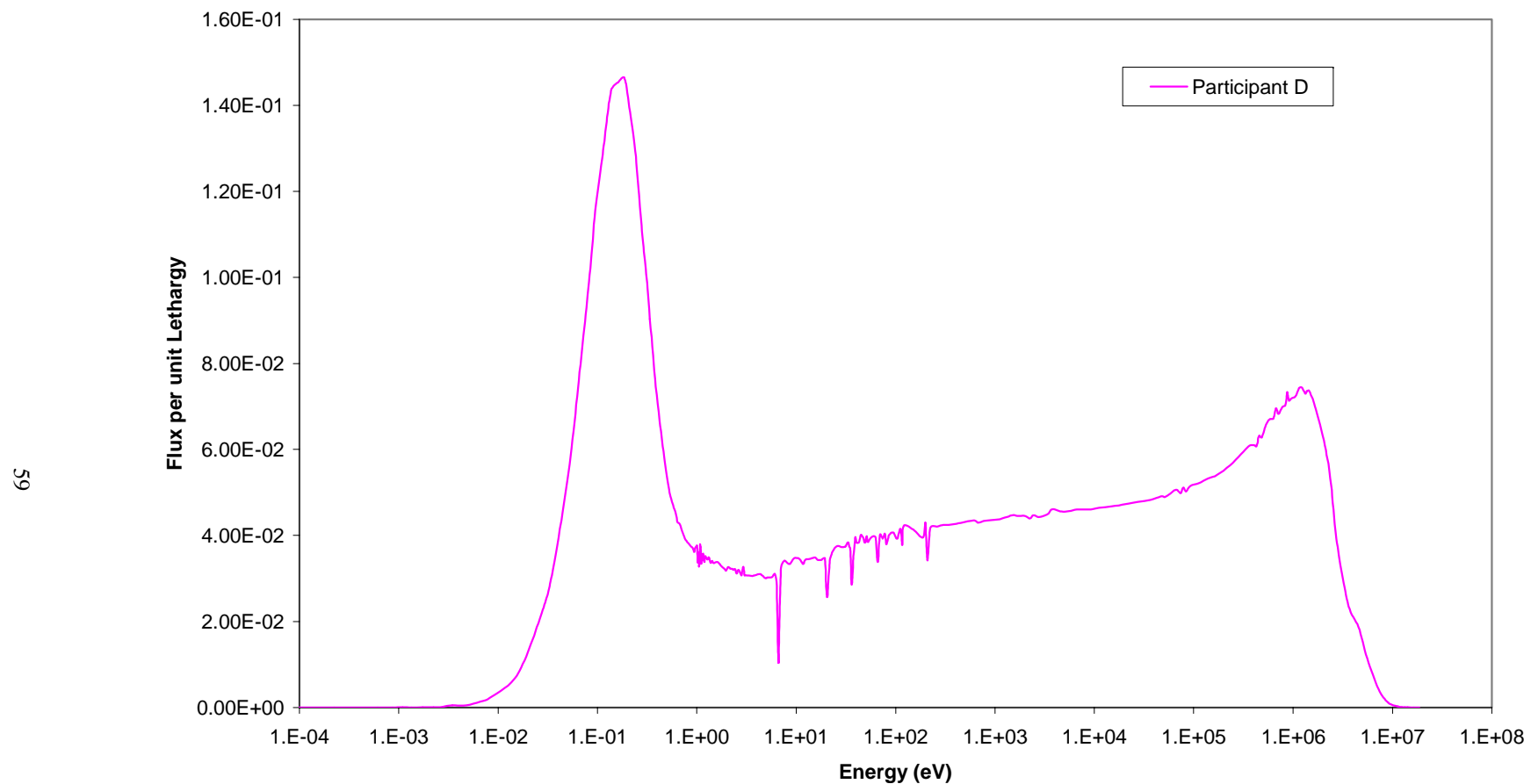


**Figure 3.2. Phase 1a – deterministic calculation: Critical fuel spectrum normalised to unit integral**

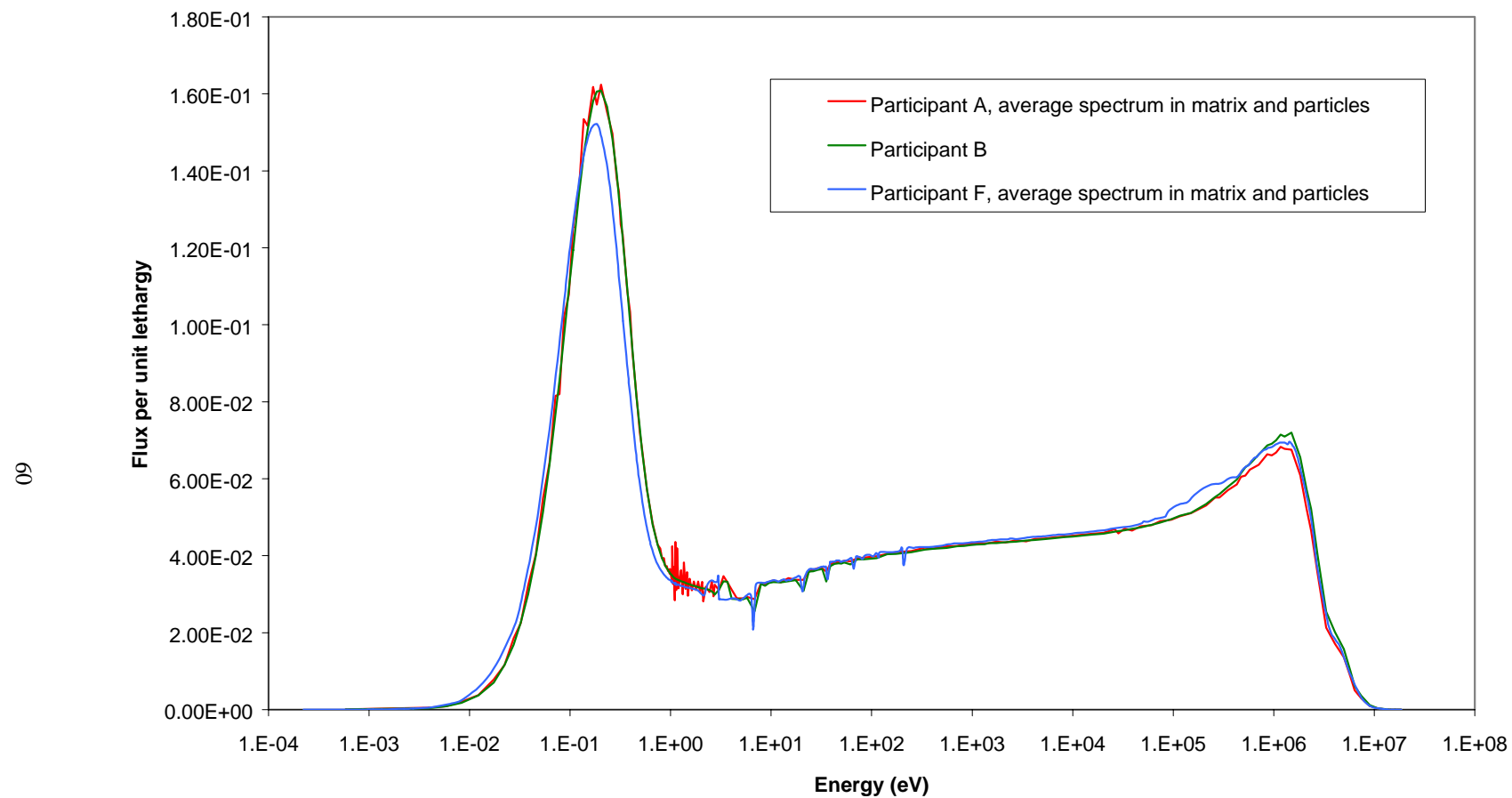


**Figure 3.3. Phase 1b – Monte Carlo calculation: Critical fuel spectrum normalised to unit integral**

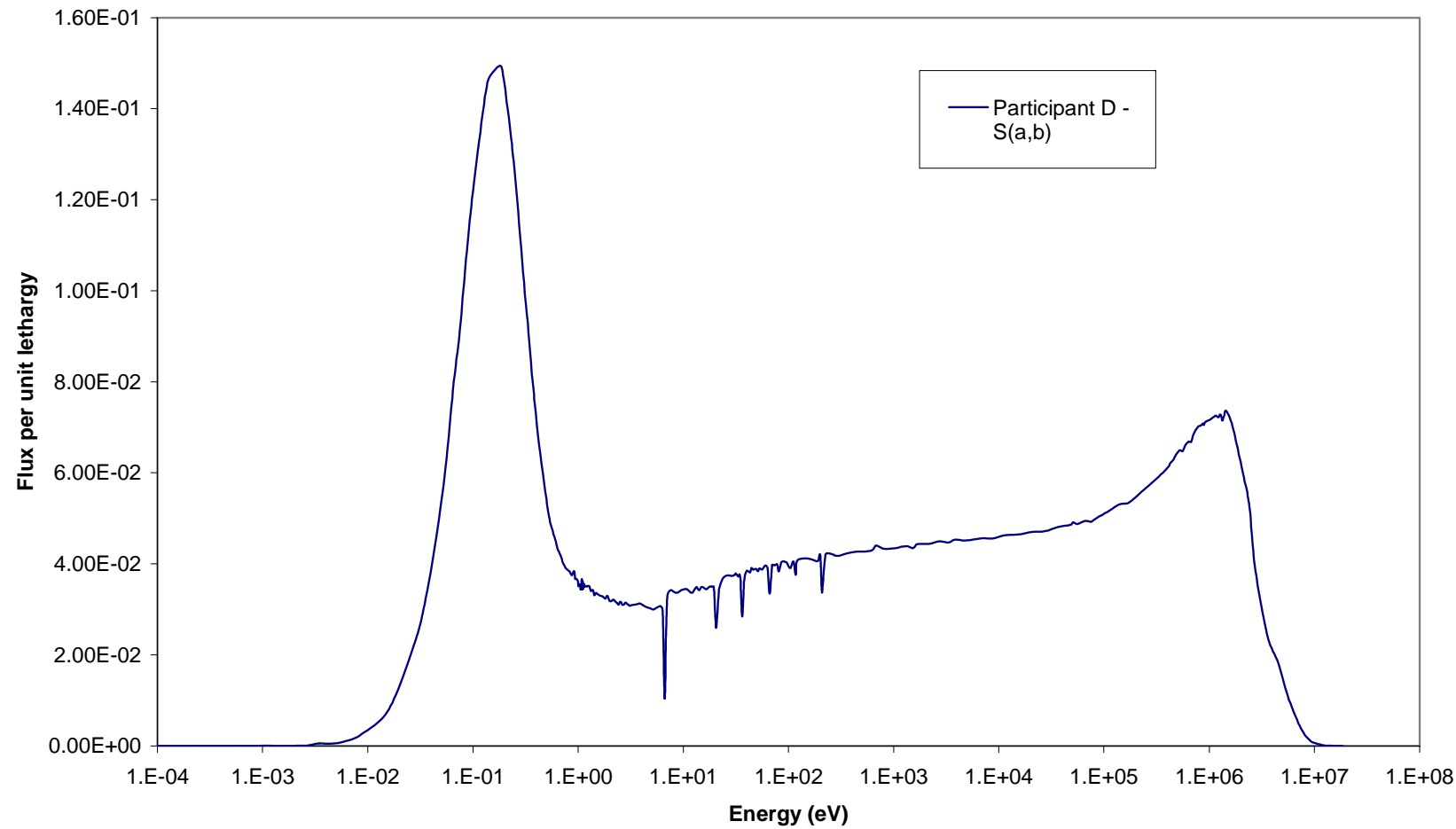


**Figure 3.4. Phase 1b – Monte Carlo calculation: Critical fuel spectrum normalised to unit integral**

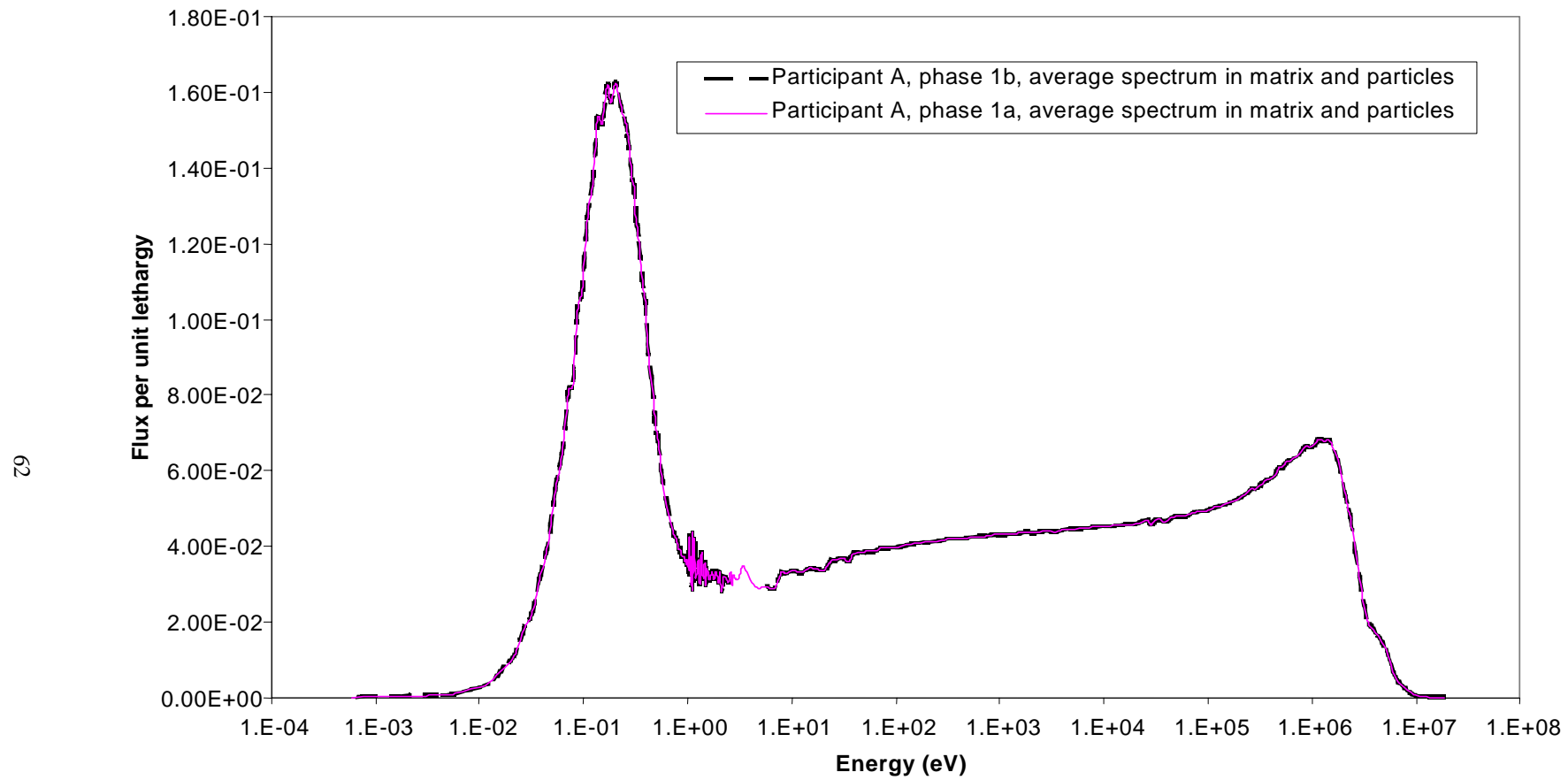


**Figure 3.5. Phase 2a – Monte Carlo calculation: Critical fuel spectrum normalised to unit integral**

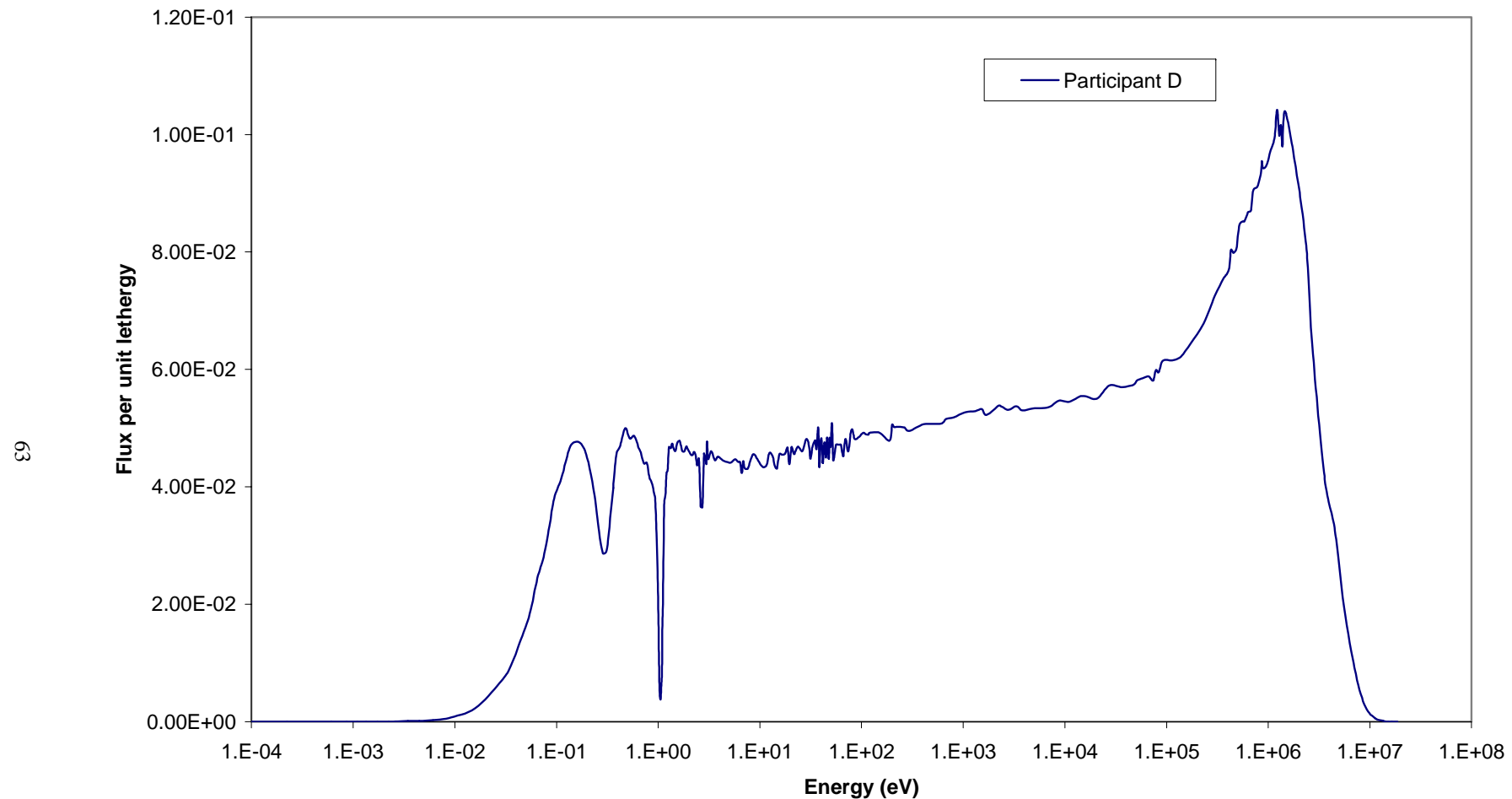


**Figure 3.6. Phase 2a – deterministic calculation: Critical fuel spectrum normalised to unit integral**

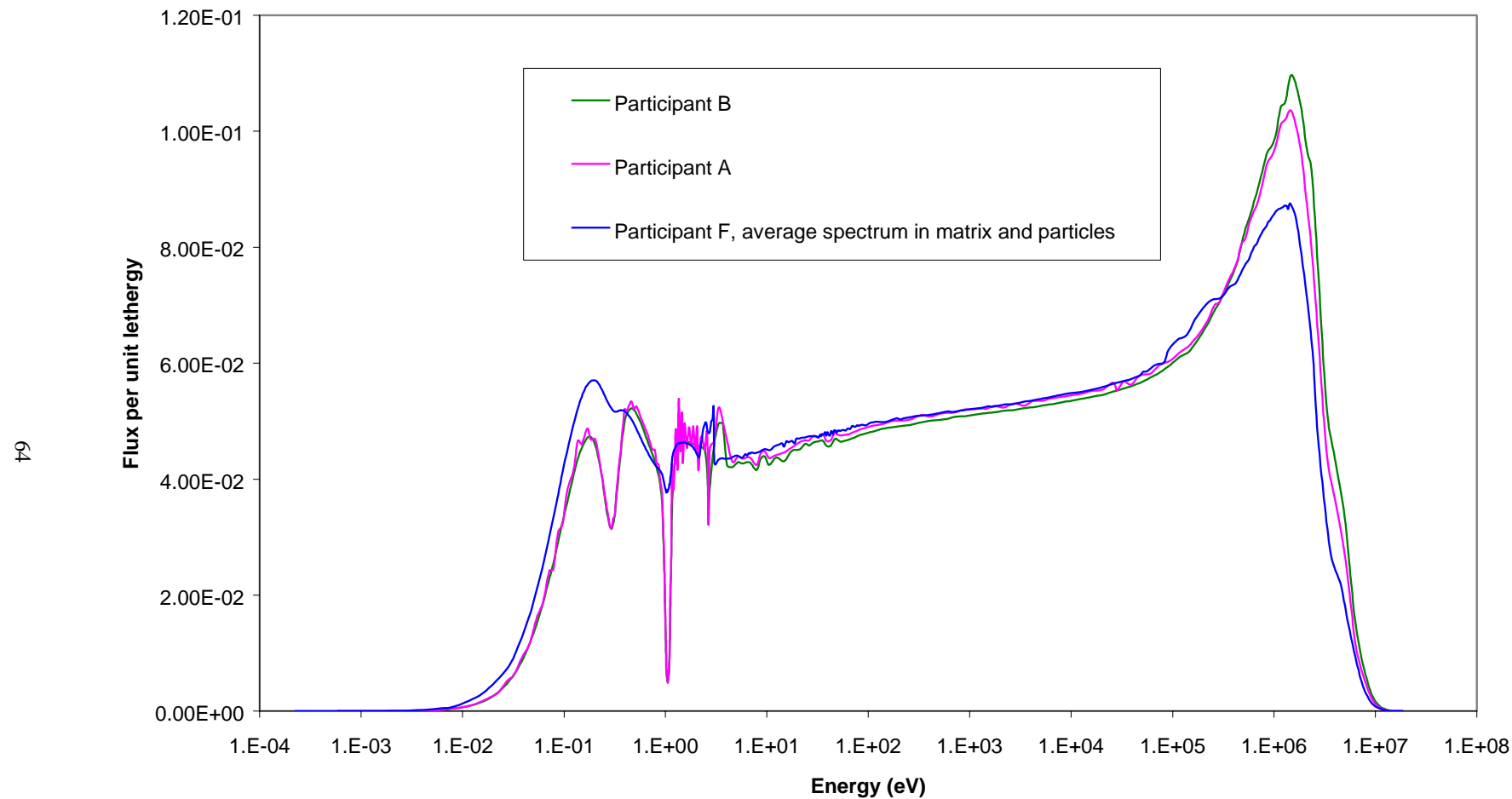


**Figure 3.7. Phase 2b – Monte Carlo calculation: Critical fuel spectrum normalised to unit integral**

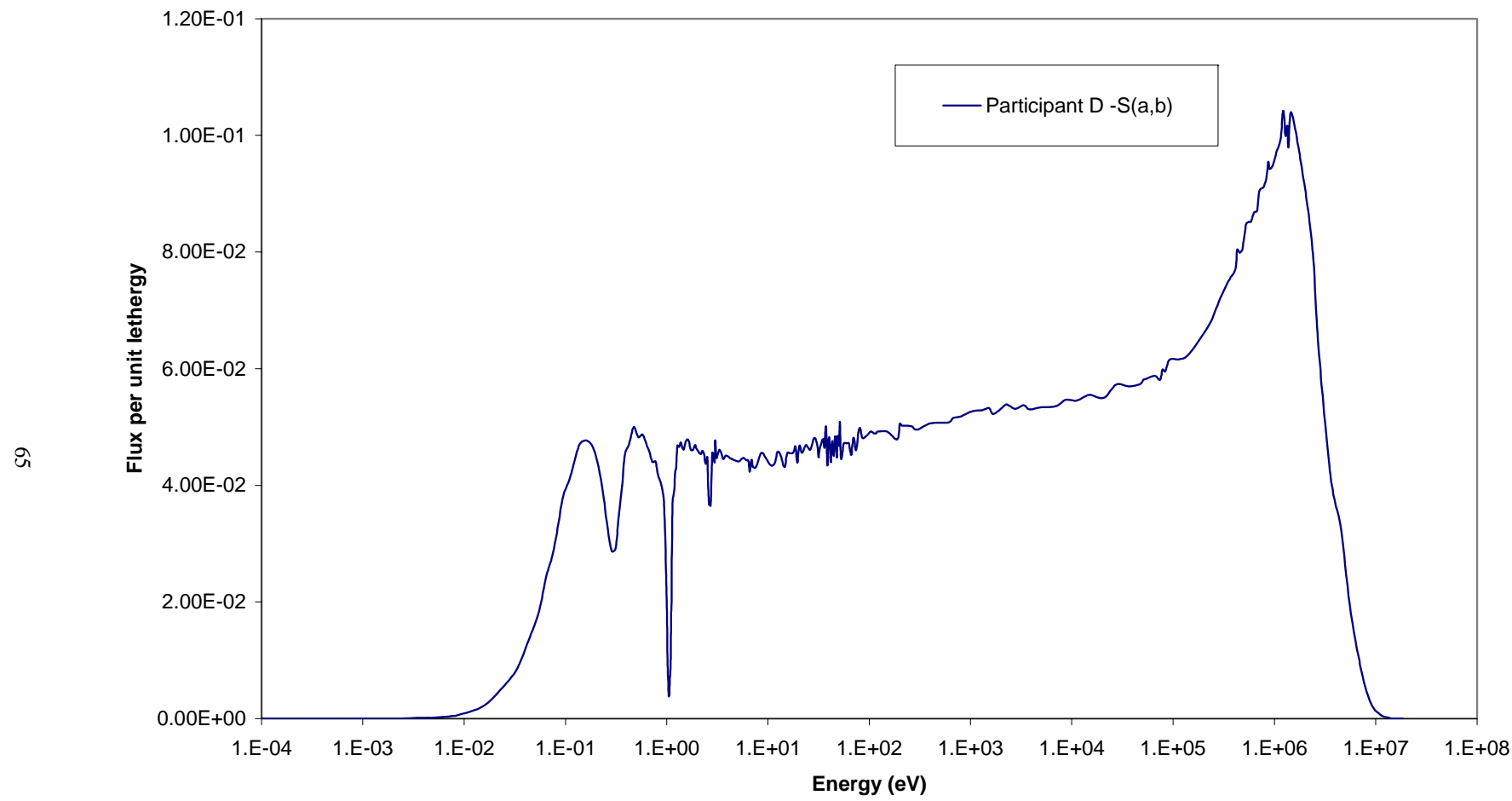


**Figure 3.8. Phase 3 – Monte Carlo calculation: Fuel region spectrum normalised to unit integral**

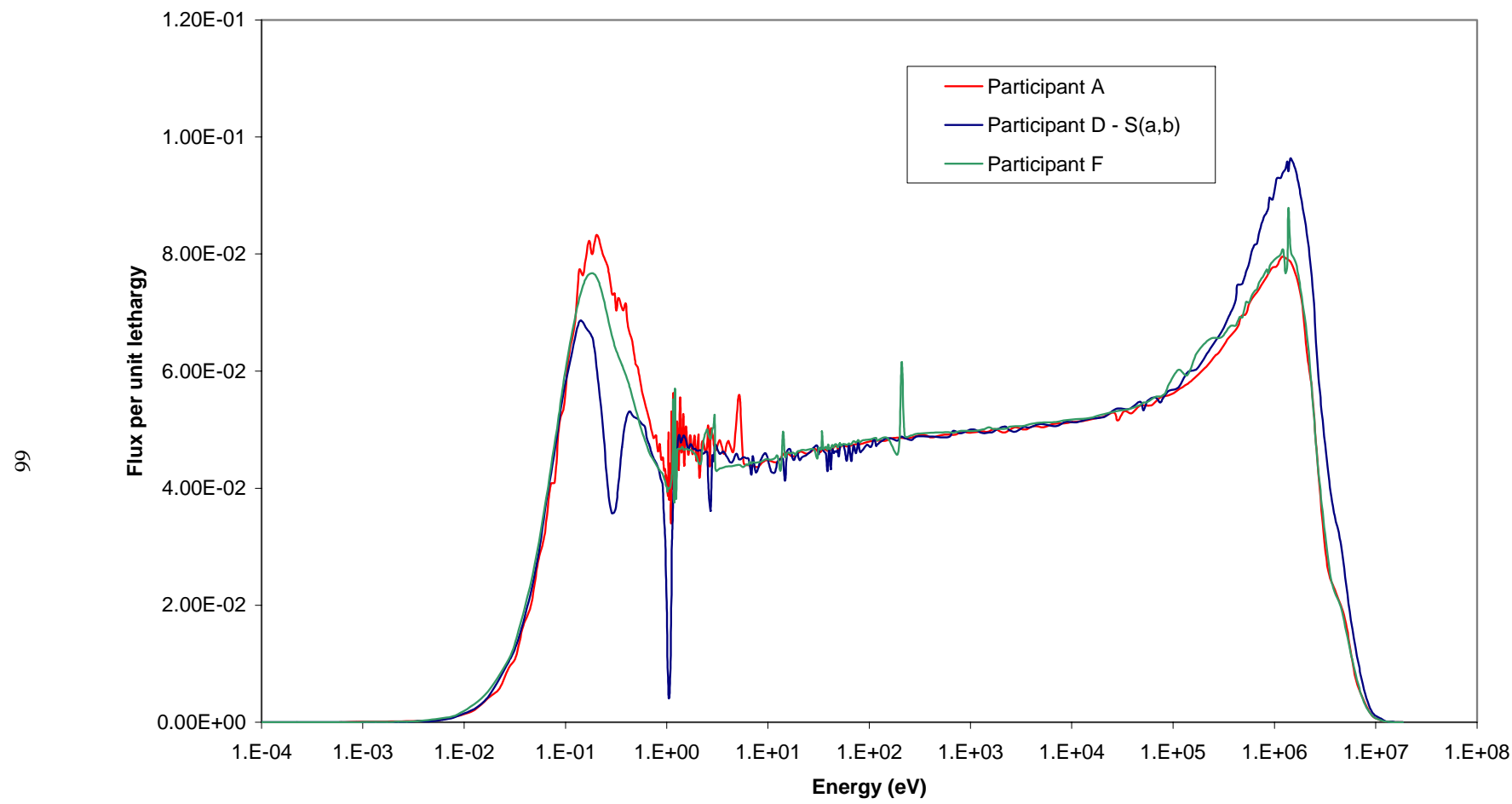
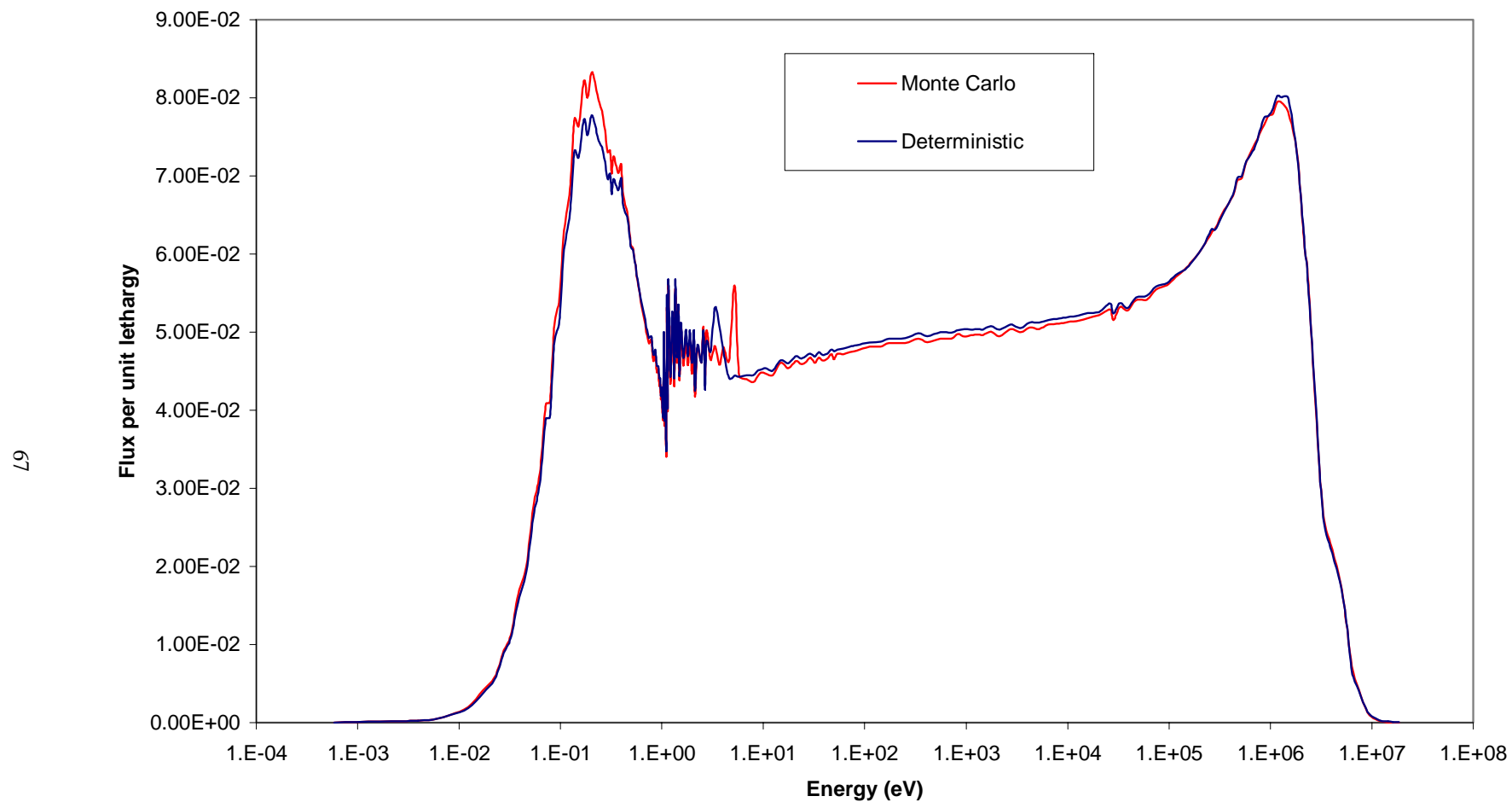
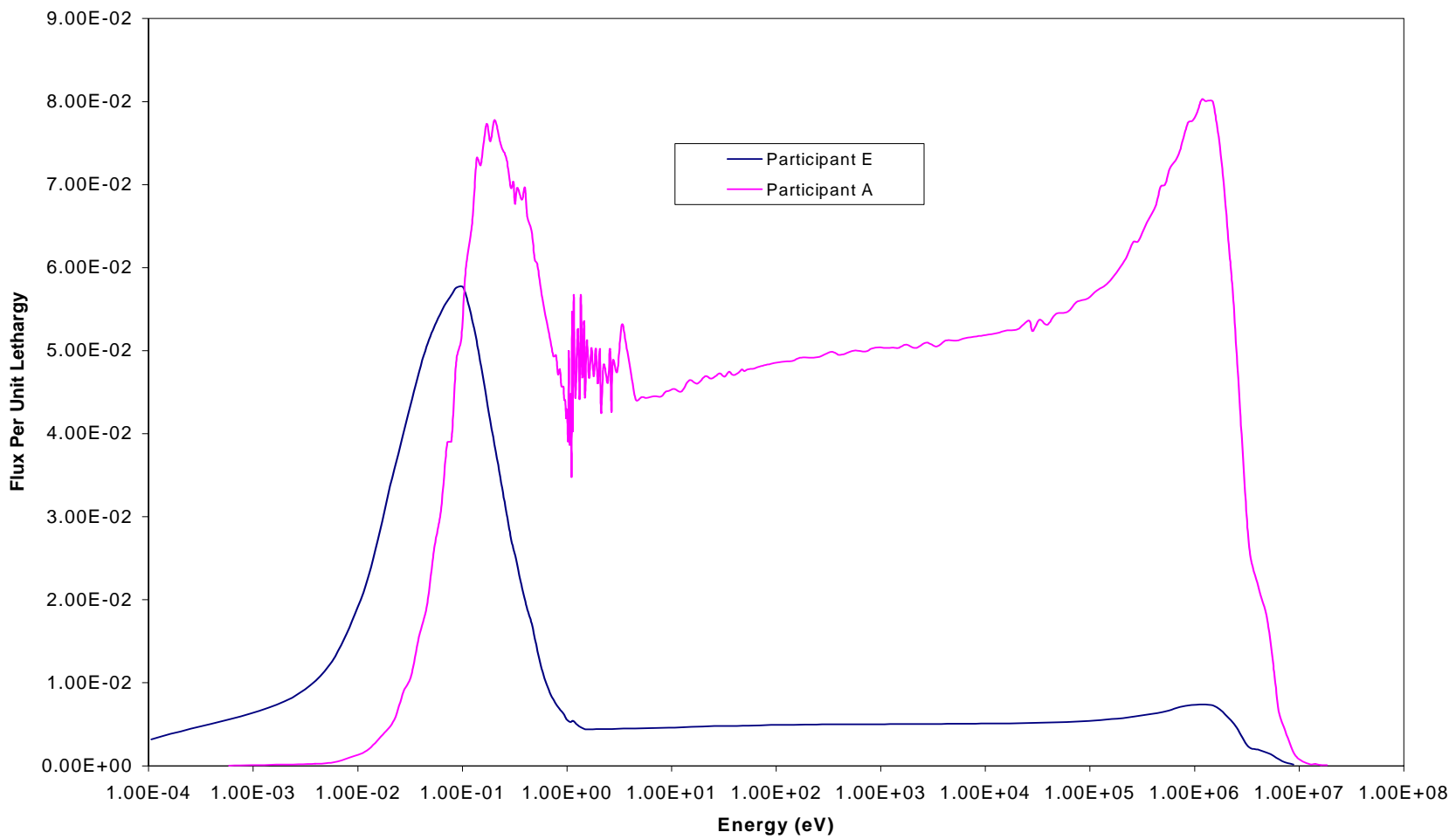


Figure 8

**Figure 3.9. Phase 3 – Serco Assurance Monte Carlo and deterministic fuel region spectra normalised to unit integral**



**Figure 3.10. Phase 3 – deterministic fuel region spectra normalised to unit integral**



**Figure 3.11. Phase 4 – comparison between Monte Carlo spectra of Participants A, D and F**

69

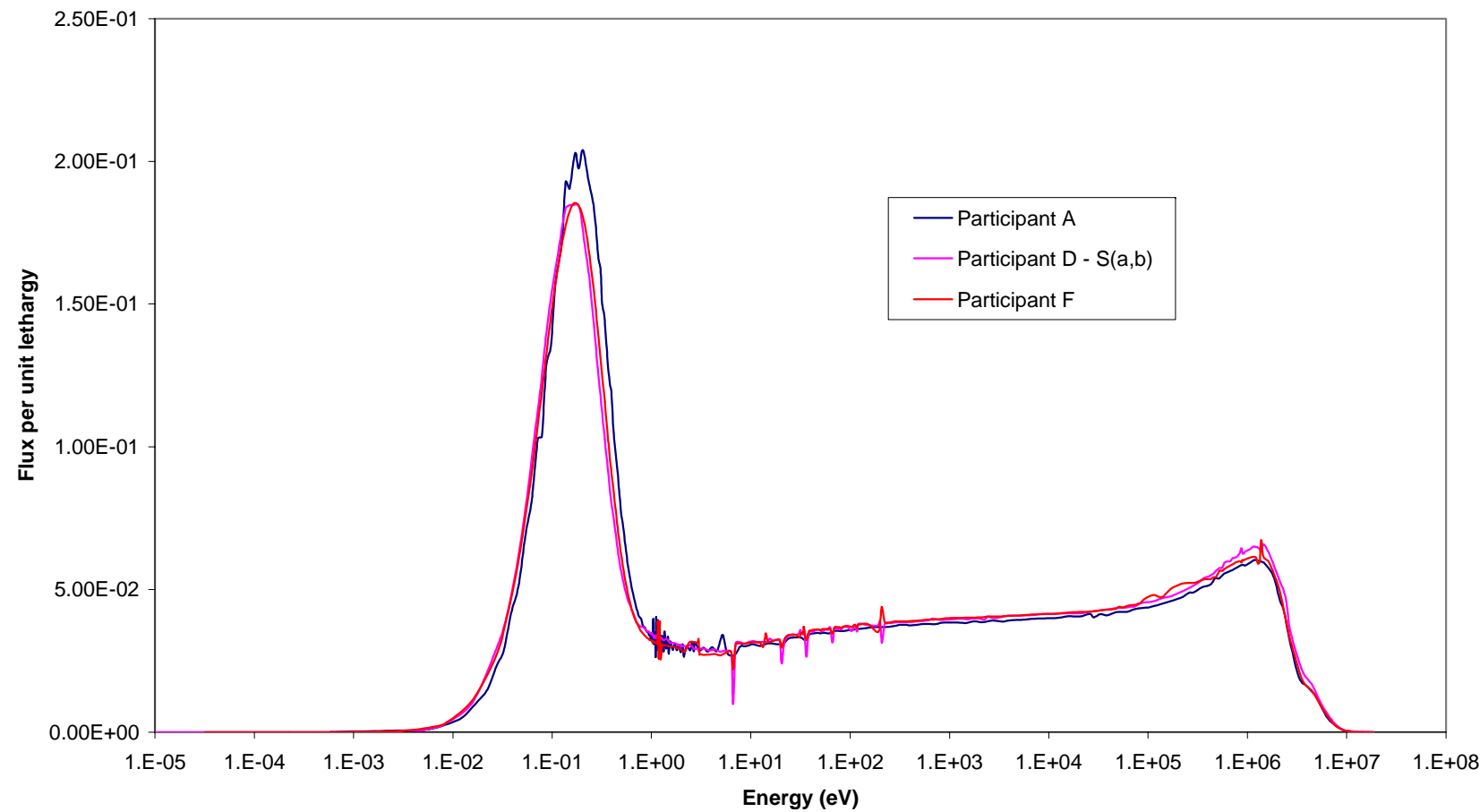


**Figure 3.12. Phase 4 – Serco Assurance Monte Carlo and deterministic fuel region spectra normalised to unit integral (172 energy groups)**

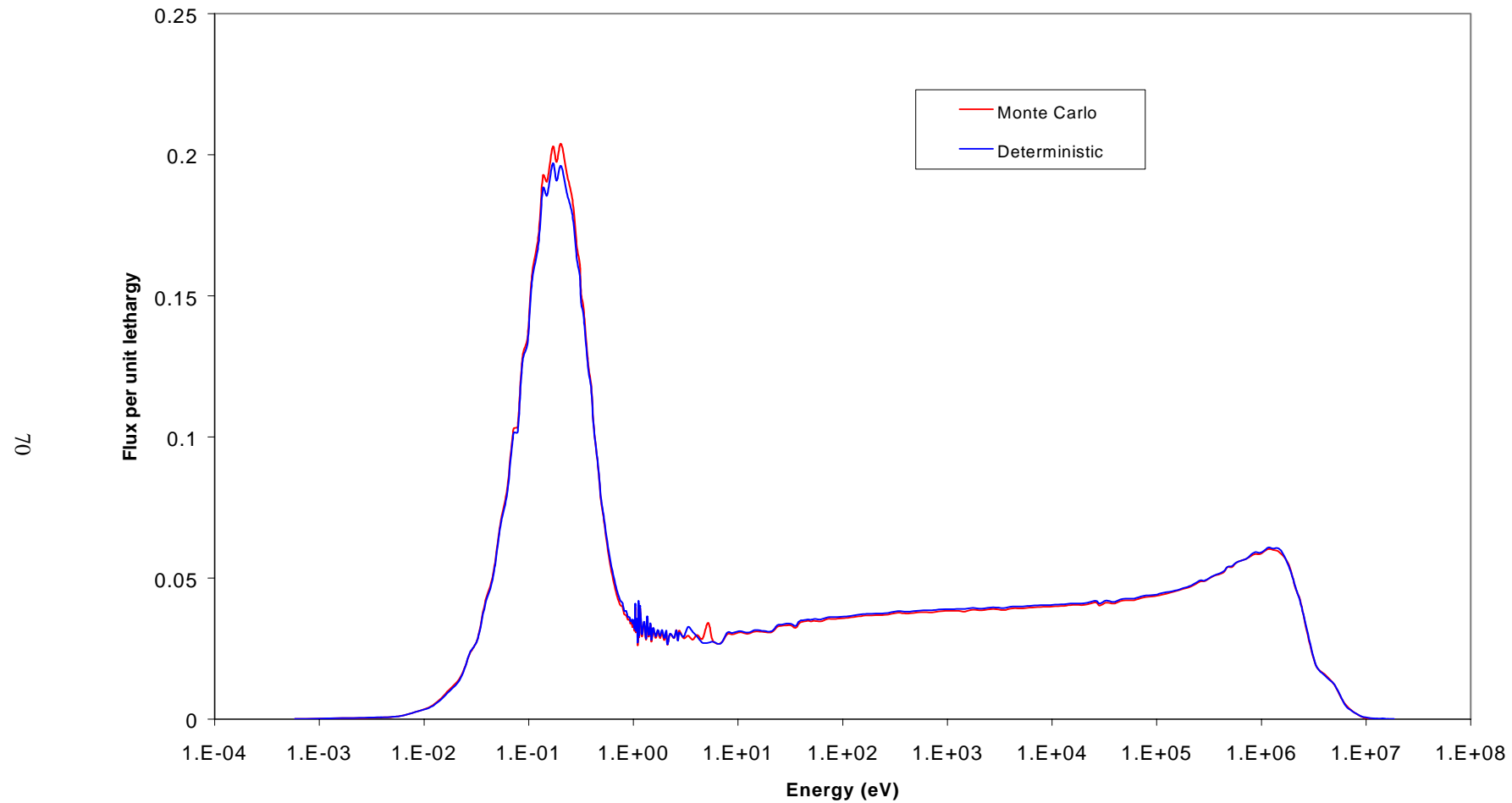


**Figure 3.13. Phase 4 – Serco Assurance Monte Carlo and deterministic fuel region spectra normalised to unit integral (4 energy groups)**

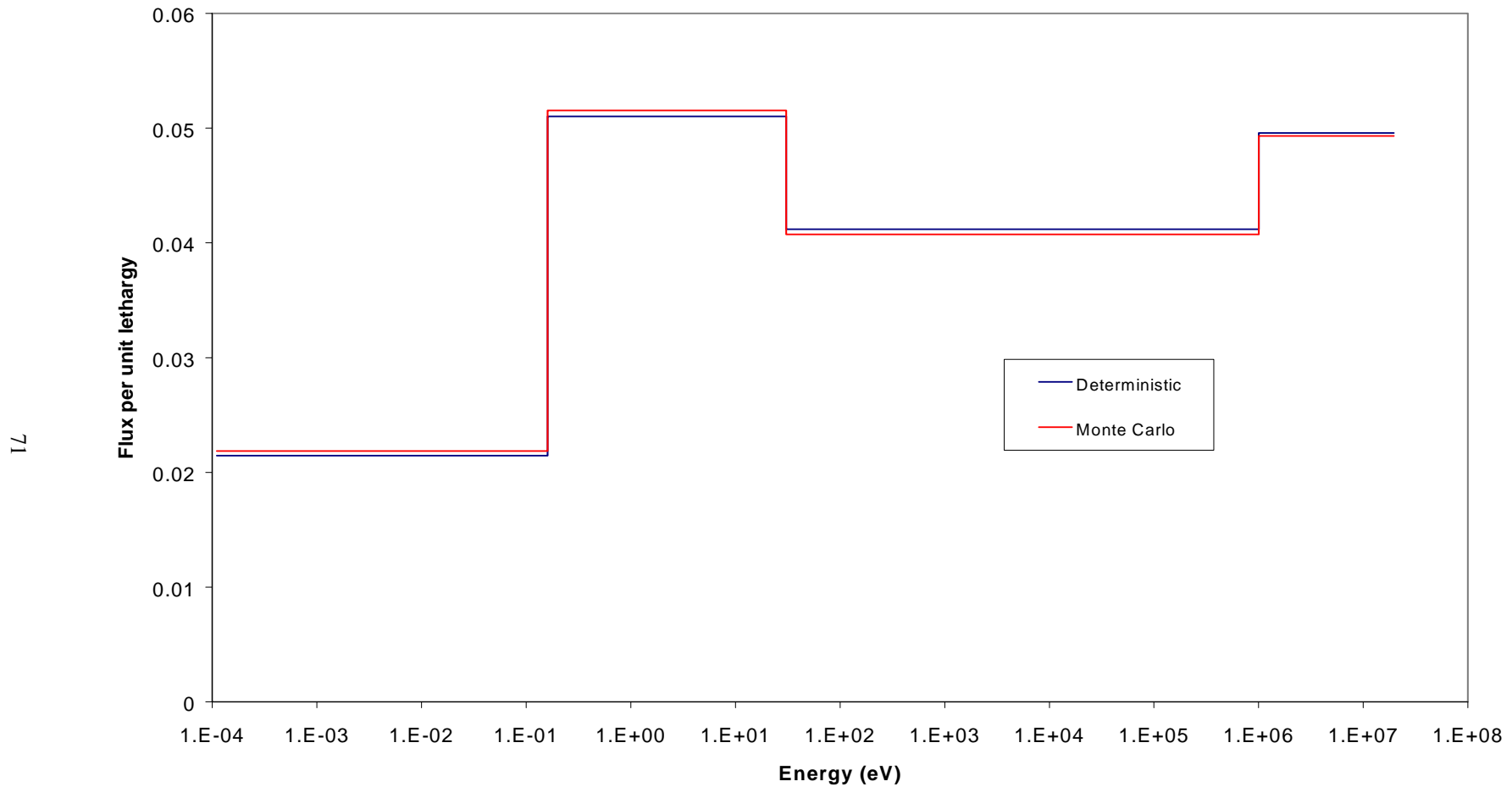


**Figure 3.14. Phase 4 – VSOP fuel region spectrum**

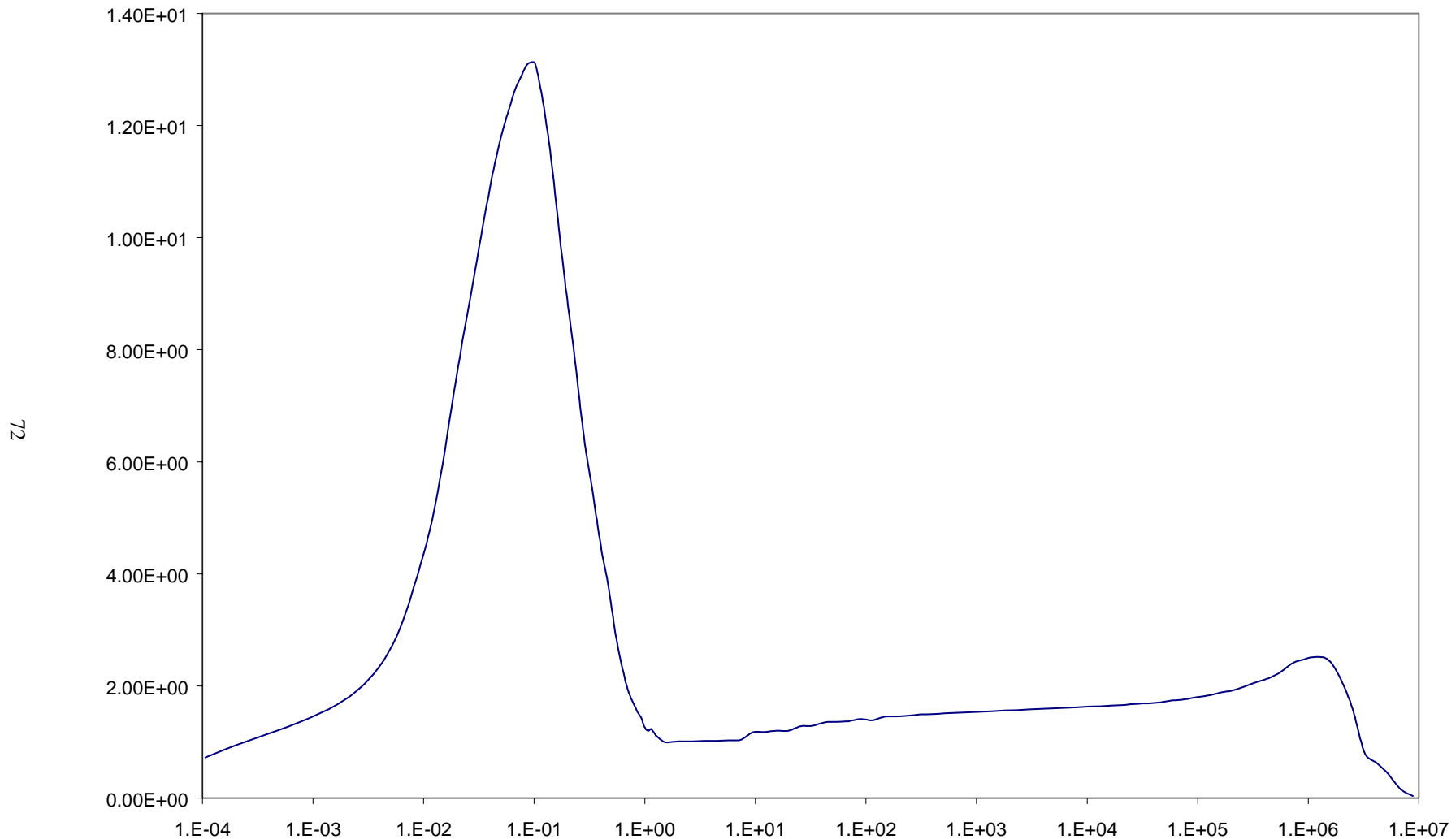


**Figure 3.15. Phase 5 – Serco Assurance deterministic spectra: Comparison between Phase 5a and Phase 5b results**

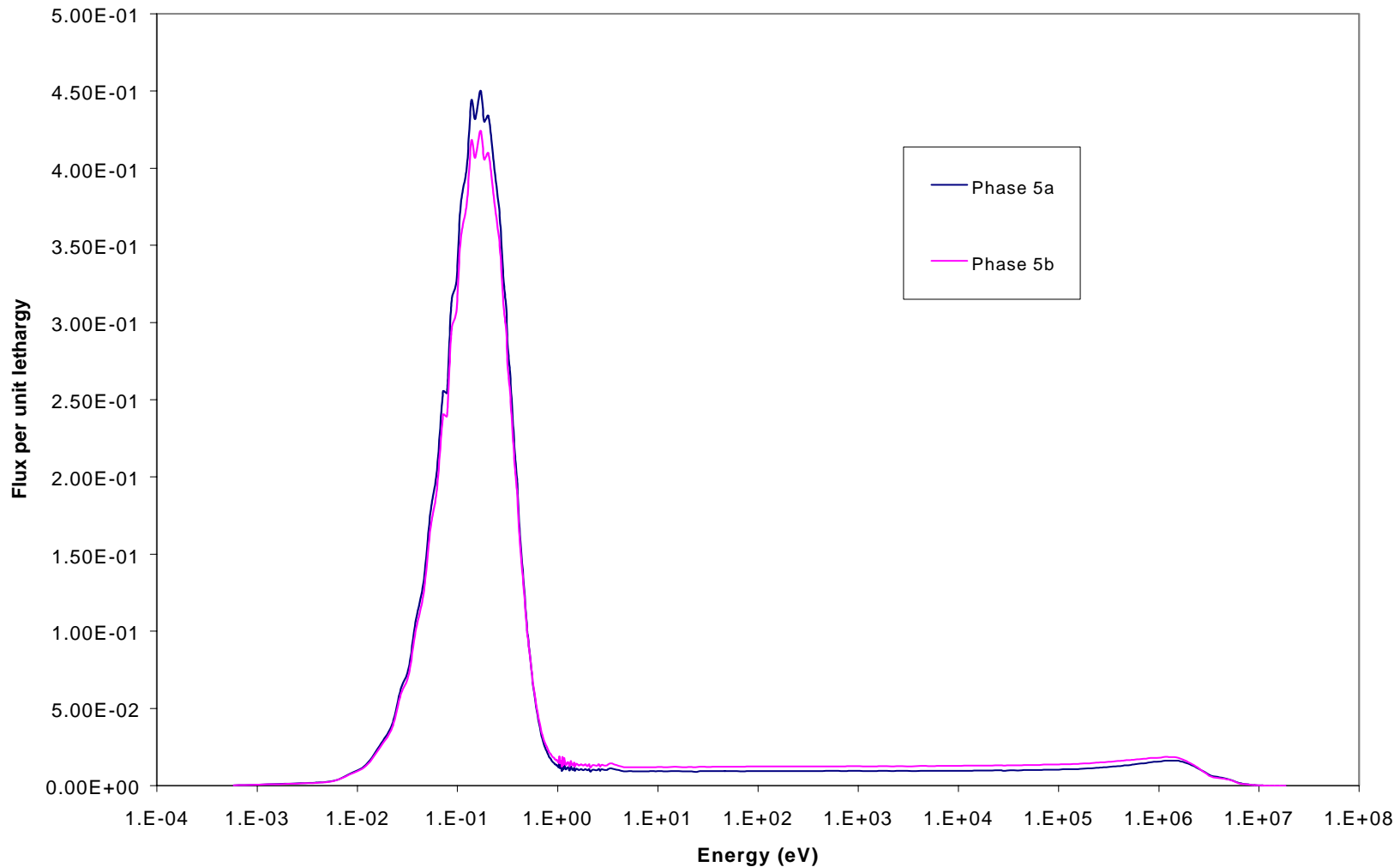
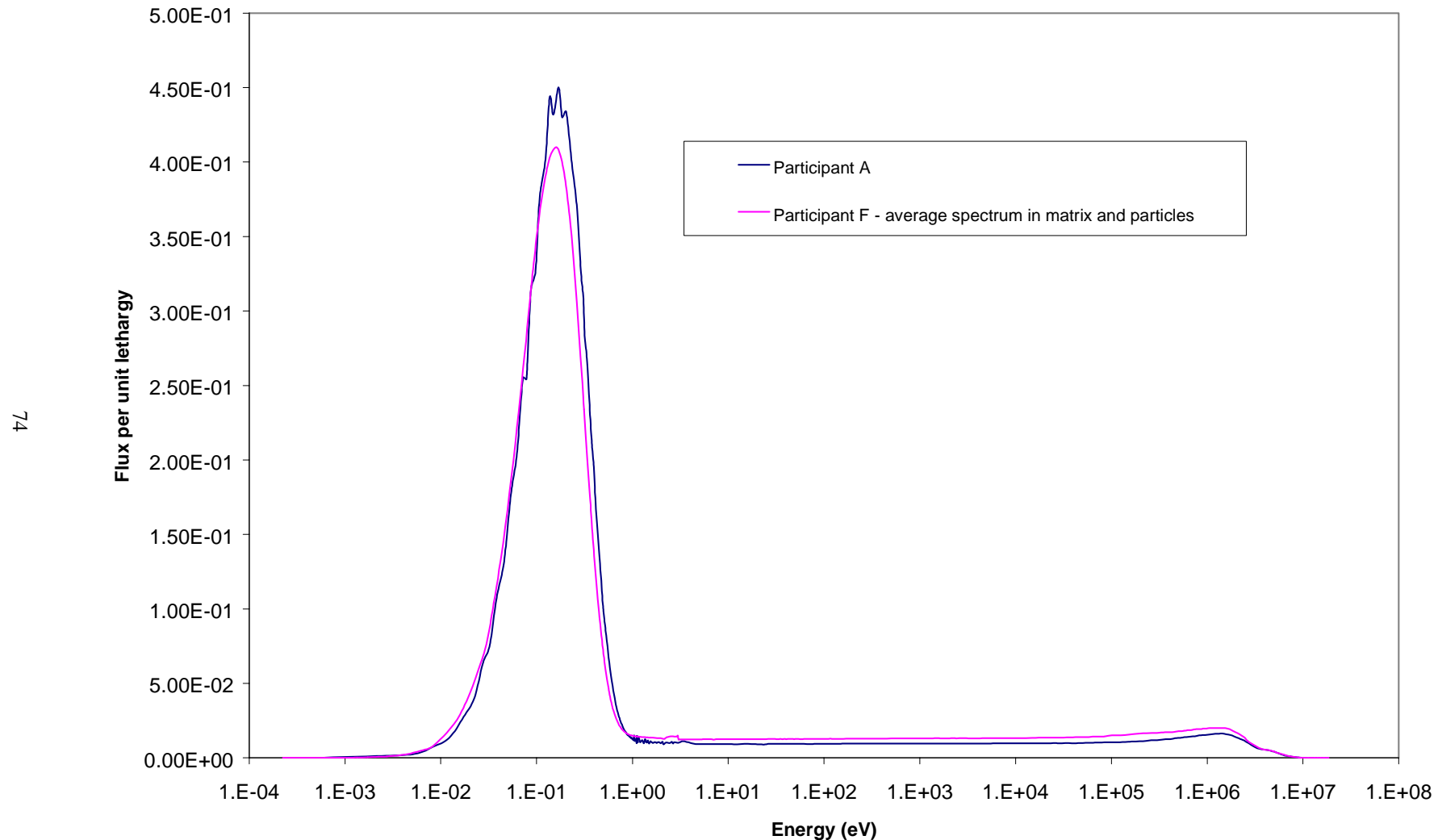


**Figure 3.16. Phase 5 – Comparison between deterministic spectra for Participants A and F**



*Appendix A*

**BENCHMARK SPECIFICATIONS**



OECD Nuclear Energy Agency  
Nuclear Science Committee  
Working Party on the Physics of Plutonium Fuels and Innovative Fuel Cycles

*Proposal version 2*

**Benchmark Specification for an HTR Fuelled with Reactor-grade Plutonium  
(or Reactor-grade Pu/Th and U/Th)**

**J.G. Hosking, T.D. Newton**  
Serco Assurance (sponsored by Nexia Solutions)

**P. Morris**  
Nexia Solutions

## **1. Background and aims**

This benchmark proposal builds upon that specified in Ref. [1]. In addition to the three phases described in that reference, another two phases have now been defined. Additional items for calculation have also been added to the existing phases. It is intended that further items may be added to the benchmark after consultation with its participants.

Although the benchmark is specifically designed to provide inter-comparisons for plutonium- and thorium-containing fuels, it is proposed that phases considering simple calculations for a uranium fuel cell and uranium core be included. The purpose of these is to identify any increased uncertainties, relative to uranium fuel, associated with the lesser-known fuels to be investigated in different phases of this benchmark.

The first phase considers an infinite array of fuel pebbles fuelled with uranium fuel. Phase 2 considers a similar array of pebbles but for plutonium fuel. Phase 3 continues the plutonium fuel inter-comparisons within the context of whole core calculations. Calculations for Phase 4 are for a uranium-fuelled core. Phase 5 considers an infinite array of pebbles containing thorium.

In setting the benchmark the requirements in the definition of the LEUPRO-12 PROTEUS benchmark have been considered.

Participants are invited to submit both deterministic results as well as, where appropriate, results from Monte Carlo calculations.

Fundamental nuclear data have been taken from Refs. [2] and [3] and are given to five decimal places. Avogadro's number and natural abundance data have been taken from Ref. [2] and atomic weights from Ref. [3].

## **2. Phase 1: Uranium cell calculations – definition**

### **2.1 Phase 1: General description**

In this phase, an infinite array of fuel pebbles is considered by modelling a single fuel pebble and using a white (isotropic flux) boundary condition. In the course of the definition of the benchmark, there has been some debate as to the form of the model to consider.

If coolant is modelled surrounding the fuel pebble, the flux on the outer boundary of the model will be anisotropic. This isotropic flux boundary condition applied in many Monte Carlo codes will not match the white boundary condition applied in deterministic collision probability calculations. Results between Monte Carlo and deterministic methods should not agree in these circumstances. This can be avoided by assuming a unit cell in a cubic array of spheres, with reflective boundary conditions. However, the introduction of a buckling in such a system, to obtain a reactor-like spectrum, would again introduce differences between Monte Carlo and deterministic solutions. To cater for the requests of all parties two cases are considered, an infinite array of fuel pebbles with reflective boundary conditions and an infinite array of pebbles arranged in a cubic lattice with reflective unit-cell boundary conditions.

The fuel pebble has a diameter of 6 cm with a central 5 cm diameter sphere containing a matrix material supporting uranium-fuelled coated particles. The pebbles have a packing fraction of 0.61, giving the outer radius of the associated spherical coolant region as 3.53735 cm, 7.0747 cm diameter. Preserving volumes would give the unit cell length for the cubic array of spheres as 5.70218 cm, however this is smaller than the pebble diameter of 6 cm. In Phase 1b, a 6 cm cubic array is to be used to match the pebble diameter. The pebble packing fraction is effectively reduced in the cubic array calculation. The coated particles have a fuel kernel of 8.2% enriched UO<sub>2</sub> with a diameter of 0.05 cm. This is surrounded by four coatings consisting of an inner carbon layer, a layer of dense pyro carbon, a layer of silicon carbide and an outer pyro carbon layer. There are 15 000 coated particles in each pebble giving a UO<sub>2</sub> mass per pebble of 10.210 g.

The absorption effect of impurities is specified in terms of equivalent-ppm natural boron content by mass. The values used are typical of those for actual cores, although there is considerable variation in impurities between different suppliers and even different batches of material from a single supplier.

## **2.2 Phase 1: Pebble and coated particle specification**

The detailed specifications of the fuel pebble and coated particle are given in Table A.1. Atomic number densities for the different regions of the pebble and coated particle are given in Table A.2. Additional data used to derive the atomic number densities are given in Table A.3.

For simplification, the He coolant composition is assumed as that at 293.6 K, even for calculations at 1 000 K.

## **2.3 Phase 1: Definition of calculations**

### **2.3.1 Phase 1a: Infinite array of fuel pebbles (spherical outer boundary)**

In Phase 1a, the benchmark considers a spherical system with an outer associated coolant region of radius 3.53735 cm and reflective or white outer boundary conditions.

### **2.3.2 Phase 1b: Infinite array of fuel pebbles (cubic array)**

In Phase 1b, the benchmark considers a cubic array of pebbles with an outer reflective boundary condition. The unit cell pitch in the array is 6 cm.

### 2.3.3 Phases 1a and 1b: Items for calculation

Isothermal temperature of 293.6 K:

- a) Reactivity ( $k_{inf}$ ).
- b) The energy-independent critical buckling  $B^2_{cr}$  and  $k_{inf}(B^2_{cr})$
- c) The migration area  $M^2$ .

Isothermal temperature of 1 000 K:

- d) Reactivity ( $k_{inf}$ ).
- e) Reactivity  $k_{eff}(B^2_{cr})$ , using the buckling from step (b), at power temperatures.
- f) The energy-independent critical buckling  $B^2_{cr}$  and  $k_{inf}(B^2_{cr})$ .
- g) The migration area  $M^2$ .
- h) The spectral indices, calculated with a critical buckling:
  - $\rho^{238} = {}^{238}U_{cap}(\text{epithermal})/{}^{238}U_{cap}(\text{thermal})$ : ratio of epithermal to thermal  ${}^{238}U$  captures.
  - $\delta^{235} = {}^{235}U_{fis}(\text{epithermal})/{}^{235}U_{fis}(\text{thermal})$ : ratio of epithermal to thermal  ${}^{235}U$  fissions.
  - $\delta^{238} = {}^{238}U_{fis}/{}^{235}U_{fis}$ : ratio of fissions in  ${}^{238}U$  to fissions in  ${}^{235}U$ .
  - $C = {}^{238}U_{cap}/{}^{235}U_{fis}$ : ratio of captures in  ${}^{238}U$  to fissions in  ${}^{235}U$ .

*Note: Epithermal is defined here as all energies above 0.625 eV and thermal as all energies below 0.625 eV.*

- i) The neutron spectrum (calculated with a critical buckling) in the fuel kernel region (flux per unit energy) with as much energy resolution as can be provided.
- j) Compositions of the actinides at irradiations of 0, 10 000, 20 000, 30 000, 40 000, 50 000, 60 000, 70 000 and 80 000 MWd/tonne, to five significant figures. The burn-up should be performed at an isothermal temperature of 1 000 K and a constant power of 556.25 watts per fuel ball. A time-dependent, energy-independent buckling should be included to give a k-effective of unity during the burn-up. Sufficient calculational steps should be used to remove the dependency of the results on the number of steps chosen.
- k) Compositions of the actinides at irradiations of 0, 10 000, 20 000, 30 000, 40 000, 50 000, 60 000, 70 000 and 80 000 MWd/tonne, to five significant figures. The burn-up should be performed at an isothermal temperature of 1 000 K and a constant power of 556.25 watts per fuel ball. No buckling should be applied during burn-up. Sufficient calculational steps should be used to remove the dependency of the results on the number of steps chosen.

## 3. Phase 2: Plutonium cell calculations – definition

### 3.1 Phase 2: General description

As for Phase 1 of the benchmark, an infinite array of fuel pebbles is again considered, as a spherical system for Phase 2a and as a cubic array for Phase 2b.

The fuel pebble has a diameter of 6 cm with the central 5 cm diameter sphere containing a matrix material supporting plutonium-fuelled coated particles. The coated particles have a fuel kernel of  $PuO_2$  with diameter of 0.024 cm. This is surrounded by four coatings consisting of an inner carbon layer,

a layer of dense pyro carbon, a layer of silicon carbide and an outer pyro carbon layer. There are 15 000 coated particles in each pebble giving a plutonium mass per pebble of 1.129 g. In Phase 2a of the benchmark, the outer diameter of the coolant associated with each pebble is 5.70218 cm as in benchmark Phase 1a. In Phase 2b a 6 cm cubic array is considered as in benchmark Phase 1b.

The isotopic plutonium vector defined for this study was suggested by B. Bonin (Cogema). It represents that arising from the irradiation of 3.7% enriched UOX fuel in a PWR with a cycle length of 274 full power days and a dwell time of four cycles. This corresponds to a burn-up of 41.2 GWd/tonne, typical of current practice. A cooling time of three years following irradiation has been allowed.

The absorption effects of impurities are specified in terms of equivalent-ppm natural boron content by mass.

### **3.2 Phase 2: Pebble and coated particle specification**

The detailed specifications of the fuel pebble and coated particle are given in Table A.4. Atomic number densities for the different regions of the pebble and coated particle are given in Table A.2. Additional data used to derive the atomic number densities are given in Table A.3 and the plutonium isotopic vector is given in Table A.6.

### **3.3 Phase 2a and 2b: Items for calculation**

Infinite array of fuel pebbles:

Isothermal temperature of 293.6 K:

- a) Reactivity ( $k_{inf}$ ).
- b) The energy-independent critical buckling  $B^2_{cr}$  and  $k_{inf}(B^2_{cr})$ .
- c) The migration area  $M^2$ .

Isothermal temperature of 1 000 K:

- d) Reactivity ( $k_{inf}$ ).
- e) Reactivity  $k_{eff}(B^2_{cr})$ , using the buckling from step (b), at power temperatures.
- f) The energy-independent critical buckling  $B^2_{cr}$  and  $k_{inf}(B^2_{cr})$ .
- g) The migration area  $M^2$ .
- h) The spectral indices, calculated with a critical buckling:
  - $\rho^{239} = {}^{239}\text{Pu}_{cap}(\text{epithermal}) / {}^{239}\text{Pu}_{cap}(\text{thermal})$ : ratio of epithermal to thermal  ${}^{239}\text{Pu}$  captures.
  - $\delta^{239} = {}^{239}\text{Pu}_{fis}(\text{epithermal}) / {}^{239}\text{Pu}_{fis}(\text{thermal})$ : ratio of epithermal to thermal  ${}^{239}\text{Pu}$  fissions.
  - $\delta^{241} = {}^{241}\text{Pu}_{fis}(\text{epithermal}) / {}^{241}\text{Pu}_{fis}(\text{thermal})$ : ratio of epithermal to thermal  ${}^{241}\text{Pu}$  fissions.
  - $F^{241} = {}^{241}\text{Pu}_{fis} / {}^{239}\text{Pu}_{fis}$ : ratio of fissions in  ${}^{241}\text{Pu}$  to fissions in  ${}^{239}\text{Pu}$ .
  - $C^8 = {}^{238}\text{Pu}_{cap} / {}^{239}\text{Pu}_{fis}$ : ratio of captures in  ${}^{238}\text{Pu}$  to fissions in  ${}^{239}\text{Pu}$ .
  - $C^9 = {}^{239}\text{Pu}_{cap} / {}^{239}\text{Pu}_{fis}$ : ratio of captures in  ${}^{239}\text{Pu}$  to fissions in  ${}^{239}\text{Pu}$ .
  - $C^0 = {}^{240}\text{Pu}_{cap} / {}^{239}\text{Pu}_{fis}$ : ratio of captures in  ${}^{240}\text{Pu}$  to fissions in  ${}^{239}\text{Pu}$ .

- $C^1 = {}^{241}\text{Pu}_{\text{cap}}/{}^{239}\text{Pu}_{\text{fis}}$ : ratio of captures in  ${}^{241}\text{Pu}$  to fissions in  ${}^{239}\text{Pu}$ .
- $C^2 = {}^{242}\text{Pu}_{\text{cap}}/{}^{239}\text{Pu}_{\text{fis}}$ : ratio of captures in  ${}^{242}\text{Pu}$  to fissions in  ${}^{239}\text{Pu}$ .

*Note: Epithermal is defined here as all energies above 0.625 eV and thermal as all energies below 0.625 eV.*

- i) The neutron spectrum (calculated with a critical buckling) in the fuel kernel region (flux per unit energy) with as much energy resolution as can be provided.
- j) Xenon reactivity effect: Reactivity ( $k_{\text{eff}}$ ) at a pebble burn-up of 1 500 MWd/tonne. The burn-up to be performed at a constant power of 556.25 watts per fuel ball with the addition of an energy independent buckling to give a k-effective of unity during the burn-up. In addition,  ${}^{135}\text{Xe}$  number density and absorption cross-section at 1 500 MWd/tonne irradiation.
- k) Compositions of the actinides at irradiations of 0, 10 000, 20 000, 30 000, 40 000, 50 000, 60 000, 70 000 and 80 000 MWd/tonne, to five significant figures. The burn-up should be performed at an isothermal temperature of 1 000 K and a constant power of 556.25 watts per fuel ball. A time-dependent, energy-independent buckling should be included to give a k-effective of unity during the burn-up. Sufficient calculational steps should be used to remove the dependency of the results on the number of steps chosen.

## 4. Phase 3: Plutonium core calculations – definition

### 4.1 Phase 3: General description

This part of the benchmark considers a whole core calculation using plutonium fuel. The schematic of the core is shown in Figure A.1 and has been taken from the first draft specification of this benchmark by H.J. Rutten of Jülich and M. Delpech and F. Dolci of the CEA. For the plutonium fuel proposed, this core design will probably be too reactive. However, as during the course of this benchmark different fuels may be investigated in different phases, there is no specific reason to optimise the design for this particular fuel type.

### 4.2 Phase 3: Core specification

The core layout is shown in Figure A.1 where the composition numbers are indicated for each region. Core parameters are defined in Table A.4 and compositions for each region are given in Table A.5. The plutonium isotopic vector is given in Table A.6. Table A.7 gives a naming convention for the different material regions and Tables A.3 and A.8 give the additional data used in deriving the composition data given in Table A.5.

The pebble and coated particle specification for Phase 3 of the benchmark is the same as for Phase 2a of the benchmark. For simplification, the He coolant temperature and pressure have been defined for zero power conditions for both the low power and power operation parts of the benchmark. The reflector regions have been assumed to have an impurity level equivalent to 2 ppm by mass of natural boron.

### **4.3 Phase 3: Definition of calculations**

Calculations for Phase 3 of the benchmark should provide:

- a) Core reactivity (k-effective) at an isothermal temperature of 293.6 K.
- b) In full-power conditions, all materials are assumed to be at an average temperature of 1 000 K. In principle, the reactor structure will be at an average temperature about 50 degrees lower than this. However, as it is not intended to model the distribution of temperature in the core, using an approximation of an isothermal temperature is adequate for the benchmark.
  - The core reactivity (k-effective).
  - The neutron spectrum averaged over the core pebble-containing region (flux per unit energy) with as much energy resolution as can be provided.
  - The absorption and fission cross-sections for the plutonium isotopes  $^{238}\text{Pu}$ ,  $^{239}\text{Pu}$ ,  $^{240}\text{Pu}$ ,  $^{241}\text{Pu}$  and  $^{242}\text{Pu}$ , averaged over the core pebble containing region, in the three energy ranges  $10^{-5}$  eV to 0.625 eV, 0.625 eV to 9.118 KeV and 9.118 KeV to 20 MeV.
- c) Xenon reactivity effect: Reactivity (k-effective) at an isothermal temperature of 1 000 K and average pebble burn-up of 1 500 MWd/tonne. The burn-up is to be performed at full power, 200.0 MW with the addition of an energy-independent buckling to give a k-effective of unity during the burn-up. The buckling is of course set to zero following the burn-up to evaluate the xenon reactivity effect. In addition, the core average  $^{135}\text{Xe}$  number density and absorption cross-section at 1 500 MWd/tonne irradiation.

## **5. Phase 4: Uranium core calculations – definition**

This part of the benchmark considers a whole core calculation using the uranium fuel defined previously in Phase 1. The schematic of the core is shown in Figure A.1 and is identical in terms of core geometry and structural material composition to the plutonium-fuelled core of Phase 3. The only difference here is the use of the uranium fuel pebble.

### **5.1 Phase 4: General description**

The core layout is shown in Figure A.1 where the composition numbers are indicated for each region. Core parameters are defined in Table A.1 and structural material compositions for each region are given in Table A.5. Fuel pebble compositions are as defined in Table A.2. Table A.7 gives a naming convention for the different material regions and Tables A.3 and A.8 give the additional data used in deriving the composition data given in Table A.5.

The pebble and coated particle specification for Phase 5 of the benchmark is the same as for Phase 1a of the benchmark. For simplification, the He coolant temperature and pressure have been defined for zero power conditions for both the low power and power operation parts of the benchmark. The reflector regions have been assumed to have an impurity level equivalent to 2 ppm by mass of natural boron.

## **5.2 Phase 4: Definition of calculations**

Calculations for Phase 4 of the benchmark should provide:

- a) Core reactivity ( $k$ -effective) at an isothermal temperature of 293.6 K. Results with and without a neutron streaming correction if available.

In full-power conditions, all materials are assumed to be at an average temperature of 1 000 K. In principle, the reactor structure will be at an average temperature about 50 degrees lower than this. However, as it is not intended to model the distribution of temperature in the core, using an approximation of an isothermal temperature is adequate for the benchmark.

- b) The core reactivity ( $k$ -effective) at an isothermal temperature of 1 000 K. Results to be provided both with and without a neutron streaming correction, if available.
- c) The tabulated, normalised (sum of flux per unit lethargy equal to unity) neutron spectrum averaged over the core pebble-containing region in as much energy resolution as can be provided. In addition, the tabulated neutron spectrum, normalised as above, for the same core region in four energy groups (lowest energy  $10^{-5}$  eV, upper group boundaries at 1.86 eV, 29 eV, 100 KeV and 20 MeV or as close as possible to these). This spectrum should be calculated at an isothermal temperature of 1 000 K.
- d) The absorption and fission cross-sections for the uranium isotopes  $^{238}\text{U}$  and  $^{235}\text{U}$  averaged over the core pebble-containing region, in the single energy range  $10^{-5}$  eV to 20 MeV. These cross-sections should be calculated at an isothermal temperature of 1 000 K.
- e) Reactivity ( $k_{\text{eff}}$ ) at an average pebble burn-up of 1 500 MWd/tonne and isothermal temperature of 1 000 K. The burn-up is to be performed at full power, 200.0 MW:
  - with the addition of an energy independent buckling to give a  $k$ -effective of unity during burn-up but with zero buckling applied following burn-up to evaluate the reactivity effect;
  - with no buckling applied;
  - the core average  $^{135}\text{Xe}$  number density and absorption cross-section at 1 500 MWd/tonne irradiation for Case 1 with the addition of an energy-independent buckling.
- f) The averaged fuelled core migration length, if available.

Participants should provide details of the calculational route they have chosen to derive values for items e) and f).

## **6. Phase 5: U/Th cell calculations – definition**

### **6.1 Phase 5: General description**

As with Phase 1 and Phase 2 of the benchmark, Phase 5 considers an infinite array of fuel pebbles. This array takes the form of a spherical system in Phase 5a and a cubic array in Phase 5b.

The fuel pebble has a diameter of 6 cm, with the central 5 cm-diameter sphere containing a matrix material supporting U/Th-fuelled coated particles. The particle design is identical to that for the plutonium system in Phase 2. Hence, each particle consists of a central fuel kernel with diameter 0.024 cm. This kernel is surrounded by four coatings, consisting of an inner carbon layer, a layer of dense pyro carbon, a layer of silicon carbide and an outer pyro carbon layer. There are 15 000 coated particles in each pebble. In Phase 5a of the benchmark, the outer diameter of the coolant associated with each pebble is 5.70218 cm. In Phase 5b, a 6 cm cubic array is considered.

The fuel is a  $^{233}\text{U}/^{232}\text{Th}$  mixed oxide, with the relative enrichment by mass of the  $^{233}\text{U}$  being 7.48%. This enrichment was chosen such that, when the particle/pebble design described above was used, the cell k-infinity at room temperature and start-of-life was comparable to that of the equivalent plutonium cell in Phase 2 of this benchmark.

As in the other phases, the absorption effects of impurities are again specified in terms of equivalent ppm natural-boron content by mass, Table 2.

Although the reactivity of this pebble configuration decreases rapidly during depletion (and therefore would not be practical for lone use in a core), the items to be calculated for this phase include some relating to burn-up. The purpose of these items is to help provide an inter-comparison of thorium burn-up in participants' codes.

## **6.2 Phase 5: Pebble and coated particle specification**

The detailed specifications of the fuel pebble and coated particle are given in Table A.9. Atomic number densities for the different regions of the pebble and coated particle are given in Table A.2. Additional data used to derive the atomic number densities are given in Table A.3.

## **6.3 Phase 5a and 5b: Items for calculation**

Infinite array of fuel pebbles:

Isothermal temperature of 293.6 K:

- a) Reactivity ( $k_{\inf}$ ).
- b) The energy-independent critical buckling  $B^2_{\text{cr}}$  and  $k_{\inf}(B^2_{\text{cr}})$ .
- c) The migration area  $M^2$ .

Isothermal temperature of 1 000 K:

- d) Reactivity ( $k_{\inf}$ ).
- e) Reactivity  $k_{\text{eff}}(B^2_{\text{cr}})$ , using the buckling from step (b), at power temperatures.
- f) The energy-independent critical buckling  $B^2_{\text{cr}}$  and  $k_{\inf}(B^2_{\text{cr}})$ .
- g) The migration area  $M^2$ .
- h) The spectral indices, calculated with a critical buckling:
  - $\rho^{232} = {}^{232}\text{Th}_{\text{cap}}(\text{epithermal})/{}^{232}\text{Th}_{\text{cap}}(\text{thermal})$ : ratio of epithermal to thermal  $^{232}\text{Th}$  captures.
  - $\delta^{233} = {}^{233}\text{U}_{\text{fis}}(\text{epithermal})/{}^{233}\text{U}_{\text{fis}}(\text{thermal})$ : ratio of epithermal to thermal  $^{233}\text{U}$  fissions.
  - $\delta^{232} = {}^{232}\text{Th}_{\text{fis}}/{}^{233}\text{U}_{\text{fis}}$ : ratio of fissions in  $^{232}\text{Th}$  to fissions in  $^{233}\text{U}$ .
  - $C = {}^{232}\text{Th}_{\text{cap}}/{}^{233}\text{U}_{\text{fis}}$ : ratio of captures in  $^{232}\text{Th}$  to fissions in  $^{233}\text{U}$ .

*Note: Epithermal, here, is defined as all energies above 0.625 eV and thermal as all energies below 0.625 eV.*

- i) The neutron spectrum (calculated with a critical buckling) in the fuel kernel region (flux per unit energy) with as much energy resolution as can be provided.

- j) Xenon reactivity effect: Reactivity ( $k_{\text{eff}}$ ) at a pebble burn-up of 1 500 MWd/tonne. The burn-up to be performed at a constant power of 556.25 watts per fuel ball with the addition of an energy independent buckling to give a k-effective of unity during the burn-up. In addition, the  $^{135}\text{Xe}$  number density and absorption cross-section at 1 500 MWd/tonne irradiation.
- k) Compositions of the actinides at irradiations of 0, 10 000, 20 000, 30 000 and 40 000 MWd/tonne, to five significant figures. The burn-up to be performed at an isothermal temperature of 1 000 K and a constant power of 556.25 watts per fuel ball. A time-dependent, energy-independent buckling to give a k-effective of unity during the burn-up should be included. Sufficient calculational steps should be used to remove the dependency of the results on the number of steps chosen.

## 7. References

- [1] Hosking, G., T.D. Newton, *Benchmark Specification for an HTR Fuelled with Reactor Grade Plutonium (or Reactor Grade Pu/Th and U/Th)*, *Proposal*, NEA/NSC/DOC(2003)22, November 2003.
- [2] Tuli, J.K., Nuclear Wallet Cards, National Nuclear Data Centre, Brookhaven National Laboratory, P.O. Box 5000 Upton, New York 11973-5000 USA, January 2000.
- [3] Atomic Data and Nuclear Data Tables, Volume 39, Number 2, Academic Press, July 1988.

**Table A.1. U benchmark: Core, pebble and coated particle parameter listing**

Item	Units	Value
<b>Reactor parameters:</b>		
Power	MW	200
Core volume	m <sup>3</sup>	66.657
He core inlet temperature (at full power)	°C	400
He core outlet temperature (at full power)	°C	950
He pressure (at full power)	MPa	4
Coolant mass flow	Kg/s	70.024
<b>Core specification:</b>		
Core height	m	9.43
Core radius	m	1.5
Number of pebbles per m <sup>3</sup>	—	5 394
Number of pebbles in core	—	359 548
Packing fraction of pebbles in core	%	61
Graphite structure natural boron impurity by mass (materials 1, 3, 4, 5, 6, 7, 8, see Table A.7)	ppm	2
<b>Fuel pebble specification:</b>		
Unit cell square pebble array pitch (cubical outer boundary)	cm	6.0
Unit cell coolant outer radius (spherical outer boundary)	cm	3.53735
Pebble diameter	cm	6.0
Radius of fuel zone	cm	2.5
Outer carbon coating thickness	cm	0.5
Outer carbon natural boron impurity by mass	ppm	0.5
Number of coated particles per pebble	—	15 000
Packing fraction of coated particles	%	9.043
Graphite matrix density	g/cm <sup>3</sup>	1.75
Graphite matrix natural boron impurity by mass	ppm	0.5
Outer carbon coating density	g/cm <sup>3</sup>	1.75
UO <sub>2</sub> fuel mass per pebble	g	10.210
<b>Coated particle specification:</b>		
Fuel in kernel UO <sub>2</sub>		
UO <sub>2</sub> fuel density	g/cm <sup>3</sup>	10.4
Uranium enrichment (by mass <sup>235</sup> U/ <sup>235</sup> U + <sup>238</sup> U)	%	8.2
Fuel natural boron impurity by mass	ppm	1
Outer coated particle radius	mm	0.455
Fuel kernel radius	mm	0.25
Coating materials	—	C/C/SiC/C
Coating thickness	mm	0.09/0.04/0.035/0.04
Coating densities	g/cm <sup>3</sup>	1.05/1.9/3.18/1.9

**Table A.2. Pebble calculations: Nuclide number density data**

Material	Nuclide	Atoms per cm <sup>3</sup> ( $\times 10^{-24}$ )
UO <sub>2</sub> fuel	<sup>238</sup> U <sup>235</sup> U O <sup>10</sup> B <sup>11</sup> B	2.12877e-02 1.92585e-03 4.64272e-02 1.14694e-07 4.64570e-07
PuO <sub>2</sub> fuel	<sup>238</sup> Pu <sup>239</sup> Pu <sup>240</sup> Pu <sup>241</sup> Pu <sup>242</sup> Pu O <sup>10</sup> B <sup>11</sup> B	6.01178E-04 1.24470e-02 5.44599e-03 3.00965e-03 1.54539e-03 4.60983e-02 1.14694e-07 4.64570e-07
<sup>233</sup> U/ <sup>232</sup> Th mixed oxide fuel	<sup>232</sup> Th <sup>233</sup> U O <sup>10</sup> B <sup>11</sup> B	2.19473E-02 1.76668E-03 4.74279E-02 1.14694E-07 4.64570E-07
Inner low-density carbon kernel coating	C	5.26449e-02
Pyro carbon kernel coatings (inner and outer)	C	9.52621e-02
Silicon carbide kernel coating	C Si	4.77240e-02 4.77240e-02
Carbon matrix	C <sup>10</sup> B <sup>11</sup> B	8.77414e-02 9.64977e-09 3.90864e-08
Carbon pebble outer coating	C <sup>10</sup> B <sup>11</sup> B	8.77414e-02 9.64977e-09 3.90864e-08
Helium coolant (at 273.16 K, 10 <sup>5</sup> Pa)	<sup>3</sup> He <sup>4</sup> He	3.71220e-11 2.65156e-05

**Table A.3. Additional composition data**

Quantity	Units	Value
<b>Physical constants:</b>		
Avagadro's number	Mol <sup>-1</sup>	6.02214E+23
Universal gas constant, R	J mol <sup>-1</sup> K <sup>-1</sup>	8.31
<b>Atomic weights:</b>		
<sup>238</sup> Pu	gm Mol <sup>-1</sup>	238.04955
<sup>239</sup> Pu	gm Mol <sup>-1</sup>	239.05216
<sup>240</sup> Pu	gm Mol <sup>-1</sup>	240.05381
<sup>241</sup> Pu	gm Mol <sup>-1</sup>	241.05685
<sup>242</sup> Pu	gm Mol <sup>-1</sup>	242.05874
<sup>233</sup> U	gm Mol <sup>-1</sup>	233.04500
<sup>235</sup> U	gm Mol <sup>-1</sup>	235.04392
<sup>238</sup> U	gm Mol <sup>-1</sup>	238.05078
<sup>232</sup> Th	gm Mol <sup>-1</sup>	232.03300
<sup>28</sup> Si	gm Mol <sup>-1</sup>	27.97693
<sup>29</sup> Si	gm Mol <sup>-1</sup>	28.97649
<sup>30</sup> Si	gm Mol <sup>-1</sup>	30.97536
Si (natural)	gm Mol <sup>-1</sup>	28.11630
<sup>12</sup> C	gm Mol <sup>-1</sup>	12.00000
<sup>13</sup> C	gm Mol <sup>-1</sup>	13.00335
C (natural)	gm Mol <sup>-1</sup>	12.01114
<sup>10</sup> B	gm Mol <sup>-1</sup>	10.01294
<sup>11</sup> B	gm Mol <sup>-1</sup>	11.00931
B (natural)	gm Mol <sup>-1</sup>	10.81203
<sup>16</sup> O	gm Mol <sup>-1</sup>	15.99491
<sup>17</sup> O	gm Mol <sup>-1</sup>	16.99913
<sup>18</sup> O	gm Mol <sup>-1</sup>	17.99916
O (natural)	gm Mol <sup>-1</sup>	15.99930
<sup>3</sup> He	gm Mol <sup>-1</sup>	3.01603
<sup>4</sup> He	gm Mol <sup>-1</sup>	4.00260
<b>Fractional abundances (by atom):</b>		
<sup>3</sup> He in natural He (coolant)	—	0.0000014
<sup>4</sup> He in natural He (coolant)	—	0.9999986
<sup>10</sup> B in natural B (impurity)	—	0.19800
<sup>11</sup> B in natural B (impurity)	—	0.80200
<sup>28</sup> Si in natural Si	—	0.92230
<sup>29</sup> Si in natural Si	—	0.04683
<sup>30</sup> Si in natural Si	—	0.03087
<sup>12</sup> C in natural C	—	0.98890
<sup>13</sup> C in Natural C	—	0.01110
<sup>16</sup> O in natural O	—	0.99762
<sup>17</sup> O in natural O	—	0.00038
<sup>18</sup> O in natural O	—	0.00200

**Table A.4. Pu benchmark: Core, pebble and coated particle parameter listing**

Item	Units	Value
<b>Reactor parameters:</b>		
Power	MW	200
Core volume	m <sup>3</sup>	66.657
He core inlet temperature (at full power)	°C	400
He core outlet temperature (at full power)	°C	950
He pressure (at full power)	MPa	4
Coolant mass flow	Kg/s	70.024
<b>Core specification:</b>		
Core height	m	9.43
Core radius	m	1.5
Number of pebbles per m <sup>3</sup>	–	5 394
Number of pebbles in core	–	359 548
Packing fraction of pebbles in core	%	61
Graphite structure natural boron impurity by mass (materials 1, 3, 4, 5, 6, 7, 8, see Table A.7)	ppm	2
<b>Fuel pebble specification:</b>		
Unit cell square pebble array pitch (cubical outer boundary)	cm	6.0
Unit cell coolant outer radius (spherical outer boundary)	cm	3.53735
Pebble diameter	cm	6.0
Radius of fuel zone	cm	2.5
Outer carbon coating thickness	cm	0.5
Outer carbon natural boron impurity by mass	ppm	0.5
Number of coated particles per pebble	–	15 000
Packing fraction of coated particles	%	3.45
Graphite matrix density	g/cm <sup>3</sup>	1.75
Graphite matrix natural boron impurity by mass	ppm	0.5
Outer carbon coating density	g/cm <sup>3</sup>	1.75
PuO <sub>2</sub> fuel mass per pebble	g	1.129
Average power per pebble	watts	556.25
<b>Coated particle specification:</b>		
Fuel in kernel PuO <sub>2</sub>		
PuO <sub>2</sub> fuel density	g/cm <sup>3</sup>	10.4
Fuel natural boron impurity by mass	ppm	1
Outer coated particle radius	mm	0.33
Fuel kernel radius	mm	0.12
Coating materials	–	C/C/SiC/C
Coating thickness	mm	0.095/0.04/0.035/0.04
Coating densities	g/cm <sup>3</sup>	1.05/1.9/3.18/1.9

**Table A.5. Core calculations: Nuclide number density data**

Material	Nuclide	Atoms per cm <sup>3</sup> ( $\times 10^{-24}$ )
UO <sub>2</sub> fuel	<sup>238</sup> U <sup>235</sup> U O <sup>10</sup> B <sup>11</sup> B	2.12877e-02 1.92585e-03 4.64272e-02 1.14694e-07 4.64570e-07
PuO <sub>2</sub> fuel	<sup>238</sup> Pu <sup>239</sup> Pu <sup>240</sup> Pu <sup>241</sup> Pu <sup>242</sup> Pu O <sup>10</sup> B <sup>11</sup> B	6.01178E-04 1.24470e-02 5.44599e-03 3.00965e-03 1.54539e-03 4.60983e-02 1.14694e-07 4.64570e-07
Inner low-density carbon kernel coating	C	5.26449e-02
Pyro carbon kernel coatings (inner and outer)	C	9.52621e-02
Silicon carbide kernel coating	C Si	4.77240e-02 4.77240e-02
Carbon matrix	C <sup>10</sup> B <sup>11</sup> B	8.77414e-02 9.64977e-09 3.90864e-08
Carbon pebble outer coating	C <sup>10</sup> B <sup>11</sup> B	8.77414e-02 9.64977e-09 3.90864e-08
Helium coolant (at 273.16 K, 10 <sup>5</sup> Pa)	<sup>3</sup> He <sup>4</sup> He	3.71220e-11 2.65156e-05
Reflector 1	C <sup>10</sup> B <sup>11</sup> B	7.72000e-02 3.39617e-08 1.37562e-07
Void	<sup>4</sup> He	1.00000e-11
Void + graphite	C <sup>10</sup> B <sup>11</sup> B	2.00000e-03 8.79837e-10 3.56378e-09
Reflector 2	C <sup>10</sup> B <sup>11</sup> B	9.03000e-02 3.97246e-08 1.60905e-07
Carbon layer surrounding system	C <sup>10</sup> B <sup>11</sup> B	8.53000e-03 3.75250e-08 1.51995e-07
Reflector + coolant channel	C <sup>10</sup> B <sup>11</sup> B	7.02000e-02 3.08823e-08 1.25089e-07
Reflector + control rods	C <sup>10</sup> B <sup>11</sup> B	3.51000e-02 1.54411e-08 6.25444e-08
Reflector 3	C <sup>10</sup> B <sup>11</sup> B	3.51000e-02 1.54411e-08 6.25444e-08

**Table A.6. Plutonium isotopic vector**

<b>Isotope</b>	<b>Units</b>	<b>% by mass</b>
$^{238}\text{Pu}$	wt.%	2.59
$^{239}\text{Pu}$	wt.%	53.85
$^{240}\text{Pu}$	wt.%	23.66
$^{241}\text{Pu}$	wt.%	13.13
$^{242}\text{Pu}$	wt.%	6.77

**Table A.7. Key to core regions shown in Figure A.1**

<b>Region</b>	<b>Number on core diagram</b>
Reflector 1	1
Void	2
Void + graphite	3
Reflector 2	4
Carbon layer surrounding system	5
Reflector + coolant channels	6
Reflector + control rods	7
Reflector 3	8

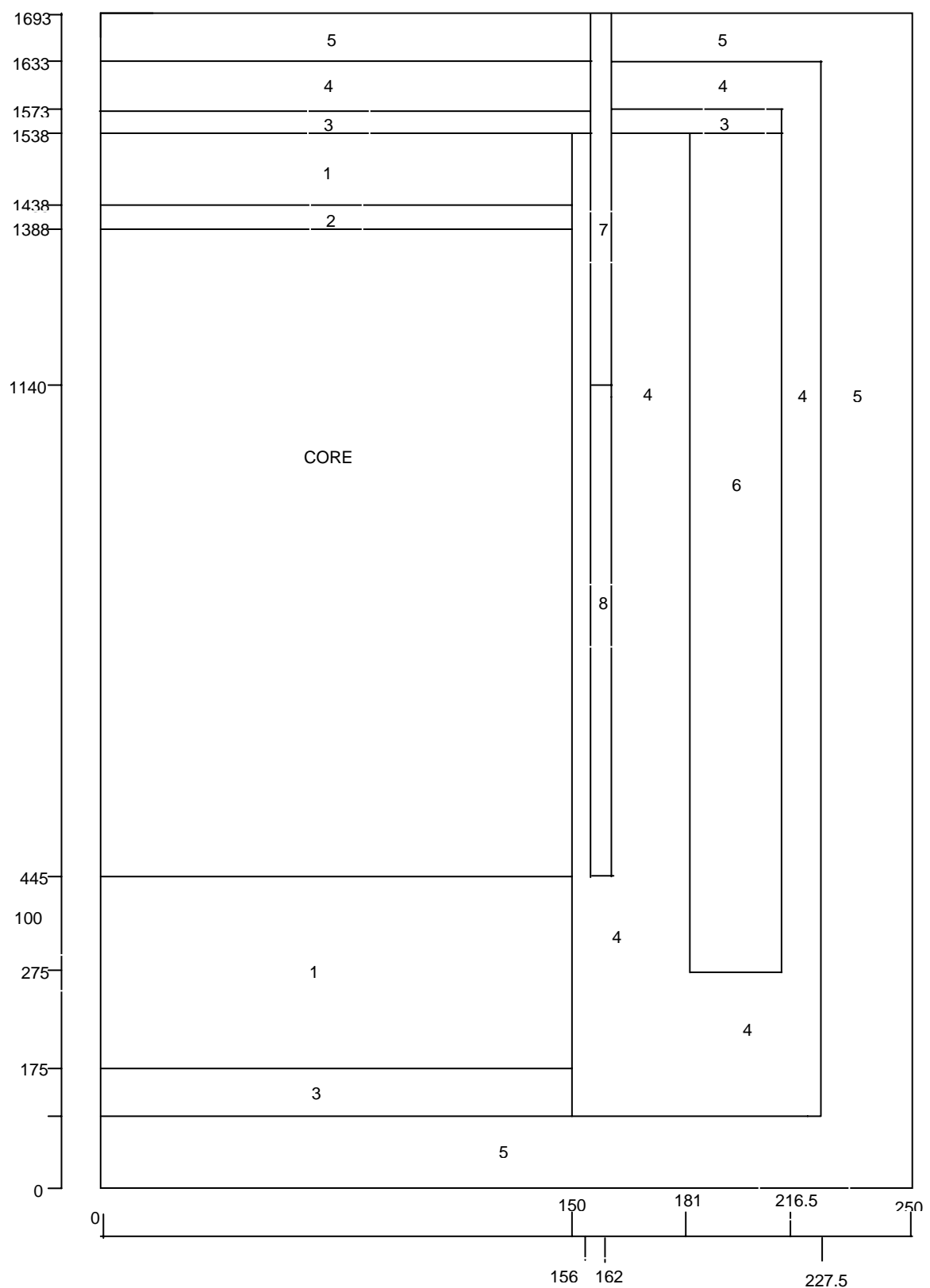
**Table A.8. Core calculations: Material mass densities**

<b>Material</b>	<b>Mass density (g/cm<sup>3</sup>)</b>
UO <sub>2</sub> fuel	10.4
PuO <sub>2</sub> fuel	10.4
Low-density carbon kernel coating	1.05
Pyro carbon kernel coating	1.9
Silicon carbide kernel coating	3.18
Carbon matrix	1.75
Carbon pebble coating	1.75
Helium coolant (at 273.16 K, 10 <sup>5</sup> Pa)	1.78E-04
Reflector 1	1.53901
Void	–
Void + graphite	3.98707e-2
Reflector 2	1.80016
Carbon layer surrounding system	1.70049
Reflector + coolant channels	1.39946
Reflector + control rods	6.99731E-01
Reflector 3	6.99731E-01

**Table A.9. U/Th benchmark: Pebble and coated particle parameter listing**

Item	Units	Value
<b>Fuel pebble specification:</b>		
Unit cell square pebble array pitch (cubical outer boundary)	cm	6.0
Unit cell coolant outer radius (spherical outer boundary)	cm	3.53735
Pebble diameter	cm	6.0
Radius of fuel zone	cm	2.5
Outer carbon coating thickness	cm	0.5
Outer carbon natural boron impurity by mass	ppm	0.5
Number of coated particles per pebble	–	15 000
Packing fraction of coated particles	%	3.45
Graphite matrix density	g/cm <sup>3</sup>	1.75
Graphite matrix natural boron impurity by mass	ppm	0.5
Outer carbon coating density	g/cm <sup>3</sup>	1.75
Fuel mass per pebble	g	1.129
<b>Coated particle specification:</b>		
Fuel in kernel: $^{233}\text{U}/^{232}\text{Th}$ mixed oxide		
Fuel density	g/cm <sup>3</sup>	10.4
$^{233}\text{U}$ enrichment (by mass $^{233}\text{U}/(^{233}\text{U} + ^{232}\text{Th})$ )	%	7.48
Fuel natural boron impurity by mass	ppm	1
Outer coated particle radius	mm	0.455
Fuel kernel radius	mm	0.12
Coating materials	–	C/C/SiC/C
Coating thickness	mm	0.095/0.04/0.035/0.04
Coating densities	g/cm <sup>3</sup>	1.05/1.9/3.18/1.9

**Figure A.1. Schematic diagram of core R-Z calculation model. Dimensions shown are in cm.**





*Appendix B*

**ENERGY GROUP SCHEMES USED  
IN THE DETERMINISTIC CALCULATIONS**



**Table B.1. 172-group energy scheme used by Participants A and B in their deterministic calculations**

Group	Upper energy boundary (eV)	Group	Upper energy boundary (eV)	Group	Upper energy boundary (eV)
1	1.964E+07	59	7.485E+02	117	1.150E+00
2	1.733E+07	60	6.773E+02	118	1.123E+00
3	1.492E+07	61	4.540E+02	119	1.110E+00
4	1.384E+07	62	3.717E+02	120	1.097E+00
5	1.162E+07	63	3.043E+02	121	1.071E+00
6	1.000E+07	64	2.040E+02	122	1.045E+00
7	8.187E+06	65	1.486E+02	123	1.035E+00
8	6.703E+06	66	1.367E+02	124	1.020E+00
9	6.065E+06	67	9.166E+01	125	9.960E-01
10	5.488E+06	68	7.567E+01	126	9.860E-01
11	4.493E+06	69	6.790E+01	127	9.720E-01
12	3.679E+06	70	5.560E+01	128	9.500E-01
13	3.012E+06	71	5.158E+01	129	9.300E-01
14	2.466E+06	72	4.825E+01	130	9.100E-01
15	2.231E+06	73	4.552E+01	131	8.600E-01
16	2.019E+06	74	4.017E+01	132	8.500E-01
17	1.653E+06	75	3.727E+01	133	7.900E-01
18	1.353E+06	76	3.372E+01	134	7.800E-01
19	1.225E+06	77	3.051E+01	135	7.050E-01
20	1.108E+06	78	2.761E+01	136	6.250E-01
21	1.003E+06	79	2.498E+01	137	5.400E-01
22	9.072E+05	80	2.260E+01	138	5.000E-01
23	8.209E+05	81	1.945E+01	139	4.850E-01
24	6.081E+05	82	1.593E+01	140	4.330E-01
25	5.502E+05	83	1.371E+01	141	4.000E-01
26	4.979E+05	84	1.122E+01	142	3.910E-01
27	4.505E+05	85	9.906E+00	143	3.500E-01
28	4.076E+05	86	9.190E+00	144	3.200E-01
29	3.020E+05	87	8.315E+00	145	3.145E-01
30	2.732E+05	88	7.524E+00	146	3.000E-01
31	2.472E+05	89	6.160E+00	147	2.800E-01
32	1.832E+05	90	5.346E+00	148	2.480E-01
33	1.228E+05	91	5.043E+00	149	2.200E-01
34	1.111E+05	92	4.129E+00	150	1.890E-01
35	8.230E+04	93	4.000E+00	151	1.800E-01
36	6.738E+04	94	3.381E+00	152	1.600E-01
37	5.517E+04	95	3.300E+00	153	1.400E-01
38	4.087E+04	96	2.768E+00	154	1.340E-01
39	3.698E+04	97	2.720E+00	155	1.150E-01
40	2.928E+04	98	2.600E+00	156	1.000E-01
41	2.739E+04	99	2.550E+00	157	9.500E-02
42	2.479E+04	100	2.360E+00	158	8.000E-02
43	1.662E+04	101	2.130E+00	159	7.700E-02
44	1.503E+04	102	2.100E+00	160	6.700E-02
45	1.114E+04	103	2.020E+00	161	5.800E-02
46	9.119E+03	104	1.930E+00	162	5.000E-02
47	7.466E+03	105	1.840E+00	163	4.200E-02
48	5.531E+03	106	1.755E+00	164	3.500E-02
49	5.005E+03	107	1.670E+00	165	3.000E-02
50	3.527E+03	108	1.590E+00	166	2.500E-02
51	3.355E+03	109	1.500E+00	167	2.000E-02
52	2.249E+03	110	1.475E+00	168	1.500E-02
53	2.035E+03	111	1.440E+00	169	1.000E-02
54	1.507E+03	112	1.370E+00	170	6.900E-03
55	1.434E+03	113	1.337E+00	171	5.000E-03
56	1.234E+03	114	1.300E+00	172	3.000E-03
57	1.010E+03	115	1.235E+00		
58	9.142E+02	116	1.170E+00		

**Table B.2. 10-group energy scheme used by Participant A in their deterministic calculations**

Group	Upper energy boundary (eV)
1	1.964E+07
2	1.162E+07
3	3.679E+06
4	2.231E+06
5	1.228E+05
6	3.043E+02
7	1.170E+00
8	9.720E-01
9	4.330E-01
10	2.480E-01

**Table B.3. 238-group energy scheme used by participant F**

Group	Upper energy boundary (eV)						
1	2.00E+07	61	3.90E+03	121	2.00E+01	181	1.09E+00
2	1.73E+07	62	3.74E+03	122	1.90E+01	182	1.08E+00
3	1.57E+07	63	3.00E+03	123	1.85E+01	183	1.07E+00
4	1.46E+07	64	2.58E+03	124	1.70E+01	184	1.06E+00
5	1.38E+07	65	2.29E+03	125	1.60E+01	185	1.05E+00
6	1.28E+07	66	2.20E+03	126	1.51E+01	186	1.04E+00
7	1.00E+07	67	1.80E+03	127	1.44E+01	187	1.03E+00
8	8.19E+06	68	1.55E+03	128	1.38E+01	188	1.02E+00
9	6.43E+06	69	1.50E+03	129	1.29E+01	189	1.01E+00
10	4.80E+06	70	1.15E+03	130	1.19E+01	190	1.00E+00
11	4.30E+06	71	9.50E+02	131	1.15E+01	191	9.75E-01
12	3.00E+06	72	6.83E+02	132	1.00E+01	192	9.50E-01
13	2.48E+06	73	6.70E+02	133	9.10E+00	193	9.25E-01
14	2.35E+06	74	5.50E+02	134	8.10E+00	194	9.00E-01
15	1.85E+06	75	3.05E+02	135	7.15E+00	195	8.50E-01
16	1.50E+06	76	2.85E+02	136	7.00E+00	196	8.00E-01
17	1.40E+06	77	2.40E+02	137	6.75E+00	197	7.50E-01
18	1.36E+06	78	2.10E+02	138	6.50E+00	198	7.00E-01
19	1.32E+06	79	2.08E+02	139	6.25E+00	199	6.50E-01
20	1.25E+06	80	1.93E+02	140	6.00E+00	200	6.25E-01
21	1.20E+06	81	1.86E+02	141	5.40E+00	201	6.00E-01
22	1.10E+06	82	1.22E+02	142	5.00E+00	202	5.50E-01
23	1.01E+06	83	1.19E+02	143	4.75E+00	203	5.00E-01
24	9.20E+05	84	1.15E+02	144	4.00E+00	204	4.50E-01
25	9.00E+05	85	1.08E+02	145	3.73E+00	205	4.00E-01
26	8.75E+05	86	1.00E+02	146	3.50E+00	206	3.75E-01
27	8.61E+05	87	9.00E+01	147	3.15E+00	207	3.50E-01
28	8.20E+05	88	8.20E+01	148	3.05E+00	208	3.25E-01
29	7.50E+05	89	8.00E+01	149	3.00E+00	209	3.00E-01
30	6.79E+05	90	7.60E+01	150	2.97E+00	210	2.75E-01
31	6.70E+05	91	7.20E+01	151	2.87E+00	211	2.50E-01
32	6.00E+05	92	6.75E+01	152	2.77E+00	212	2.25E-01
33	5.73E+05	93	6.50E+01	153	2.67E+00	213	2.00E-01
34	5.50E+05	94	6.10E+01	154	2.57E+00	214	1.75E-01
35	5.00E+05	95	5.90E+01	155	2.47E+00	215	1.50E-01
36	4.70E+05	96	5.34E+01	156	2.38E+00	216	1.25E-01
37	4.40E+05	97	5.20E+01	157	2.30E+00	217	1.00E-01
38	4.20E+05	98	5.06E+01	158	2.21E+00	218	9.00E-02
39	4.00E+05	99	4.92E+01	159	2.12E+00	219	8.00E-02
40	3.30E+05	100	4.83E+01	160	2.00E+00	220	7.00E-02
41	2.70E+05	101	4.70E+01	161	1.94E+00	221	6.00E-02
42	2.00E+05	102	4.52E+01	162	1.86E+00	222	5.00E-02
43	1.50E+05	103	4.40E+01	163	1.77E+00	223	4.00E-02
44	1.28E+05	104	4.24E+01	164	1.68E+00	224	3.00E-02
45	1.00E+05	105	4.10E+01	165	1.59E+00	225	2.53E-02
46	8.50E+04	106	3.96E+01	166	1.50E+00	226	1.00E-02
47	8.20E+04	107	3.91E+01	167	1.45E+00	227	7.50E-03
48	7.50E+04	108	3.80E+01	168	1.40E+00	228	5.00E-03
49	7.30E+04	109	3.70E+01	169	1.35E+00	229	4.00E-03
50	6.00E+04	110	3.55E+01	170	1.30E+00	230	3.00E-03
51	5.20E+04	111	3.46E+01	171	1.25E+00	231	2.50E-03
52	5.00E+04	112	3.38E+01	172	1.22E+00	232	2.00E-03
53	4.50E+04	113	3.33E+01	173	1.20E+00	233	1.50E-03
54	3.00E+04	114	3.18E+01	174	1.17E+00	234	1.20E-03
55	2.50E+04	115	3.13E+01	175	1.15E+00	235	1.00E-03
56	1.70E+04	116	3.00E+01	176	1.14E+00	236	7.50E-04
57	1.30E+04	117	2.75E+01	177	1.13E+00	237	5.00E-04
58	9.50E+03	118	2.50E+01	178	1.12E+00	238	1.00E-04
59	8.03E+03	119	2.25E+01	179	1.11E+00		
60	6.00E+03	120	2.10E+01	180	1.10E+00		



OECD PUBLICATIONS, 2 rue André-Pascal, 75775 PARIS CEDEX 16  
Printed in France.